

ON QUASIPARTICLE LIFETIMES AND TRANSPORT IN ORDERED
AND DISORDERED METALS

by

João Manuel Borregana Lopes dos Santos

Thesis submitted for the degree of Doctor of
Philosophy of the University of London

Physics Department
Imperial College of Science and Technology
London SW7 2BZ

July 1983

ABSTRACT

A theoretical analysis of electronic quasiparticle lifetimes in ordered and disordered metals is presented in this work.

In the first part of the thesis we consider the case of electron-phonon interactions in pure metals. At low temperatures the quasiparticle inverse lifetime varies as T^2 (T , temperature). The effective inter-electron interaction mediated by virtual phonons dominates real phonon scattering processes which give a T^3 contribution. It is shown that, to obtain correctly the scattering amplitude, to lowest order in ν_D/ϵ_F (ν_D and ϵ_F are the Debye and Fermi energies respectively), Migdal's theorem for the electron-phonon interaction must be modified. We derive a formal expression for the full electron-electron scattering amplitude including direct and phonon exchange interactions. These results provide a microscopic justification of MacDonald's suggestion that phonon mediated interactions should contribute significantly to the electron-electron resistivity of simple metals.

The case of disordered metals is considered in the second part of the thesis.

It is known that static disorder scattering affects the temperature dependences of the quasiparticle inverse lifetime at low temperatures. We extend and improve a method of calculation recently proposed by Abrahams, Anderson, Lee and Ramakrishnan. For dynamically screened interactions we find a $T^{3/2}$ and $T \ln(T_2/T)$ temperature dependences ^{in three and two dimensions} results previously found by Schmid and Abrahams, Anderson, Lee and Ramakrishnan. Our result in two dimensions differs in detail from that of the latter authors. Its relation to the theory of weak localization, and some experimental results are also discussed.

Finally, we consider the case of electron-phonon interactions for a simple model Hamiltonian. At the lowest temperatures we recover the behaviour characteristic of electron-electron interactions, i.e. $T^{d/2}$ (d , dimensionality). The extra logarithmic factor in two dimensions occurs only for dynamically screened Coulomb interactions.

To my parents;
To Manuela and Pedro Nuno.

ACKNOWLEDGEMENTS

On this occasion I would like to express my gratitude to:

- Dr. David Sherrington, for suggesting the topic of this thesis, for his constant advice and encouragement, and, especially, for showing great confidence in my ability to carry out this work.
- The members of the Solid State Theory Group of Imperial College, for providing such a friendly atmosphere. In particular, Dr. N. Rivier, David Elderfield and Malcolm Dunlop for innumerable discussions.
- The staff of the Physics Department of the University of Oporto, who put up with increased lecturing loads during my leave of absence.
- Prof. A. Houghton, Dr. A. MacKinnon and J.R. Senna for many fruitful discussions on the topics of this thesis.
- Miss Deanne Eastwood for her very quick and accurate typing of this thesis.
- Malcolm and Helen, our true hosts in this country.
- Finally, to Manuela, who made it all worthwhile (and even did the drawings for this work).

A Fellowship from INIC (Ministry of Education of Portugal) and an award from the "Overseas Research Students - Fees Support Scheme" of the U.K. are also gratefully acknowledged.

List of Publications

Part of the material contained in this thesis has been the subject of the following publications:

"Microscopic Derivation of the Role of Phonon-Mediated Electron-Electron Interactions in the Low Temperature Resistivity of Simple Metals". J.M.B. Lopes dos Santos and D. Sherrington, 1983, J. Phys. F13, 1233

"Self-Consistent Calculation of the Quasiparticle Lifetime in Two Dimensional Disordered Metals". J.M.B. Lopes dos Santos - Phys. Rev. B. (in press).

TABLE OF CONTENTS

	<u>Page</u>
Title	
Abstract	i
Dedication	iii
Acknowledgements	iv
List of Publications	v
Table of Contents	vi
CHAPTER 1 : PROBLEMS AND METHODS	1
CHAPTER 2 : PHONON EXCHANGE INTERACTIONS	
2.1 Electron-Electron Resistivity of Simple Metals	4
2.2 The "Direct" Interaction	8
2.3 The Exchange Contribution	19
2.4 Physical Interpretation	29
CHAPTER 3 : DIRECT AND PHONON MEDIATED INTERACTIONS	
3.1 The Scattering Amplitude and the Four-Point Vertex Function	34
3.2 The Scattering Amplitude and Migdal's Theorem	42
CHAPTER 4 : WEAK LOCALIZATION AND QUASIPARTICLE LIFETIMES IN TWO DIMENSIONAL METALS	
4.1 Introduction	46
4.2 Impurity Scattering Perturbation Theory and Diffusive Poles	47
4.3 Weak Localization and the Inelastic Scattering Time	61
4.4 Inelastic Scattering Time in Two Dimensions	63
CHAPTER 5 : SELF-CONSISTENT CALCULATION OF THE QUASIPARTICLE LIFETIME IN TWO DIMENSIONAL METALS	
5.1 The Method of AALR in Momentum Space	70
5.2 Clean Limit Contribution to the Quasiparticle Lifetime	75

5.3	Contribution of the Particle-hole Diffusion Pole to the Quasiparticle Lifetime	82
5.4	The Lifetime of the Particle-Hole Propagator D	93
5.5	Experimental Results	108
CHAPTER 6 : PHONON MEDIATED INTERACTIONS IN DISORDERED METALS : A MODEL CALCULATION		
6.1	Introduction	111
6.2	The Phonon Spectral Function	113
6.3	The Clean Limit Contribution	116
6.4	Contribution of the Particle Hole Diffusion Pole	117
APPENDIX A THE PHONON SELF-ENERGY AND SPECTRAL FUNCTION IN PURE METALS		
A.1	The Self-Energy	124
A.2	Spectral Function	128
APPENDIX B INTERMEDIATE STATES AND THE IMAGINARY PART OF THE SELF-ENERGY		
APPENDIX C	THE INTEGRAL $I(q; i\epsilon_m + i\omega_\ell, i\epsilon_m)$	134
APPENDIX D	THE MOMENTUM INTEGRALS I_{pq}	139
APPENDIX E	THE POLARIZATION INSERTION $\Pi(q, i\omega_\ell)$ AND THE SCREENED COULOMB INTERACTION	141
REFERENCES		150

CHAPTER 1

PROBLEMS AND METHODS

The single most important property of quasiparticle lifetimes is that they are long. Indeed, the very concept of quasiparticle as a well defined excitation of a many-body system requires that the corresponding lifetime be very long.

In this work we shall be concerned exclusively with electronic quasiparticles in metals. And these are not very accessible to experimental measurement. The reason is, of course, that no physical probes couple to a single fermion. By conservation of spin, fermions must be created or destroyed in pairs and therefore all electronic response functions are two particle Green's functions. In many instances then, one concerns oneself with quasiparticle lifetimes only when they become a bit too short for comfort. And yet these quantities reflect in a very direct way the characteristics of the interactions within the system.

Quasiparticle lifetimes are most often calculated from one particle Green's functions. In a clean metal the Green's function has the form

$$G(\mathbf{k}, i\epsilon_m) = \frac{1}{i\epsilon_m - \omega_{\mathbf{k}} - \Sigma(\mathbf{k}, i\epsilon_m)} \quad (1.1)$$

where $\omega_{\mathbf{k}}$ is the bare particle energy measured with respect to the chemical potential μ , $\Sigma(\mathbf{k}, i\epsilon_m)$ is the self-energy and $\epsilon_m = (2m+1)\pi k_B T$ is a Fermion Matsubara frequency. The location of the poles of the advanced or retarded Green's functions gives the quasiparticle energy $\tilde{\omega}_{\mathbf{k}}$ and inverse lifetime $\Gamma_{\mathbf{k}}$ (Nozières 1964)

$$\tilde{\omega}_{\mathbf{k}} = \omega_{\mathbf{k}} + \Sigma_1(\mathbf{k}, \tilde{\omega}_{\mathbf{k}}) \quad (1.2a)$$

$$\Gamma_{\mathbf{k}} = z_{\mathbf{k}} \Sigma_2(\mathbf{k}, \tilde{\omega}_{\mathbf{k}}) \quad (1.2b)$$

where $\Sigma_1(\mathbf{k}, \omega)$ and $\Sigma_2(\mathbf{k}, \omega)$ are the real and imaginary parts of the advanced self-energy $\Sigma(\mathbf{k}, \omega - i0^+)$, and $z_{\mathbf{k}}$ the quasiparticle renormalization factor is

$$z_{\mathbf{k}} = \left(1 - \left. \frac{\partial \Sigma_1(\mathbf{k}, \omega)}{\partial \omega} \right|_{\omega = \tilde{\omega}_{\mathbf{k}}} \right)^{-1} \quad (1.3)$$

and gives the spectral weight of the quasiparticle state ($z_{\mathbf{k}} \leq 1$).

The physical interpretation of $\Gamma_{\mathbf{k}}$ is that it gives the rate of decay of the amplitude of finding a particle in state \mathbf{k} after one has been added, in that state, to a system which is otherwise in thermal equilibrium. In the cases where a Boltzmann equation is valid this quantity can be calculated by computing the rate of decay of the occupation of a state \mathbf{k} which is changed with respect to its equilibrium value. In this case, however, one obtains the rate of decay of the probability of finding the particle in state \mathbf{k} which is twice the quasiparticle inverse lifetime as defined in eq. (1.2(b)).

In Chapters 2 and 3 we use Green's function methods to derive a formal expression for the quasiparticle inverse lifetime in a clean metal, in which the right hand side has the form of a Boltzmann electron-electron collision integral. This allows us to identify the form of the scattering amplitude which involves phonon mediated interactions as well as direct electron-electron ones. We find that Migdal's theorem (Migdal 1958), as it is usually stated, in terms of the electron self-energy, does not give the phonon exchange scattering amplitude correctly to

lowest order in ν_D/ϵ_F (ν_D and ϵ_F are the Debye and Fermi energies respectively). This investigation was prompted by a suggestion of MacDonald (1980) and MacDonald, Taylor and Geldart (1981), that the phonon mediated interaction should contribute significantly to the electron-electron resistivity of simple metals. This work provides a microscopic derivation of the full electron-electron scattering amplitude in the Boltzmann collision integral and supports MacDonald's suggestion.

The second part of the thesis, Chapters 4 to 6, deals with the question of quasiparticle lifetimes in disordered systems. We are here referring not to the lifetime of a momentum state, which is dominated by elastic impurity scattering, but to the lifetime of an exact eigenstate of the Hamiltonian in the absence of interactions. Recent theoretical advances have opened the possibility of measuring directly this latter quantity (see Chapter 4). What is measured, in fact, is the lifetime of a two particle propagator, but it turns out to be closely related to the quasiparticle lifetime. This has created a lot of experimental and theoretical activity in this field. In fact, the interplay of interactions and disorder is proving to be one of the most fascinating areas of condensed matter physics in recent years.

Finally, some words on notation. In defining our Green's functions we have used the conventions of Fetter and Walecka (1971) (the book from which I learned the subject). We have set $\hbar = 1$ throughout the work. A slightly unconventional notation is that the superscripts 'R' or 'A' (retarded or advanced) are used in the Green's functions or self-energies to mean that their frequency arguments have positive or negative imaginary parts, irrespective of whether or not they have been analytically continued to the real axis.

CHAPTER 2PHONON EXCHANGE INTERACTIONS2.1 Electron-Electron Resistivity of Simple Metals

It has been suggested recently by MacDonald and co-workers (MacDonald 1980, MacDonald, Taylor and Geldart 1981) that the effective electron-electron interaction due to the exchange of phonons should contribute to the electrical resistivity in exactly the same way as the direct Coulomb interaction, namely, giving rise to a T^2 term in the low temperature resistivity ($T \ll \theta_D$, where θ_D is the Debye temperature). This contribution was calculated by relating effective scattering probability to the electronic four-point function in the limit of zero energy transfer, and substantially alters the coefficient of the T^2 term in the resistivity of simple metals (MacDonald 1980; MacDonald, Taylor and Geldart 1981; see Table I).

MacDonald's assumption is tantamount to saying that a correct Boltzmann equation for the electron-phonon system would have an effective electron-electron collision integral.

On the other hand, conventional Boltzmann treatment of transport in the electron-phonon system (Ziman 1962) gives a limiting low temperature behaviour for the resistivity of T^5 and microscopic derivations of transport equations by Prange and Kadanoff (1964) and Prange and Sachs (1967) apparently confirmed the results of this conventional theory.

To the best of our knowledge the only (indirect) microscopic basis for MacDonald's suggestion lies in the work of Abrikosov, Gorkov and Dzyaloshinskii (1963) (AGD), who did a diagrammatic calculation of the electron self-energy based on Migdal's theorem (Migdal 1958), which provides a classification

METAL	ρ_{ee}/T^2 ($10^{-16} \Omega \text{ m K}^{-1}$)		
	COULOMB	COULOMB + PHONON EXCHANGE	Exp
Li	0.6	21	~ 200
Na	0.1	13	18 ~ 19.5
K	0.4	17	5.5 ~ 29
Al	1.8	41	28

TABLE I

Values of the T^2 coefficient of the resistivity of various simple metals. Theoretical values are calculated with Coulomb interactions only (first column) and with inclusion of phonon exchange interactions (second column). Shown also are experimental values (from MacDonald, Taylor and Geldart (81) and MacDonald (80)).

of diagrams in powers of ν_D / ϵ_F (ν_D is the Debye energy and ϵ_F the Fermi energy). Typically this ratio is of order 1%. At the very lowest temperatures, $T \ll (\nu_D / \epsilon_F) \theta_D$, they showed that the electronic inverse lifetime varies as T^2 when account is taken of finite phonon lifetimes and not as T^3 as one would expect from electron-phonon real scattering (a similar result for the electron inverse lifetime as a function of energy away from the Fermi level at $T = 0$ was found earlier by Migdal (1958)). The T^2 dependence is characteristic of fermion interactions and AGD attribute this contribution to the sort of effective interaction that MacDonald invoked.

The resistivity is proportional to a transport inverse lifetime which does not, necessarily, have the same temperature dependence as the quasiparticle inverse lifetime. The latter is essentially the rate of collisions whereas the transport inverse lifetime is basically the rate of decay of current. For electron-phonon scattering, in the transport inverse lifetime, the scattering probability $P_{\underline{k} \rightarrow \underline{k}'}$ is weighted with a factor $1 - \underline{v}_{\underline{k}} \cdot \underline{v}_{\underline{k}'} / v_{\underline{k}}^2$ ($v_{\underline{k}}$ is the velocity of a state \underline{k}) which gives the fractional change of current along the initial direction in a scattering event $\underline{k} \rightarrow \underline{k}'$. For simple metals with almost spherical Fermi surfaces this factor may be replaced by $1 - \underline{k} \cdot \underline{k}' / k^2$. At low temperatures ($T \ll \theta_D$) the typical phonon wavevector is very small

$$q \sim \frac{k_B T}{c_s} \ll k_F$$

where c_s is the sound velocity. Hence the angle θ between \underline{k} and \underline{k}' is also very small and

$$1 - \frac{\underline{k} \cdot \underline{k}'}{k^2} = 1 - \cos \theta \sim \theta^2 \sim \left(\frac{q}{k_F}\right)^2 \sim \left(\frac{T}{\theta_D}\right)^2$$

It is for this reason that the resistivity varies as T^5 whereas the quasiparticle inverse lifetime varies as T^3 .

On the other hand electron-electron scattering only contributes to the resistivity for nonspherical Fermi surfaces with Umklapp scattering. Otherwise the current is conserved in a collision and does not decay. Provided this condition is satisfied, though, one normally finds that the transport and quasiparticle inverse lifetimes show the same T^2 dependence which arises from well known phase space restrictions in the Boltzmann fermion-fermion collision integral (see for instance Baym and Pethick 1978).

This fact will be used to attempt a more definite microscopic justification of MacDonald's suggestion than that provided by the calculation of AGD.

In section 2.2 we rederive the result of AGD but cast it into a form that makes it obvious that the T^2 inverse lifetime, for the electron-phonon system, can be obtained from a Boltzmann equation with an effective electron-electron collision integral. However, we find that the corresponding scattering probability only includes the direct term and omits an exchange contribution which is expected to be of the same order of magnitude. This leads us to reconsider Migdal's theorem and we find that we must calculate another skeleton diagram - usually discarded on the basis of Migdal's result - in order to obtain the complete electron-electron effective scattering probability. This is done in section 2.3. These two sections are somewhat technical, but the final result - eq. (2.27) - is very intuitive. In section 2.4 we discuss the physical reason for our choice of diagrams and argue that all remaining contributions are smaller by a factor v_D / v_F . In

the following chapter these results are generalized to include Coulomb interactions.

Given the nature of our purpose, we consider the simplest possible electron-phonon hamiltonian - a jellium model with longitudinal Debye phonons and electron-phonon matrix elements $M_{\mathbf{k}-\mathbf{k}'}$ dependent only on $|\mathbf{k}-\mathbf{k}'|$ and behaving as $|M_{\mathbf{k}-\mathbf{k}'}|^2 \propto |\mathbf{k}-\mathbf{k}'|$ for $|\mathbf{k}-\mathbf{k}'| \ll k_F$. Our essential conclusions will certainly go through for more realistic models.

2.2 The "Direct" Interaction

The one particle Green's functions for the electron-phonon system can be obtained from a set of integral equations which involve the full vertex function. This function is obtained by summing all linked diagrams with one phonon and two electron external lines in which all propagators are renormalized (see Fig. 2.1). Migdal showed, as early as 1958, that all corrections to the bare vertex involve a small multiplicative factor of order v_D/ϵ_F , i.e. $(m/M)^{1/2}$ where m and M are the electronic and ionic masses (Migdal 1958 and AGD).

One is then led to the conclusion that the dominant electron and phonon self-energies are given by the diagrams in Fig. 2.2 (see AGD). We shall, in fact, see that to obtain the low temperature electronic self-energy completely to dominant order in v_D/ϵ_F we have to consider an extra diagram. In this paragraph, however, we sketch the main steps in the calculation of the diagram of Fig. 2.2(a), which already involves a T^2 correction to the usual T^3 contribution.

By using the spectral representations for the Green's functions we can perform the frequency sums in the usual way (see Schrieffer 1964 for details) and obtain for the imaginary part of the electron self-energy,

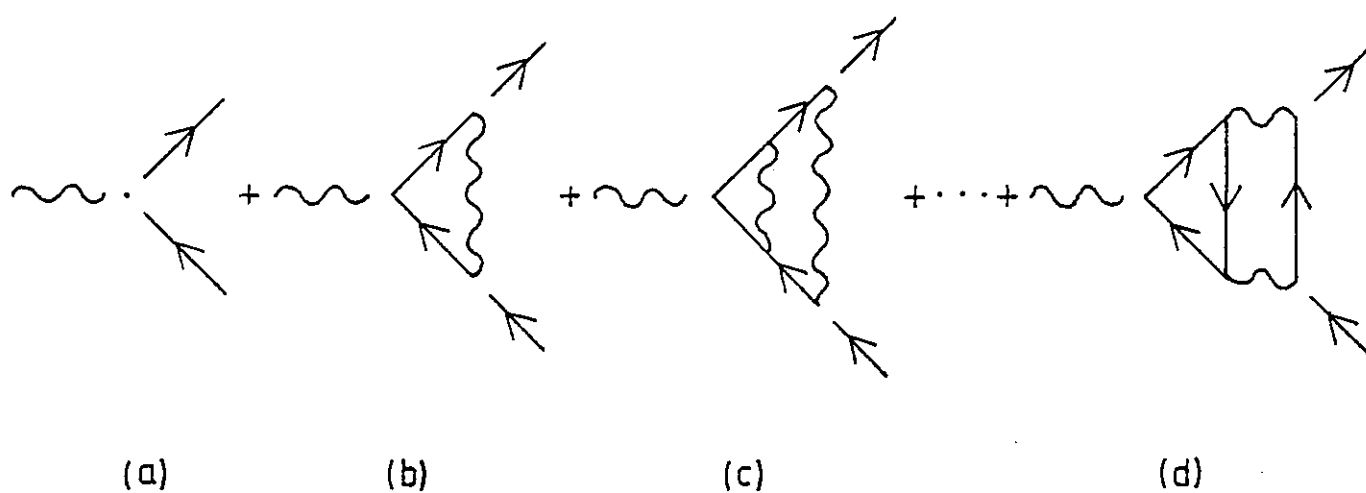


FIG 2.1

Bare electron phonon vertex (a) and some corrections (b, c, d).
 External lines are not included in the definition of the vertex
 function

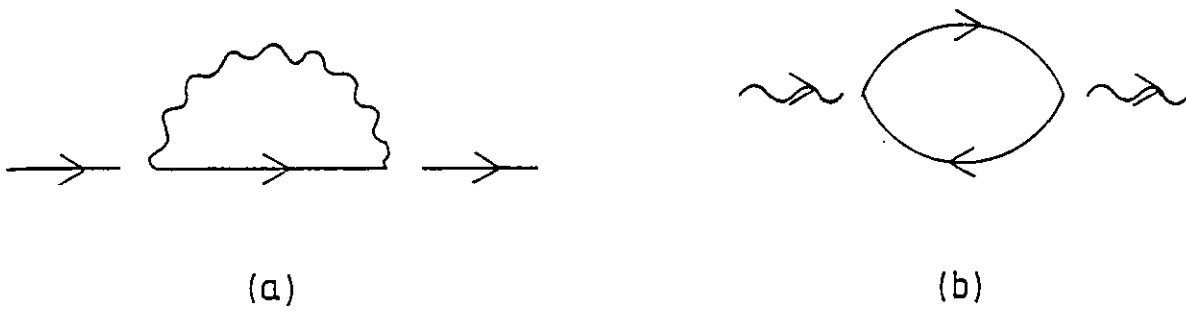


FIG 2.2

Electron (a) and phonon (b) self-energies in the context of Migdal's theorem. All propagators are renormalized.

$$\Sigma_2(\underline{k}, \xi) = \pi \int \frac{d^3 k'}{(2\pi)^3} |M_{\underline{k}-\underline{k}'}^0|^2 \left(\frac{d\xi'}{2\pi} \frac{d\eta}{2\pi} \rho(\underline{k}', \xi') \sigma(\underline{k}-\underline{k}', \eta) \right. \\ \left. \times [N(\eta) + 1 - f(\xi')] \right) \delta(\xi - \xi' - \eta) \quad (2.1)$$

where $\rho(\underline{k}, \xi)$ and $\sigma(\underline{q}, \eta)$ are the electron and phonon spectral functions and $f(\xi)$ and $N(\eta)$ are the fermion and boson thermal occupation factors. Equation (2.1) apparently includes only phonon emission processes. This is because we are integrating η between $\pm\omega$. Using the property

$$\sigma(\underline{q}, \eta) = -\sigma(\underline{q}, -\eta)$$

(which can be proved from the Lehman representation for $\sigma(\underline{q}, \eta)$ for a system with a centre of symmetry) we can rewrite eq. (2.1) with η integrated between 0, $+\omega$ and, then, the phonon absorption term would appear explicitly.

From the imaginary part of the self-energy we can get the real part using the well known dispersion relation

$$\Sigma_1(\underline{k}, \xi) = P \int \frac{d\xi'}{\pi} \frac{\Sigma_2(\underline{k}, \xi')}{\xi - \xi'} \quad (2.2)$$

The electronic spectral function is itself given in terms of $\Sigma_1(\underline{k}, \xi)$ and $\Sigma_2(\underline{k}, \xi)$ by

$$\rho(\underline{k}, \xi) = \frac{2 \Sigma_2(\underline{k}, \xi)}{[\xi - \omega_{\underline{k}} - \Sigma_1(\underline{k}, \xi)]^2 + \Sigma_2^2(\underline{k}, \xi)} \quad (2.3)$$

(all electronic energies are measured with respect to the

Fermi energy).

We shall now argue that in the frequency and temperature ranges we are interested in, $|\xi|, k_B T \ll v_D$, it is possible, without further approximation, to make the replacement

$$\rho(\underline{k}', \xi') \rightarrow 2\pi z_{\underline{k}'} \delta(\xi - \epsilon_{\underline{k}'}) \quad (2.4)$$

where $z_{\underline{k}'}$, the quasiparticle renormalization factor, and $\epsilon_{\underline{k}'}$, the renormalized electron energy, are defined by

$$z_{\underline{k}'} = \left(1 - \frac{\partial \Sigma_1(\underline{k}', \xi)}{\partial \xi} \Big|_{\xi = \epsilon_{\underline{k}'}} \right)^{-1} \quad (2.5)$$

$$\epsilon_{\underline{k}'} = \omega_{\underline{k}'} + \Sigma_1(\underline{k}_F, \epsilon_{\underline{k}'}) \quad (2.6)$$

where $\omega_{\underline{k}'}$ is the bare electron energy.

To prove the validity of eq. (2.4) we need to invoke some properties of $\Sigma_2(\underline{k}, \xi)$ which will be borne out self-consistently by the calculation.

- (i) $\Sigma_2(\underline{k}, \xi)$ varies slowly with $\omega_{\underline{k}}$ - on a scale or order ϵ_F - but much more quickly with ξ or $k_B T$ - on a scale of order v_D . We shall see shortly that we only need, in eq. (2.1), values of $\omega_{\underline{k}'}$ such that $|\omega_{\underline{k}'}| \lesssim \text{Max} \{ |\xi|, k_B T \}$. Hence we can neglect entirely the \underline{k}' variation of $\Sigma_2(\underline{k}', \xi')$ (and by eq. (2.2) of $\Sigma_1(\underline{k}', \xi')$ and set $|\underline{k}'| = k_F$).
- (ii) As $\xi, k_B T \rightarrow 0$, $\Sigma_2(\underline{k}, \xi)$ goes to zero at least as fast as $\text{Max} \{ \xi^2, (k_B T)^2 \}$.

These two properties imply that $\rho(\underline{k}', \xi')$, as a function of ξ' , is strongly peaked near the renormalized energy $\epsilon_{\underline{k}'}$ having a lorentzian form near the peak, i.e. for

$$|\xi - \epsilon_{\underline{k}'}| \lesssim \Sigma_2(\underline{k}', \epsilon_{\underline{k}'}) \ll \text{Max}\{|\xi|, k_B T\}$$

$$\rho(\underline{k}', \xi') = \frac{2 Z_{\underline{k}'} \Gamma_{\underline{k}'}}{(\xi - \epsilon_{\underline{k}'})^2 + \Gamma_{\underline{k}'}} \quad (2.7)$$

where

$$\Gamma_{\underline{k}'} = Z_{\underline{k}'} \Sigma_2(\underline{k}', \epsilon_{\underline{k}'}) \quad (2.8)$$

is the quasiparticle inverse lifetime.

Note that the important values of ξ' in eq. (2.1) are $\xi' \lesssim \text{Max}\{|\xi|, k_B T\}$ since the thermal factors are cut off exponentially for $|\xi'| \gg \text{Max}\{|\xi|, k_B T\}$.

In the region of integration for which $|\omega_{\underline{k}'}| \lesssim \text{Max}\{|\xi|, k_B T\}$, $\rho(\underline{k}', \xi')$ is well represented by the lorentzian of eq. (2.7) for the important values of ξ' . But the width $\Gamma_{\underline{k}'}$ is then at most of order $\text{Max}\{\xi^2, (k_B T)^2\}$ whereas the thermal occupation factors vary on a scale of order $k_B T$ or $|\xi|$. It follows, then, that the replacement of eq. (2.4) is correct to lowest order in temperature or frequency.

For $|\omega_{\underline{k}'}| \gg \text{Max}\{|\xi|, k_B T\}$ eq. (2.7) no longer gives a good representation of $\rho(\underline{k}', \xi')$ for $|\xi'| \lesssim \text{Max}\{|\xi|, k_B T\}$. But in this case we have $|\xi'| \ll \omega_{\underline{k}'}$ and we can write

$$\rho(\underline{k}', \xi') \approx \frac{2 \Sigma_2(\underline{k}', \xi')}{\omega_{\underline{k}'}} \quad (2.9)$$

($\Sigma_1(\underline{k}, \xi')$ goes to zero as $\xi' \rightarrow 0$ as well). As we have $\Sigma_2(\underline{k}, \xi') \sim \text{Max}\{\xi'^2, (k_B T)^2\}$ it follows that this region of values of $\omega_{\underline{k}}$ gives a contribution which is of higher order in T or ξ compared to the one coming from $\omega_{\underline{k}'} \leq \text{Max}\{|\xi|, k_B T\}$.

Although the justification of eq. (2.4) was presented in the context of eq. (2.1), we find that this simplification is also valid in other expressions that we shall encounter later and can be justified by very similar arguments.

It is implicit in the previous argument that $\sigma(\underline{k}-\underline{k}', \xi-\xi')$ varies slowly with $\xi-\xi'$ compared to $\rho(\underline{k}', \xi')$ and we shall soon see that this is correct. In fact, our results can be obtained without using eq. (2.4) by taking advantage of property (i) above and the fact that the electronic self-energy is at most of order ν_D , following a method due to Prange and Kadanoff (1964). However, for the range of temperatures we are interested in, eq. (2.4) is valid and does not involve an approximation. Then eq. (2.1) becomes,

$$\Sigma_2(\underline{k}, \xi) = \pi \int \frac{d^3 k'}{(2\pi)^3} \underline{x}_{\underline{k}'} |M_{\underline{k}-\underline{k}'}^0|^2 [N(\xi - \epsilon_{\underline{k}'}) + 1 - f(\epsilon_{\underline{k}'})] \times \frac{1}{2\pi} \sigma(\underline{k}-\underline{k}', \xi - \epsilon_{\underline{k}'}) \quad (2.10)$$

The phonon spectral function is discussed in appendix A (see also AGD). For $\eta \leq \nu_q$ it can be represented as a difference of two lorentzians centred around $\pm \nu_q$, where ν_q is the phonon renormalized energy, with a width γ_q of order $(\nu_D/\epsilon_F) \nu_q$. It is linear in η for $\eta \ll \nu_q$ (eqs. (A.14)-(A.16)).

For simplicity we consider in eq. (2.10) the limit

$|\xi| \ll k_B T$; in the opposite limit we can apply similar arguments with $|\xi|$ in place of $k_B T$. The term in square brackets in eq. (2.10) varies with $\epsilon_{\underline{k}}$, on a scale of order $k_B T$ and is exponentially small for $|\epsilon_{\underline{k}}| \gg k_B T$. Let us then consider first the contribution of phonons with $\nu_{\underline{k}-\underline{k}'} \leq k_B T$. The integral over $\epsilon_{\underline{k}'}$ is then dominated by the peaks of $\sigma(\underline{k}-\underline{k}', -\epsilon_{\underline{k}'})$ and, as $\gamma_{\underline{k}-\underline{k}'} \sim (\nu_{\mathcal{D}}/\epsilon_F) \nu_{\underline{k}-\underline{k}'} \ll k_B T$ we can make the replacement

$$\sigma(\underline{k}-\underline{k}', -\epsilon_{\underline{k}'}) \rightarrow 2\pi \left(\frac{\nu_{\underline{k}-\underline{k}'}^0}{\nu_{\underline{k}-\underline{k}'}} \right) \left[\delta(\nu_{\underline{k}-\underline{k}'} + \epsilon_{\underline{k}'}) - \delta(\nu_{\underline{k}-\underline{k}'} - \epsilon_{\underline{k}'}) \right] \quad (2.11)$$

where $\nu_{\underline{q}}^0$ is the bare phonon frequency. The \underline{k}' integral can now be performed over all values of \underline{k}' because the modes with $\nu_{\underline{k}-\underline{k}'} \gg k_B T$ give an exponentially small contribution. We see that except for minor scale factors and energy renormalization we recovered the result of first order perturbation theory. Taking into account that $|M_{\underline{k},\underline{k}'}^0| \propto |\underline{k}-\underline{k}'|$ for $|\underline{k}-\underline{k}'| \ll k_F$ it is straightforward to show that $\Sigma_2(k_F, 0)$ is of order $\lambda_0 (T/\theta_{\mathcal{D}})^3 \nu_{\mathcal{D}}$ (AGD) where $\lambda_0 = \lim_{q \rightarrow 0} n_0 |M_q|^2 / \nu_q$ which is of order one for most metals (n_0 is the electronic unrenormalized density of states per unit volume and spin state at the Fermi level).

However, in the region $|\epsilon_{\underline{k}'}| \leq k_B T$ eq. (2.11) is not a good representation of the spectral function for modes with $\nu_{\underline{k}-\underline{k}'} \gg k_B T$. In this case we have $|\epsilon_{\underline{k}'}| \ll \nu_{\underline{k}-\underline{k}'}$ and (see eq. (A.16))

$$\sigma(\underline{k}-\underline{k}', -\epsilon_{\underline{k}'}) = \frac{8 \nu_{\underline{k}-\underline{k}'}^0 S_2(\underline{k}-\underline{k}', -\epsilon_{\underline{k}'})}{[\nu_{\underline{k}-\underline{k}'}^0{}^2 + 2 \nu_{\underline{k}-\underline{k}'}^0 S_1(\underline{k}-\underline{k}', 0)]^2} \quad (2.12)$$

$$\approx 8 \left(\frac{\nu_{\underline{k}-\underline{k}'}^0}{\nu_{\underline{k}-\underline{k}'}^0} \right)^2 \frac{S_2(\underline{k}-\underline{k}', -\epsilon_{\underline{k}'})}{\nu_{\underline{k}-\underline{k}'}^0{}^2}$$

where $S_1(q, \eta)$ and $S_2(q, \eta)$ are the real and imaginary parts of the phonon self-energy, the latter being linear in for $|\eta| \ll \nu_q$. These modes will then give a contribution of order T^2 which will dominate, at low enough temperatures, ($T \ll (\nu_q/\epsilon_F) \theta_D$, as we shall see) over the conventional T^3 term (see Fig. 2.3).

We shall now demonstrate explicitly the electron-electron coupling nature of this dominant low temperature contribution to the electron lifetime.

The imaginary phonon self-energy is given by

$$S_2(q, \eta) = \int \frac{d^3 k_2}{(2\pi)^3} |M_q^0|^2 \int \frac{d\xi_2}{2\pi} \rho(\underline{k}_2, \xi_2) \rho(\underline{k}_2 + \underline{q}, \xi_2 + \eta) \times [f(\xi_2) - f(\xi_2 + \eta)] \quad (2.13)$$

We are interested only in the term linear in η for small η . By similar arguments to those that led to eq. (2.4) one can show that one can replace both electronic spectral functions by the corresponding delta functions to get (see Appendix A),

$$S_2(q, \eta) = 2\pi \int \frac{d^3 k_2}{(2\pi)^3} |M_q^0|^2 x_{\underline{k}_2} x_{\underline{k}_2 + \underline{q}} [f(\epsilon_{\underline{k}_2}) - f(\epsilon_{\underline{k}_2 + \underline{q}})] \times \delta(\epsilon_{\underline{k}_2} + \eta - \epsilon_{\underline{k}_2 + \underline{q}}) \quad (2.14)$$

Substituting this in eq. (2.12) and the resulting expression in eq. (2.10), we get

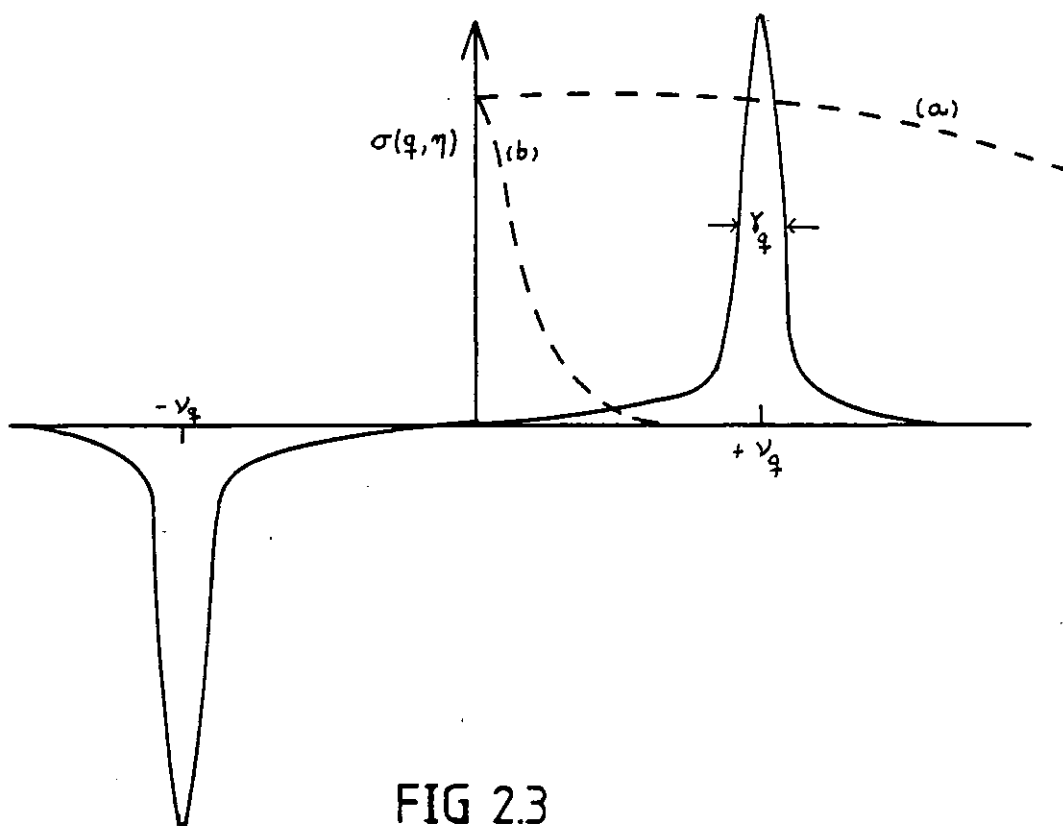


FIG 2.3

Schematic representation of the phonon spectral function. The broken lines are intended to suggest the variation of thermal occupation factors in eq. (2.10') in the limits

$$(a) \quad k_B T > \nu_q$$

$$(b) \quad k_B T \ll \nu_q \quad ; \quad q \equiv k - k'$$

$$\begin{aligned} \Sigma_2(\underline{k}_1, \underline{\epsilon}_1) = & \pi \int \frac{d^3 k_2}{(2\pi)^3} \frac{d^3 k_3}{(2\pi)^3} \frac{8 |M_{\underline{k}_1 - \underline{k}_3}|^4}{v_{\underline{k}_1 - \underline{k}_3}^2} z_{\underline{k}_2} z_{\underline{k}_3} z_{\underline{k}_4} \\ & \times [N(\underline{\epsilon}_1 - \underline{\epsilon}_{\underline{k}_3}) + 1 - f(\underline{\epsilon}_{\underline{k}_3})] [f(\underline{\epsilon}_{\underline{k}_2}) - f(\underline{\epsilon}_{\underline{k}_4})] \delta(\underline{\epsilon}_1 + \underline{\epsilon}_{\underline{k}_2} - \underline{\epsilon}_{\underline{k}_3} - \underline{\epsilon}_{\underline{k}_4}) \end{aligned} \quad (2.15)$$

where $\underline{k}_4 \equiv \underline{k}_1 + \underline{k}_2 - \underline{k}_3$ and the factor $(v_{\underline{k}_1 - \underline{k}_3}^0 / v_{\underline{k}_1 - \underline{k}_3})^2$ is incorporated in $|M_{\underline{k}_1 - \underline{k}_3}^0|^4$ by replacing the unrenormalized phonon energies which appear in the definition of the electron-phonon matrix elements by renormalized ones (Holstein 1964). Using well known transformations of thermal occupation factors one can rewrite eq. (2.15) as

$$\begin{aligned} \Sigma_2(\underline{k}_1, \underline{\epsilon}_1) = & 2\pi \int \frac{d^3 k_2}{(2\pi)^3} \frac{d^3 k_3}{(2\pi)^3} z_2 z_3 z_4 \frac{4 |M_{\underline{k}_1 - \underline{k}_3}|^4}{v_{\underline{k}_1 - \underline{k}_3}^2} \\ & \times [f_2(1-f_3)(1-f_4) + f_3 f_4(1-f_2)] \delta(\underline{\epsilon}_1 + \underline{\epsilon}_{\underline{k}_2} - \underline{\epsilon}_{\underline{k}_3} - \underline{\epsilon}_{\underline{k}_4}) \end{aligned} \quad (2.16)$$

where $f_i \equiv f(\underline{\epsilon}_{\underline{k}_i})$ and $z_i \equiv z_{\underline{k}_i}$.

The reader familiar with the Boltzmann equation will probably recognize in eq. (2.16) the expression one would get for the quasiparticle relaxation rate,

$$\frac{1}{\tau_{\underline{k}_1}(\underline{\epsilon}_1)} \equiv 2 z_{\underline{k}_1} \Sigma_2(\underline{k}_1, \underline{\epsilon}_1) \quad (2.17)$$

from an electron-electron collision integral with a transition probability given by

$$\begin{aligned} \omega(1,2 \rightarrow 3,4) = & \omega^{\uparrow\uparrow}(1,2 \rightarrow 3,4) + \omega^{\uparrow\downarrow}(1,2 \rightarrow 3,4) \\ = & 4\pi \left[\sqrt{z_1 z_2 z_3 z_4} \frac{2 |M_{\underline{k}_1 - \underline{k}_3}|^2}{v_{\underline{k}_1 - \underline{k}_3}} \right]^2 \end{aligned} \quad (2.18)$$

where $\omega^{\uparrow\uparrow}$ and $\omega^{\uparrow\downarrow}$ are the transition probabilities for

parallel and antiparallel spins of \underline{k}_1 and \underline{k}_2 ($\omega^{\uparrow\uparrow} = \omega^{\uparrow\downarrow}$)

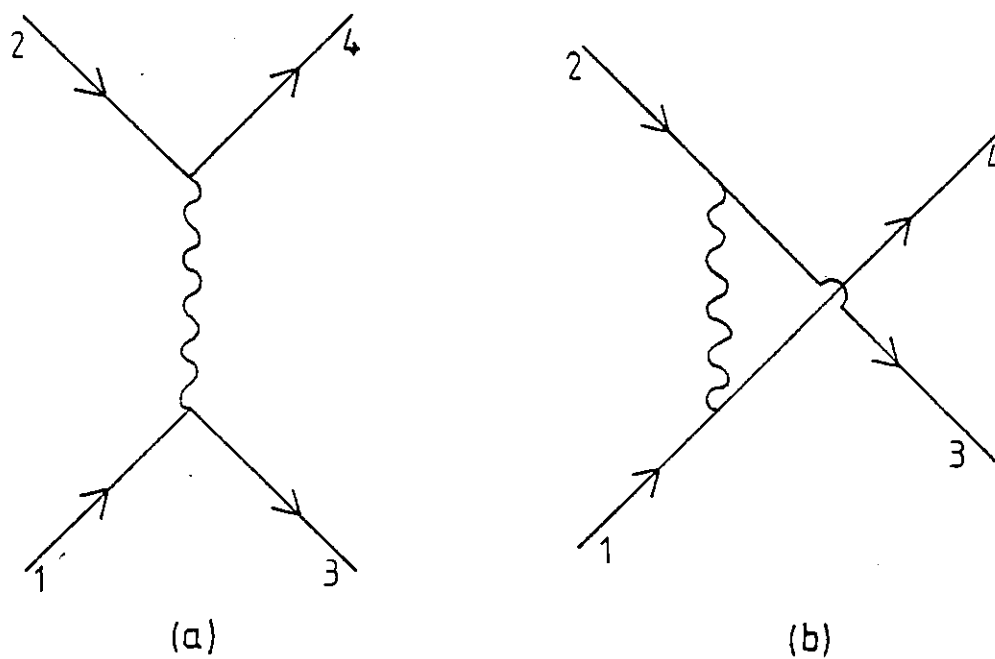
In a Boltzmann equation formulation one generally takes $\xi_i = \epsilon_{\underline{k}_i}$, on the energy shell. Equation (2.17) then describes the effects of a collision of the type illustrated in Fig. 2.4(a) in which the interaction line is obtained by taking the product of two electron-phonon matrix elements, the zero frequency limit of the phonon propagators, and the square roots of the quasiparticle renormalization factors for each of the electronic states involved in the collision. The T^2 dependence of the quasiparticle inverse lifetime is now clearly seen to originate from the well known phase space restrictions on fermion-fermion scattering in a degenerate Fermi Gas (see for instance Baym and Pethick 1978).

However, the attentive reader will have noticed that, although we have derived an analogue of the direct electron-electron collision integral, we have as yet no analogue of the corresponding exchange contribution (Fig. 2.4(b)) which is expected to be of the same order of magnitude. This omission will be rectified in the next paragraph.

2.3 The Exchange Contribution

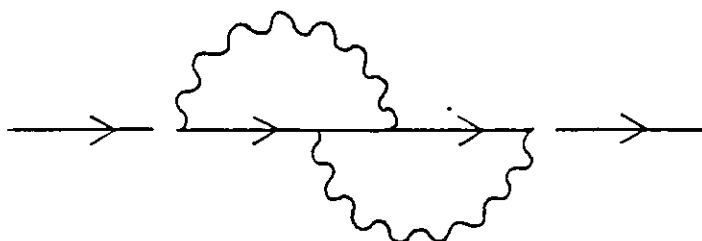
It is clear from the previous analysis that the missing exchange scattering term must come from diagrams which are usually discarded on the basis of Migdal's theorem. We shall now show that it comes from the electron-phonon diagram in Fig. 2.5 and, lest the alarmed reader ask himself, "If the theorem fails, why only this diagram and not all others?", we shall also argue in section 2.4 that this is the only extra diagram needed to lowest order in v_D/ϵ_F . A more conclusive proof may be found in the following chapter.

The full contribution of this diagram is

**FIG 2.4**

Electron-electron interactions

- (a) Direct
- (b) Exchange

**FIG 2.5**

Electron self-energy diagram which is normally ignored on the basis of Migdal's theorem but which is shown to give a T^2 contribution of the same order of magnitude as that given in Fig. 2.2(a).

$$\begin{aligned}
\Sigma(\underline{k}, i\epsilon_1) &= \int \frac{d^3 k_1}{(2\pi)^3} \frac{d^3 k_3}{(2\pi)^3} |M_{\underline{k}_1 - \underline{k}_3}^0|^2 |M_{\underline{k}_3 - \underline{k}_2}^0|^2 \\
&\times \int \frac{d\xi_1}{2\pi} \frac{d\xi_3}{2\pi} \frac{d\xi_4}{2\pi} \frac{d\eta_1}{2\pi} \frac{d\eta_2}{2\pi} \rho(\underline{k}_1, \xi_1) \rho(\underline{k}_3, \xi_3) \rho(\underline{k}_4, \xi_4) \\
&\times \sigma(\underline{k}_1 - \underline{k}_3, \eta_1) \sigma(\underline{k}_3 - \underline{k}_2, \eta_2) \\
&\times \left(\frac{1}{\beta}\right)^2 \sum_{\epsilon_2, \epsilon_3} \frac{1}{i\epsilon_3 - \xi_3} \frac{1}{i(\epsilon_1 - \epsilon_3) - \eta_1} \frac{1}{i\epsilon_2 - \xi_2} \frac{1}{i(\epsilon_1 + \epsilon_2 - \epsilon_3) - \xi_4} \frac{1}{i(\epsilon_3 - \epsilon_2) - \eta_2}
\end{aligned}$$

where $\underline{k}_4 = \underline{k}_1 + \underline{k}_2 - \underline{k}_3$ and the ϵ_i are fermion Matsubara frequencies $\epsilon_i = (2n_i + 1)\pi k_B T$ ($\beta = (k_B T)^{-1}$).

The calculation of the frequency sums is quite straightforward, albeit tedious, but the final result can be cast into a very appealing form. The imaginary part of the self-energy can be written as a sum of terms which can be identified with the various possible scattering events. For example, two of the terms are

$$-\frac{1}{\xi_4 - \xi_1 - \eta_1} \frac{1}{\xi_3 - \xi_2 - \eta_2} \left\{ f_2 (1 - f_3) (1 - f_4) + f_3 f_4 (1 - f_2) \right\} \delta(\xi_1 + \xi_2 - \xi_3 - \xi_4) \quad (2.20a)$$

$$\frac{1}{\xi_3 - \xi_2 - \eta_2} \frac{1}{\xi_4 - \xi_1 - \eta_1} \left\{ (N_2 + 1 - f_2) (N_1 + 1 - f_3) \right\} \delta(\xi_1 - \xi_3 - \eta_1) \quad (2.20b)$$

The term in eq. (2.20a) can be viewed as describing a collision between electrons $1, 2 \rightarrow 3, 4$ whereas the one in eq. (2.20b) corresponds to a one phonon emission/absorption process via an intermediate state involving the emission and

reabsorption of another phonon. Other terms imply scattering into states with one electron plus two phonons and other processes leading finally to one electron and one phonon.

The full contribution corresponding to the term in eq. (2.20a) is

$$\begin{aligned}
 \Sigma_2^{(ex)}(\underline{k}_1, \xi_1) = & -\pi \int \frac{d^3 \underline{k}_2}{(2\pi)^3} \frac{d^3 \underline{k}_3}{(2\pi)^3} |M_{\underline{k}_1 - \underline{k}_3}^0|^2 |M_{\underline{k}_3 - \underline{k}_2}^0|^2 \\
 & \times \int \frac{d\xi_2}{2\pi} \frac{d\xi_3}{2\pi} \frac{d\xi_4}{2\pi} \rho(\underline{k}_2, \xi_2) \rho(\underline{k}_3, \xi_3) \rho(\underline{k}_4, \xi_4) \\
 & \times \int \frac{d\eta_1}{2\pi} \frac{d\eta_2}{2\pi} \sigma(\underline{k}_1 - \underline{k}_3, \eta_1) \sigma(\underline{k}_3 - \underline{k}_2, \eta_2) \frac{1}{\xi_4 - \xi_2 - \eta_1} \frac{1}{\xi_3 - \xi_2 - \eta_2} \\
 & \times [f_2(1-f_3)(1-f_4) + f_3 f_4(1-f_2)] \delta(\xi_1 + \xi_2 - \xi_3 - \xi_4). \quad (2.21)
 \end{aligned}$$

We recall that

$$\rho \int \frac{d\eta}{2\pi} \sigma(q, \eta) \frac{1}{\omega - \eta} = \text{Re } \mathcal{D}(q, \omega) \quad (2.22)$$

where $\mathcal{D}(q, \omega)$ is the (retarded or advanced) phonon propagator. Hence the η_1, η_2 integrations just give a factor

$$\text{Re } \mathcal{D}(\underline{k}_1 - \underline{k}_3, \xi_4 - \xi_2) \text{Re } \mathcal{D}(\underline{k}_3 - \underline{k}_2, \xi_3 - \xi_2) \quad (2.23)$$

The thermal occupation factors and the energy conserving delta function restrict $|\xi_2|, |\xi_3|, |\xi_4| \lesssim \text{Max}\{|\xi_1|, k_B T\}$.

As $\text{Max}\{|\xi_1|, k_B T\} \ll v_D$, for most values of \underline{k}_2 and \underline{k}_3 we have $\text{Max}\{|\xi_1|, k_B T\} \ll v_{\underline{k}_1 - \underline{k}_3}, v_{\underline{k}_3 - \underline{k}_2}$ in which case we can take the zero frequency limit of the phonon propagators in eq.

(2.23). Noting that

$$Re \mathcal{D}(q, 0) = \left(\frac{v_q^0}{v_q} \right) \left(- \frac{z}{v_q} \right) \quad (2.24)$$

we get

$$\begin{aligned} \Sigma_2^{(ex)}(\underline{k}_1, \underline{\xi}_1) &= -\pi \int \frac{d^3 k_2}{(2\pi)^3} \frac{d^3 k_3}{(2\pi)^3} \frac{z |M_{\underline{k}_1 - \underline{k}_3}|^2}{v_{\underline{k}_1 - \underline{k}_3}} \frac{z |M_{\underline{k}_3 - \underline{k}_2}|^2}{v_{\underline{k}_3 - \underline{k}_2}} \\ &\times \int \frac{d\underline{\xi}_2}{(2\pi)} \frac{d\underline{\xi}_3}{(2\pi)} \frac{d\underline{\xi}_4}{2\pi} \rho(\underline{k}_2, \underline{\xi}_2) \rho(\underline{k}_3, \underline{\xi}_3) \rho(\underline{k}_4, \underline{\xi}_4) \\ &\times \left\{ f_2 (1-f_3)(1-f_4) + f_3 f_4 (1-f_2) \right\} \delta(\underline{\xi}_1 + \underline{\xi}_2 - \underline{\xi}_3 - \underline{\xi}_4) \end{aligned} \quad (2.25)$$

where the factors (v_q^0 / v_q) are absorbed in the matrix elements as before.

This expression, apart from the first line, is in fact entirely identical to the contribution calculated in section 2.2. This is easily seen by inserting eq. (2.14) in eq. (2.12) and the resulting expression in eq. (2.1). The arguments we applied to get eq. (2.16) now lead to

$$\begin{aligned} \Sigma_2^{(ex)}(\underline{k}_1, \underline{\xi}_1) &= -\pi \int \frac{d^3 k_2}{(2\pi)^3} \frac{d^3 k_3}{(2\pi)^3} z_2 z_3 z_4 \left\{ \frac{z |M_{\underline{k}_1 - \underline{k}_3}|^2}{v_{\underline{k}_1 - \underline{k}_3}} \frac{z |M_{\underline{k}_3 - \underline{k}_2}|^2}{v_{\underline{k}_3 - \underline{k}_2}} \right\} \\ &\times \left[f_2 (1-f_3)(1-f_4) + f_3 f_4 (1-f_2) \right] \delta(\underline{\xi}_1 + \underline{\xi}_2 - \underline{\xi}_3 - \underline{\xi}_4) \end{aligned} \quad (2.26)$$

which is precisely the exchange partner of eq. (2.16).

The sum of these two contributions to the quasiparticle relaxation rate is

$$\begin{aligned}
\frac{1}{\tau_{\underline{k}_1}(\xi_1)} &\equiv \sum_{\underline{z}_1, \underline{z}_2} Z_2(\underline{k}_1, \xi_1) \\
&= 2\pi \int \frac{d^3 \underline{k}_2}{(2\pi)^3} \frac{d^3 \underline{k}_3}{(2\pi)^3} \sum_{\underline{z}_1, \underline{z}_2, \underline{z}_3, \underline{z}_4} \left\{ 2 \left[\frac{2 |M_{\underline{k}_1 - \underline{k}_3}|^2}{v_{\underline{k}_1 - \underline{k}_3}} \right]^2 - \frac{2 |M_{\underline{k}_1 - \underline{k}_2}|^2}{v_{\underline{k}_1 - \underline{k}_2}} \frac{2 |M_{\underline{k}_3 - \underline{k}_2}|^2}{v_{\underline{k}_3 - \underline{k}_2}} \right\} \\
&\quad \times \left[f_{\underline{z}_1} (1 - f_{\underline{z}_3}) (1 - f_{\underline{z}_4}) + f_{\underline{z}_3} f_{\underline{z}_4} (1 - f_{\underline{z}_2}) \right] \delta(\xi_1 + \epsilon_{\underline{k}_1} - \epsilon_{\underline{k}_2} - \epsilon_{\underline{k}_3} - \epsilon_{\underline{k}_4})
\end{aligned} \tag{2.27}$$

The effective transition probability (summed over the spins of \underline{k}_2 , \underline{k}_3 and \underline{k}_4) is

$$\omega(12 \rightarrow 34) = 2\pi \sum_{\underline{z}_1, \underline{z}_2, \underline{z}_3, \underline{z}_4} \left\{ 2 \left[\frac{2 |M_{\underline{k}_2 - \underline{k}_3}|^2}{v_{\underline{k}_2 - \underline{k}_3}} \right]^2 - \frac{2 |M_{\underline{k}_1 - \underline{k}_3}|^2}{v_{\underline{k}_1 - \underline{k}_3}} \frac{2 |M_{\underline{k}_1 - \underline{k}_2}|^2}{v_{\underline{k}_3 - \underline{k}_2}} \right\} \tag{2.28}$$

This can be written as (Baym and Pethick 1978)

$$\omega(12 \rightarrow 34) = \frac{1}{2} \omega^{\uparrow\uparrow}(1,2 \rightarrow 3,4) + \omega^{\uparrow\downarrow}(1,2 \rightarrow 3,4) \tag{2.29}$$

where $\omega^{\uparrow\uparrow}$ and $\omega^{\uparrow\downarrow}$, the scattering probabilities for spin 1 and 2 parallel and antiparallel, are given by

$$\omega^{\uparrow\uparrow} = 2\pi \left[\sqrt{\sum_{\underline{z}_1, \underline{z}_2, \underline{z}_3, \underline{z}_4} \left(2 \frac{|M_{\underline{k}_1 - \underline{k}_3}|^2}{v_{\underline{k}_1 - \underline{k}_3}} - 2 \frac{|M_{\underline{k}_1 - \underline{k}_2}|^2}{v_{\underline{k}_1 - \underline{k}_2}} \right)} \right]^2 \tag{2.30a}$$

$$\omega^{\uparrow\downarrow} = 2\pi \left[\sqrt{\sum_{\underline{z}_1, \underline{z}_2, \underline{z}_3, \underline{z}_4} \frac{|M_{\underline{k}_1 - \underline{k}_3}|^2}{v_{\underline{k}_1 - \underline{k}_3}}} \right]^2 \tag{2.30b}$$

The factor $\frac{1}{2}$ in eq. (2.29) accounts for the fact that we must only sum over distinguishable states of the electrons 3 and 4. In eqs. (2.30) we also used the conservation of momentum $\underline{k}_3 - \underline{k}_2 = \underline{k}_1 - \underline{k}_4$ and invariance under permutation of \underline{k}_3 and \underline{k}_4 in the integral in eq. (2.27). Equations (2.30) are the ones proposed by MacDonald, Taylor and Geldart (1981), except

for the quasiparticle renormalization factors.

The integral in the right hand side of eq. (2.30) is discussed in detail in Baym and Pethick (1978). The thermal occupation factors and the delta-function restrict $|\epsilon_{\underline{k}_2}|, |\epsilon_{\underline{k}_3}|, |\epsilon_{\underline{k}_4}| \lesssim \text{Max}\{|\xi_1|, k_B T\}$ hence for $|\xi_1| \ll k_B T$ we obtain a $k_B T$ factor for each of the $\epsilon_{\underline{k}_2}, \epsilon_{\underline{k}_3}$ integrations. The geometry of the scattering is illustrated in Fig. 2.6. The momenta have all modules k_F to within correction of order $k_B T$. The angle θ_3 between \underline{k}_3 and the total momentum is fixed by momentum conservation to be $\theta_3 \approx \theta/2$ where θ is the angle between \underline{k}_1 and \underline{k}_2 . Thus the scattering probability becomes a function of the angle θ and φ - the angle between the planes of the initial and final momenta.

The result one obtains is then, for $|\xi_1| \ll k_B T$,

$$\frac{1}{\tau_{k_F}(T)} = \frac{\pi^2}{2} \frac{n_0^2}{8\epsilon_F} (k_B T)^2 \int \frac{d\Omega}{4\pi} \frac{\omega(\theta, \varphi)}{\cos\theta/2} \quad (2.31)$$

Recalling that $n_0 |M_{\underline{k}, \underline{k}'}|^2 / v_{\underline{k}, \underline{k}'}$ is of order one for most metals, we can estimate this term to be of order

$$\frac{1}{\tau_{k_F}(T)} \sim \left(\frac{k_B T}{\epsilon_F}\right)^2 \sim \frac{v_D^2}{\epsilon_F} \left(\frac{T}{\theta_D}\right)^2 \quad (2.32)$$

We see then that this contribution from virtual phonon exchange dominates real phonon scattering ($\sim (T/\theta_D)^3 v_D$) for $T < (v_D/\epsilon_F) \theta_D$, i.e. for temperatures below a few percent of the Debye temperature.

It remains to be shown that the other terms arising from the diagram of Fig. 2.5 are small. For purposes of illustration we consider the one-phonon term in eq. (2.20b).

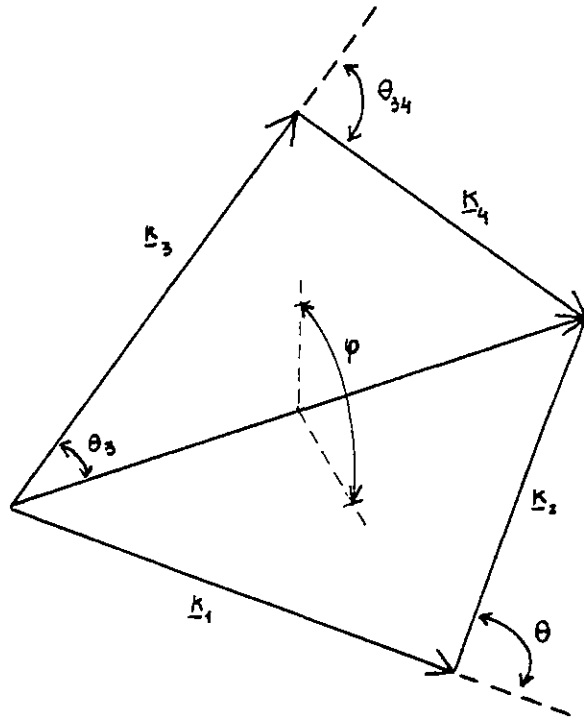


FIG 2.6

Geometry of an electron-electron scattering event in a degenerate Fermi gas. Conservation of energy and the Fermi exclusion principle restrict all momenta to the vicinity of k_F . Conservation of momenta then imposes $\theta_3 \sim \theta_{34}/2 \sim \theta/2$.

$$Z_2(\underline{k}_1, \underline{\xi}_1)$$

$$\propto \int \frac{d^3 k_3}{(2\pi)^3} \frac{d\underline{\xi}_3}{2\pi} \frac{d\eta_1}{2\pi} |M_{\underline{k}_3, -\underline{k}_3}^0|^2 \rho(\underline{k}_3, \underline{\xi}_3) \sigma(\underline{k}_1 - \underline{k}_3, \eta_1) [N_1 + 1 - f_3] \delta(\underline{\xi}_1 - \underline{\xi}_3 - \eta_1)$$

$$\times \left\{ \int \frac{d^3 k_2}{(2\pi)^3} \frac{d\underline{\xi}_2}{2\pi} \frac{d\underline{\xi}_4}{2\pi} \frac{d\eta_2}{2\pi} \rho(\underline{k}_2, \underline{\xi}_2) \sigma(\underline{k}_3 - \underline{k}_2, \eta_2) \rho(\underline{k}_4, \underline{\xi}_4) |M_{\underline{k}_3 - \underline{k}_4}^0| \right.$$

$$\times \left. \frac{1}{\underline{\xi}_4 - \underline{\xi}_2 - \eta_1} \frac{N_2 + 1 - f_2}{\underline{\xi}_3 - \underline{\xi}_2 - \eta_2} \right\}. \quad (2.33)$$

The term outside the curly brackets is identical to that found in eq. (2.1) for Fig. 2.2(a). We compare the term in curly brackets with unity which appears in its place in eq. (2.1). Doing the $\underline{\xi}_4$ integration we get for this term

$$\left\{ \dots \right\} = \int \frac{d^3 k_2}{(2\pi)^3} \frac{d\underline{\xi}_2}{2\pi} \frac{d\eta_2}{2\pi} |M_{\underline{k}_3 - \underline{k}_2}^0|^2 \rho(\underline{k}_2, \underline{\xi}_2) \sigma(\underline{k}_3 - \underline{k}_2, \eta_2)$$

$$\times \frac{N_2 + 1 - f_2}{\underline{\xi}_3 - \underline{\xi}_2 - \eta_2} \left[-\text{Re } G(\underline{k}_4, \underline{\xi}_2 + \eta_1) \right]$$

where G is the electronic Green function. Apart from the factor $-\text{Re } G(\underline{k}_4, \underline{\xi}_2 + \eta_1)$ this is just the real part of the self-energy $Z_1(\underline{k}_3, \underline{\xi}_3)$ as calculated from the diagram of section 2.2. For most values of $\underline{k}_2, \underline{k}_3$ we have

$$\omega_{\underline{k}_1 + \underline{k}_2 - \underline{k}_3} \sim \epsilon_F \quad \text{and so}$$

$$\text{Re } G(\underline{k}_1 + \underline{k}_2 - \underline{k}_3, \underline{\xi}_2 + \eta_1) \sim \frac{1}{\epsilon_F}$$

and we estimate this factor to be of order

$$\left\{ \dots \right\} \sim Z_1(\underline{k}_3, \underline{\xi}_3) \frac{1}{\epsilon_F} \sim \frac{v_D}{\epsilon_F} \ll 1$$

In fact, what we have just calculated is the lowest order vertex correction (see Fig. 2.1(b)) and so, on the basis of usual beliefs, it is not surprising that it is of order v_D/ϵ_F . But, as we have seen, not all contributions from the diagram

of Fig. 2.5 are negligible at low temperatures. In the next paragraph we discuss more carefully our choice of diagrams and give what we believe to be the correct statement of Migdal's theorem.

2.4 Physical Interpretation

The quasiparticle scattering rate may be viewed as made up of a sum of transition probabilities of the injected electron plus background into all possible final states - one electron and one phonon, one electron and two phonons, electron and electron-hole pair, etc. The contribution of any diagram to the imaginary part of the self-energy breaks up into a sum of terms, each involving an energy conserving delta-function and appropriate thermal occupation factors that identify the corresponding scattering process. In the self-energy diagrams these final scattering states appear as intermediate states for one or more of the possible time orderings. There is a subtlety involved in the use of renormalized propagators insofar as the intermediate states involved may not be obvious from the diagrams. For instance, we saw mathematically in section 2.2 that the diagram of Fig. 2.2(a) includes, as effective scattered final states, ones containing an electron plus electron-hole pair. This becomes pictorially more apparent if we consider one of the unrenormalized diagrams making up Fig. 2.2(a); this is done in Fig. 2.7.

Indeed, the dominant processes at low temperatures are precisely the ones corresponding to final states with an electron plus an electron-hole pair, just as for direct electron-electron scattering. The diagram of Fig. 2.7 describes such a process mediated by the exchange of a renormalized phonon with bare vertices. We can draw the diagram of Fig. 2.5 in a way that

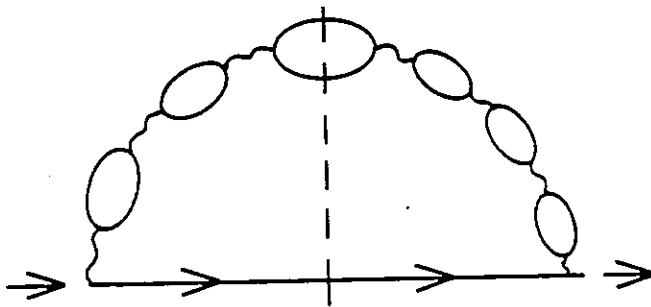


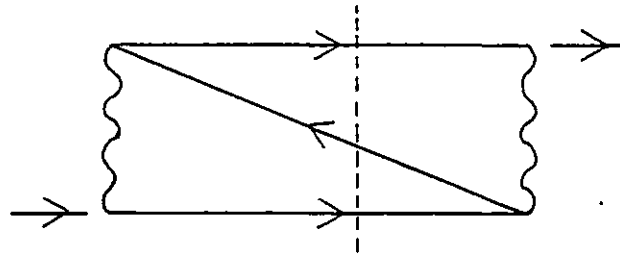
FIG 2.7

Electron self-energy diagram included in the renormalized diagram of Fig. 2.2(a) but drawn to emphasize the inclusion of an intermediate state having one electron and an electron-hole pair. The phonon lines are unrenormalized in this figure.

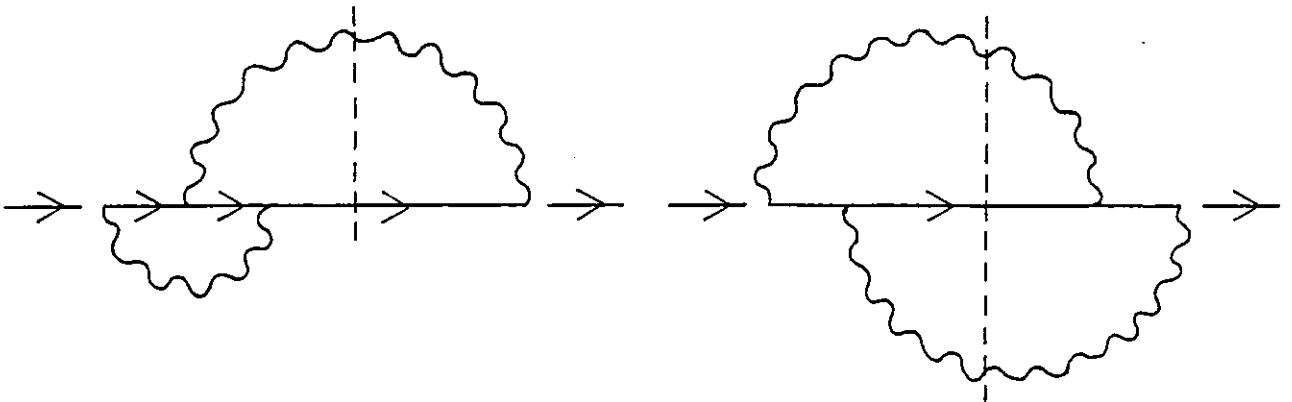
shows that it also includes the same type of process and so should be of the same order (Fig. 2.8(a)). As we have already noted, the diagram of Fig. 2.5 also includes other contributions arising from scattering to different final states - one electron plus phonon, one electron plus two phonons, etc. - see Figs. 2.8(b) and 2.8(c). These contributions are, however, of higher order in T or have vertex insertions which reduce their value by a factor v_D/ϵ_F . For example, the one-phonon term we analysed in section 2.3 does give a T^2 contribution (the term outside curly brackets in eq. (2.33) is identical to the term calculated in section 2.2) but the electron-electron effective interaction now contains a vertex insertion, so this term is of order $(v_D/\epsilon_F)^2 (T/\theta_D)^2 v_D$.

In the following chapter we shall carry these considerations a little further and include also Coulomb interactions. We shall see that eq. (2.27) does give the dominant low temperature contribution to the quasiparticle inverse lifetime to within corrections smaller by a factor v_D/ϵ_F .

At this point we would like to stress that the quasiparticle inverse lifetime, although strictly an equilibrium quantity, can be calculated from a transport equation by linearizing the collision integral about a change in occupation of a single state. We noted before that eq. (2.27) is exactly what we would obtain from an electron-electron collision integral. It is quite certain that if we were to derive a transport equation in the manner of Kadanoff and Baym (1963) we would obtain a Boltzmann equation in which, as well as the usual electron-phonon collision integral (Prange and Kadanoff 1964) arising from the on shell part of $\sigma(q, \eta)$, $\eta \approx \pm v_q$ there would be an effective electron-electron collision integral with a phonon exchange term arising from the low frequency,



(a)



(b)

(c)

FIG 2.8

Diagram of Fig. 2.5 redrawn in various ways to emphasize several possible final states:

- (a) Electron plus electron-hole pair
- (b) Electron plus phonon
- (c) Electron plus two phonons

off-shell region of $\sigma(q, \eta)$, $|\eta| \ll v_q$ in the diagram of Fig. 2.2(a) and from the diagram of Fig. 2.5. In the presence of Umklapp scattering - our results would certainly go through with minor modifications - such a term would contribute to the usual electron-electron T^2 contribution to the resistivity as MacDonald suggested.

CHAPTER 3

DIRECT AND PHONON MEDIATED INTERACTIONS

It was shown in the previous chapter that, at low temperatures, the dominant contribution to the electronic quasiparticle relaxation rate, due to electron-phonon interactions, is due to scattering into states with one electron plus a single electron-hole pair, mediated by the exchange of a virtual phonon. The same scattering processes are known to be dominant for direct electron-electron interactions. We shall use this fact to derive a formal expression for the effective electron-electron scattering probability in the presence of Coulomb and electron-phonon interactions.

3.1 The Scattering Amplitude and the Four-point Vertex Function

The contribution of any diagram to the imaginary part of the electronic self-energy is a sum of terms corresponding to each of the intermediate states contained in the diagram. These states are defined as sets of propagators, such that, when cut, the diagram falls into two - only two - parts, each linked to one of the external vertices. The contribution of each such intermediate state is identified by a delta-function which conserves energy between the initial single particle state plus background and the intermediate state itself (for proof of this see Langer (1961) or Appendix B). To obtain the dominant low temperature behaviour of the quasiparticle relaxation rate we need to isolate the terms arising from the intermediate states with one electron and an electron-hole pair. A general diagram with such a state is shown in Fig. 3.1. We assume now

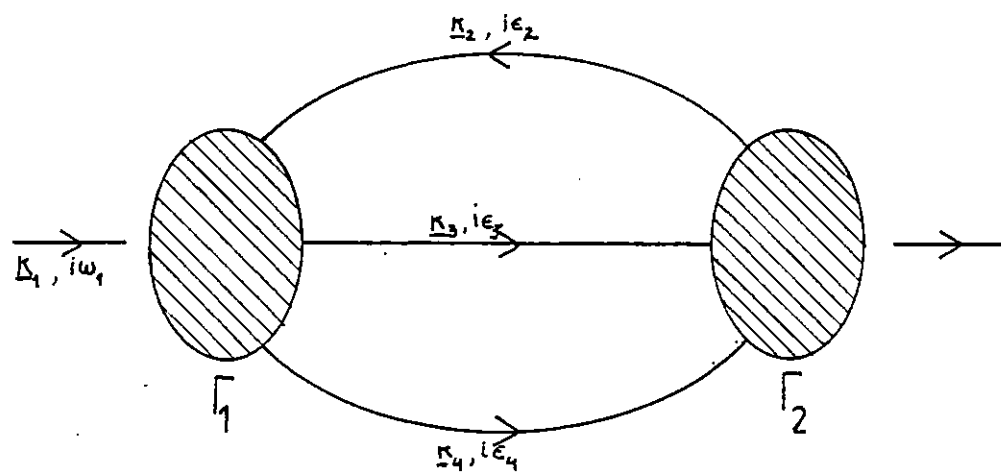


FIG 3.1

A general diagram with an intermediate state with an electron and an electron-hole pair. By conservation of frequency and momentum $\omega_1 + \epsilon_2 - \epsilon_3 - \epsilon_4 = 0$ and $\underline{k}_1 + \underline{k}_2 = \underline{k}_3 + \underline{k}_4$.

that the phonon lines are unrenormalized so that all such states appear explicitly in the diagram; electron propagators, however, are fully renormalized as before. We label the three propagators of the intermediate state with different Matsubara frequencies and ensure frequency conservation with the Kronecker delta $\delta_{\omega_1 + \epsilon_2 - \epsilon_3 - \epsilon_4, 0}$

The frequency sums to be performed have the form

$$S = (-) \left(\frac{1}{\beta}\right)^3 \sum_{\{\epsilon\}} T_1(i\omega_1, \{\epsilon\}) T_2(i\omega_1, \{\epsilon\}) \times \frac{1}{i\epsilon_2 - \xi_2} \frac{1}{i\epsilon_3 - \xi_3} \frac{1}{i\epsilon_4 - \xi_4} \beta \delta_{\omega_1, \epsilon_2 - \epsilon_3 - \epsilon_4} \quad (3.1)$$

where T_1 and T_2 are products of energy denominators which are linear combinations, with coefficients 0, ± 1 , of the external frequency $i\omega_1$, $\{\epsilon\} \equiv \{\epsilon_2, \epsilon_3, \epsilon_4\}$ and the spectral frequencies of the propagators occurring in the diagrams Γ_1 and Γ_2 . These are obtained from the original diagram by deleting the three propagators of the intermediate state. When we sum over the frequencies $\{\epsilon\}$ by the usual method of contour integration we pick up contributions from the poles which are explicitly displayed in eq. (3.1) and from the poles in T_1 and T_2 . We shall see that the former give the term associated with this intermediate state. Denoting their contribution by S' ,

$$S' = (-) \left(\frac{1}{\beta}\right)^3 \sum_{\{\epsilon\}} T_1 T_2 \times \int_0^\beta d\tau e^{i\omega_1 \tau} \frac{e^{i\epsilon_2 \tau}}{i\epsilon_2 - \xi_2} \frac{e^{-i\epsilon_3 \tau}}{i\epsilon_3 - \xi_3} \frac{e^{-i\epsilon_4 \tau}}{i\epsilon_4 - \xi_4} \quad (3.2)$$

where we used

$$\beta \delta_{\nu_{n,0}} = \int_0^\beta d\tau e^{i\nu_n \tau}$$

ν_n being a boson Matsubara frequency. The frequency summation is now straightforward,

$$\begin{aligned} S' &= (-) T_1(i\omega_1, \{\xi\}) T_2(i\omega_1, \{\xi\}) \\ &\times \int_0^\beta e^{(i\omega_1 + \xi_2 - \xi_3 - \xi_4)\tau} f(\xi_2) [1 - f(\xi_3)] [1 - f(\xi_4)] \\ &= (-) T_1(i\omega_1, \{\xi\}) T_2(i\omega_1, \{\xi\}) \frac{e^{(i\omega_1 + \xi_2 - \xi_3 - \xi_4)\beta} - 1}{i\omega_1 + \xi_2 - \xi_3 - \xi_4} \quad (3.4) \\ &\times f_2 (1 - f_3) (1 - f_4) . \end{aligned}$$

Using

$$\begin{aligned} e^{i\omega_1 \beta} &= -1 \\ e^{\beta \xi} f(\xi) &= 1 - f(\xi) \end{aligned}$$

one obtains

$$\begin{aligned} S' &= T_1(i\omega_1, \{\xi\}) T_2(i\omega_1, \{\xi\}) \\ &\times \frac{f_2(1-f_3)(1-f_4) + f_3 f_4 (1-f_2)}{i\omega_1 + \xi_2 - \xi_3 - \xi_4} \quad (3.5) \end{aligned}$$

It is important to note that no other contribution to S contains the energy denominator $i\omega_1 + \xi_2 - \xi_3 - \xi_4$. If, in

the frequency sums in eq. (3.1) we pick one of the poles in T_1 or T_2 we cannot generate a denominator which only involves the external frequency and the three spectral frequencies ξ_2, ξ_3 and ξ_4 . And, in S' this energy denominator does not occur either in $T_1 (i\omega_1, \{\xi\})$ or $T_2 (i\omega_1, \{\xi\})$ because all the energy denominators in T_1 and T_2 contain at least another spectral frequency.

We conclude then that the total contribution to the imaginary part of the self-energy associated with the intermediate state shown is

$$\begin{aligned} \sum^{(S')}(\underline{k}_1, \xi_1) &= \pi \int \frac{d^3 k_2}{(2\pi)^3} \frac{d^3 k_3}{(2\pi)^3} \int \frac{d\xi_2}{2\pi} \frac{d\xi_3}{2\pi} \frac{d\xi_4}{2\pi} \\ &\times Re \Gamma_1(\underline{k}_1, \xi_1; \underline{k}_2, \xi_2; \underline{k}_3, \xi_3; \underline{k}_4, \xi_4) Re \Gamma_2(\underline{k}_3, \xi_3, \underline{k}_4, \xi_4; \underline{k}_1, \xi_1, \underline{k}_2, \xi_2) \\ &\times \rho(\underline{k}_2, \xi_2) \rho(\underline{k}_3, \xi_3) \rho(\underline{k}_4, \xi_4) \\ &\times [f_2(1-f_3)(1-f_4) + f_3 f_4(1-f_2)] \delta(\xi_1 + \xi_2 - \xi_3 - \xi_4) \end{aligned} \quad (3.6)$$

where $\underline{k}_4 \equiv \underline{k}_1 + \underline{k}_2 - \underline{k}_3$; $\Gamma_1(\underline{k}_i, \xi_i)$ and $\Gamma_2(\underline{k}_i, \xi_i)$ are the contributions to the electronic four-point function from the diagrams Γ_1 and Γ_2 after the external frequencies are continued to real values $i\epsilon_i \rightarrow \xi_i$. It is convenient at this point to write the spin sums explicitly. We assume that spin σ_1 of the incoming particle with momentum \underline{k}_1 is up (the result is independent of σ_1). By conservation of spin if σ_2 is up, so are σ_3 and σ_4 . If σ_1 and σ_2 are anti-parallel, so are σ_3 and σ_4 . Writing the spin sums explicitly only changes the Γ_1, Γ_2 factors in eq. (3.6) which now read

$$\begin{aligned}
\text{Re } \Gamma_1 \text{ Re } \Gamma_2 \longrightarrow & \text{Re } \Gamma_1^{\uparrow\uparrow}(\underline{k}_i, \xi_i) \text{ Re } \Gamma_2^{\uparrow\uparrow}(\underline{k}_i, \xi_i) \\
& + \text{Re } \Gamma_1^{\uparrow\downarrow}(\underline{k}_i, \xi_i) \text{ Re } \Gamma_2^{\uparrow\downarrow}(\underline{k}_i, \xi_i)
\end{aligned} \tag{3.7}$$

where the arrows denote the spins of the incoming electrons in each of Γ_1 and Γ_2 .

Summing over all intermediate states of this type is equivalent to summing over all Γ_1 and Γ_2 . The result is

$$\begin{aligned}
\Sigma_2(\underline{k}_1, \xi_1) = & \frac{1}{2} \int \frac{d^3 k_2}{(2\pi)^3} \frac{d^3 k_3}{(2\pi)^3} \frac{d\xi_2}{2\pi} \frac{d\xi_3}{2\pi} \\
& \times \left\{ \frac{1}{2} \left(\text{Re } \Gamma^{\uparrow\uparrow}(\underline{k}_i, \xi_i) \right)^2 + \left(\text{Re } \Gamma^{\uparrow\downarrow}(\underline{k}_i, \xi_i) \right)^2 \right\} \\
& \times \rho(\underline{k}_1, \xi_1) \rho(\underline{k}_2, \xi_2) \rho(\underline{k}_3, \xi_3) \rho(\underline{k}_4, \xi_4) \\
& \times \left[f_2 (1-f_3)(1-f_4) + f_3 f_4 (1-f_2) \right]
\end{aligned} \tag{3.8}$$

where $\xi_4 \equiv \xi_1 + \xi_2 - \xi_3$ and $\Gamma^{\sigma_1 \sigma_2}(\underline{k}_1, \xi_1; \underline{k}_2, \xi_2; \underline{k}_3, \xi_3; \underline{k}_4, \xi_4)$ is the electronic four-point function with the external Matsubara frequencies analytically continued to real values. It is defined as the sum of all Feynman diagrams with four external electron lines. External lines, external momentum and frequency conserving delta functions are excluded from the definition of $\Gamma(\underline{k}_i, \xi_i)$ (see Fig. 3.2). The 1/2 factor in the parallel spin term accounts for the fact that exchanging the intermediate electron lines 3,4 in both four-point functions leads to the same self-energy diagram. Permuting these lines in the case of antiparallel spin leads to a diagram which violates spin conservation. We also used the relation

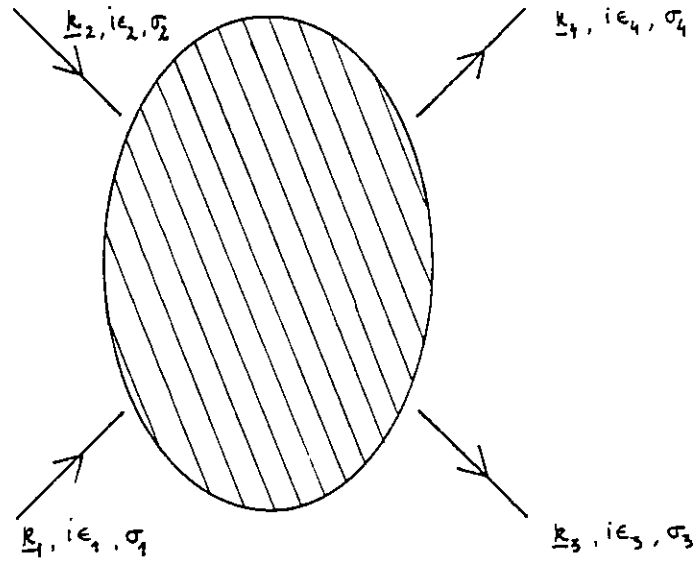


FIG 3.2

The four point vertex function $\Gamma^{\sigma_1 \sigma_2}(\underline{k}_1, i\epsilon_1; \underline{k}_2, i\epsilon_2; \underline{k}_3, i\epsilon_3; \underline{k}_4, i\epsilon_4)$

By conservation of momentum frequency and spin, $\underline{k}_1 + \underline{k}_2 = \underline{k}_3 + \underline{k}_4$,

$$\epsilon_1 + \epsilon_2 = \epsilon_3 + \epsilon_4, \quad \sigma_1 + \sigma_2 = \sigma_3 + \sigma_4.$$

$$\text{Re } \Gamma(1, 2 \rightarrow 3, 4) = \text{Re } \Gamma(3, 4 \rightarrow 1, 2)$$

which is guaranteed by time reversal symmetry.

The four-point vertex function is well behaved and slowly varying for frequencies close to zero (the fermi energy). Hence, to find the dominant, low temperature, low frequency behaviour of $\Sigma_2(\underline{k}, \xi)$, we may use the quasiparticle approximation for the spectral functions (eq. (2.4)). This is justified by arguments similar to those presented in Chapter 2. We obtain for the relaxation rate

$$\begin{aligned} \frac{1}{\tau_{\underline{k}_i}(\xi_i)} &= 2\pi \int \frac{d^3 k_2}{(2\pi)^3} \frac{d^3 k_3}{(2\pi)^3} \\ &\times z_1 z_2 z_3 z_4 \left\{ \frac{1}{2} \left(\text{Re } \Gamma^{\uparrow\uparrow}(\underline{k}_i, \epsilon_{\underline{k}_i}) \right)^2 + \left(\text{Re } \Gamma^{\uparrow\downarrow}(\underline{k}_i, \epsilon_{\underline{k}_i}) \right)^2 \right\} \\ &\times \left[f_1 (1-f_3)(1-f_4) + f_3 f_4 (1-f_2) \right] \\ &\times \delta(\xi_i + \epsilon_{\underline{k}_2} - \epsilon_{\underline{k}_3} - \epsilon_{\underline{k}_4}) \end{aligned} \quad (3.9)$$

where, now $f_i \equiv f(\epsilon_{\underline{k}_i})$.

We recognize again the familiar structure of the Boltzmann electron-electron collision integral with a transition probability given by

$$\omega^{\sigma_1 \sigma_2}(1, 2 \rightarrow 3, 4) = 2\pi \left(\sqrt{z_1 z_2 z_3 z_4} \Gamma^{\sigma_1 \sigma_2}(\underline{k}_i, \epsilon_{\underline{k}_i}) \right)^2 \quad (3.10)$$

This identification of the scattering amplitude with the four-point vertex function for electron-electron interactions can be found in Nozières (1964) or AGD where it is derived by completely different methods. To the best of our knowledge an explicit derivation of eq. (3.9) with electron-phonon interaction

included has not been presented before.

3.2 The Scattering Amplitude and Migdal's Theorem

The remaining task is to calculate the four-point vertex function $\Gamma^{\sigma_1\sigma_2}(\underline{k}_i, \epsilon_{\underline{k}_i})$. Fortunately this has already been done by Rice (1968) and Prange and Sachs (1967).

Rice defines $\Gamma^{\sigma_1\sigma_2}(\underline{k}_i, \epsilon_{\underline{k}_i})$ as the sum of a Coulomb term (all diagrams with no phonon lines) and a phonon term (all diagrams that include at least one phonon line). He then uses arguments similar to those used by Migdal in his calculation of vertex corrections, to show that the phonon term is given by the diagrams of Fig. 3.3, i.e. a single renormalized phonon propagator with electron-phonon vertices renormalized with respect to Coulomb interactions.

Hence

$$\text{Re } \Gamma_{\text{el-ph}}^{\uparrow\uparrow} = - \left(\frac{2 |M_{\underline{k}_1 - \underline{k}_3}|^2}{v_{\underline{k}_1 - \underline{k}_3}} - \frac{2 |M_{\underline{k}_1 - \underline{k}_4}|^2}{v_{\underline{k}_1 - \underline{k}_4}} \right) \quad (3.11a)$$

$$\text{Re } \Gamma_{\text{el-ph}}^{\uparrow\downarrow} = - \left(\frac{2 |M_{\underline{k}_1 - \underline{k}_3}|^2}{v_{\underline{k}_1 - \underline{k}_3}} \right) \quad (3.11b)$$

where we have taken the limit $\epsilon_{\underline{k}_i} \rightarrow 0$ which is a valid approximation given that we are interested in the dominant low temperature behaviour. Note that for electron-phonon interactions alone this result is what we found in Chapter 2 (see eqs. (2.30)). It should be said that nothing in our analysis suggests that Migdal's arguments should fail, in the estimation of corrections to the four-point function, as they do in the calculation of the self-energy. The problem with the latter one is that sufficient account of the dominant type of scattering events was not taken. When that is done it becomes very clear that the diagram of

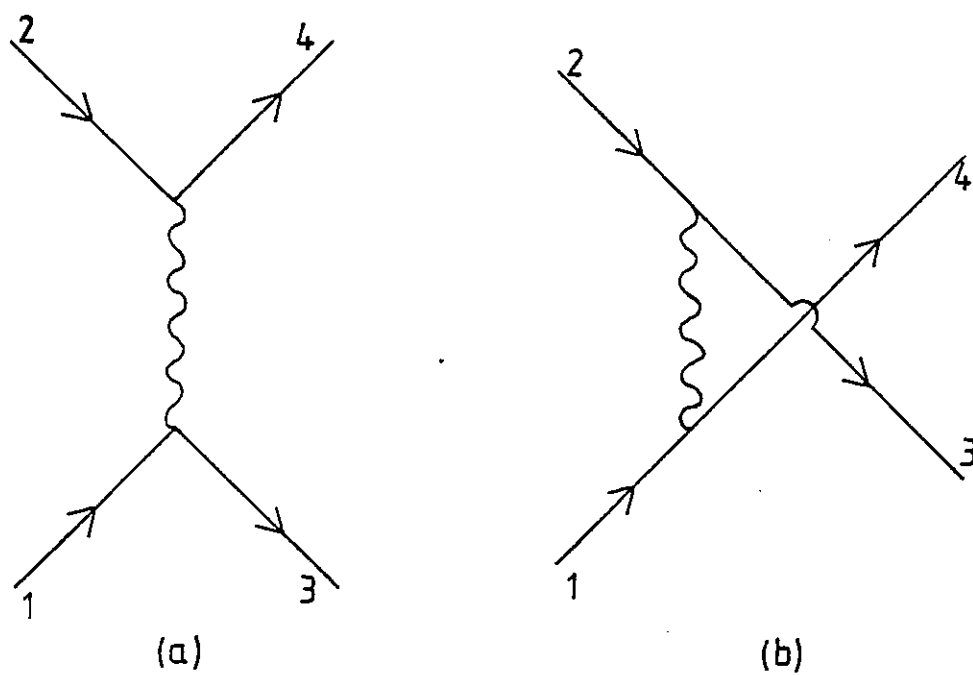


FIG 3.3

The electron-phonon contribution to the four-point vertex function $\Gamma^{\sigma_1, \sigma_2}(1, 2; 3, 4)$ to lowest order in γ_D/ϵ_F For antiparallel spins only one term is present.

Fig. 2.5 is in fact of the same order as that of Fig. 2.2(a).

Unfortunately, for the Coulomb term, no reasonable expansion parameter, such as v_D / ϵ_F , exists. The usual approximation is to take for the four-point vertex function the Thomas-Fermi potential

$$\text{Re } \Gamma_{\text{Coulomb}}^{\uparrow\uparrow}(1,2 \rightarrow 3,4) = V_{\text{TF}}(\underline{k}_1 - \underline{k}_3) - V_{\text{TF}}(\underline{k}_1 - \underline{k}_4) \quad (3.12a)$$

$$\text{Re } \Gamma_{\text{Coulomb}}^{\uparrow\downarrow}(1,2 \rightarrow 3,4) = V_{\text{TF}}(\underline{k}_1 - \underline{k}_3) \quad (3.12b)$$

where

$$V_{\text{TF}}(q) = \frac{4\pi a^2}{q^2 + \kappa^2}$$

where κ^{-1} is the Debye screening radius ($\kappa^2 = 8\pi n_0 e^2$).

The full scattering probability is then

$$\begin{aligned} \omega^{\uparrow\uparrow}(1,2 \rightarrow 3,4) = 2\pi \left\{ \sqrt{z_1 z_2 z_3 z_4} \left[(V_{\text{TF}}(\underline{k}_1 - \underline{k}_3) - V_{\text{TF}}(\underline{k}_1 - \underline{k}_4)) \right. \right. \\ \left. \left. - \left(\frac{z |m_{\underline{k}_1 - \underline{k}_3}|^2}{v_{\underline{k}_1 - \underline{k}_3}} - \frac{z |m_{\underline{k}_1 - \underline{k}_4}|^2}{v_{\underline{k}_1 - \underline{k}_4}} \right) \right] \right\}^2 \end{aligned} \quad (3.13a)$$

$$\omega^{\uparrow\downarrow}(1,2 \rightarrow 3,4) = 2\pi \left\{ \sqrt{z_1 z_2 z_3 z_4} \left[V_{\text{TF}}(\underline{k}_1 - \underline{k}_3) - z \frac{|m_{\underline{k}_1 - \underline{k}_3}|^2}{v_{\underline{k}_1 - \underline{k}_3}} \right] \right\}^2 \quad (3.13b)$$

The Coulomb and the phonon exchange interaction appear with opposite signs because the first is repulsive and the latter is attractive. Equations (3.13) apart from the quasiparticle renormalization factors are the ones proposed by MacDonald, Taylor and Geldart (1981). These factors contain Coulomb and electron-

phonon contributions.

In conclusion we would say that while we cannot comment on the accuracy of the calculations of MacDonald and co-workers we find that the physical ideas behind them are physically sound and perfectly justified from a microscopic point of view.

CHAPTER 4

WEAK LOCALIZATION AND QUASIPARTICLE LIFETIMES IN

TWO DIMENSIONAL METALS

4.1 Introduction

It has been known for some time that static impurity scattering can alter the electron-electron and electron-phonon scattering rates in metals (Schmid 1973, 1974; Keck and Schmid 1976; Bergmann 1971; Al'tschuler 1978; Al'tschuler and Aronov 1979).

As was discussed in the previous chapters, in clean metals the electron-electron scattering rate, at low temperatures, is of order $(k_B T)^2 / \epsilon_F$. Schmid (1974) showed that in the presence of static impurity scattering one obtains an additional correction which varies as $T^{3/2}$ and dominates the previous term at low enough temperatures. Though very interesting, this result failed to arouse attention, possibly because the inelastic scattering rate was not directly accessible to experimental measurement, more likely because physicists' minds were turned elsewhere.

However, recent advances in the theory of weakly disordered metals have changed this situation dramatically.

On the one hand, following the scaling theory of localization of Abrahams, Anderson, Licciardello and Ramakrishnan (1979), we now have a way of measuring experimentally the inelastic scattering rate, τ_{in}^{-1} , in two dimensions (2D) (silicon inversion layers, thin films). On the other hand, the interplay between interactions and impurity scattering which is responsible for the result discovered by Schmid, has been found to lead to much more

dramatic consequences in the transport properties of disordered metals, following the work of Al'tschuler and Aronov (1979), Al'tschuler, Aronov and Lee (1980) and Fukuyama (1980).

In this chapter we will try to review some aspects of this field which are more relevant to the problem of quasi-particle lifetimes. For more details the reader is referred to the recent extensive review of Fukuyama (1983).

4.2 Impurity Scattering Perturbation Theory and Diffusive Poles

It should now come as a surprise to no one that the effect of disorder on the properties of a metal can be so drastic that it can turn it into an insulator by localizing the single particle states (Anderson 1958). We are interested here, though, in properties of systems which have high electrical conductivity so that the effect of impurities can be treated as a perturbation of the clean metal. This requires that $k_F \ell \gg 1$ where ℓ is the impurity mean free path, i.e. ℓ^{-1} is the average momentum uncertainty of an energy eigenstate at the Fermi level.

We shall work with a simple model Hamiltonian of free electrons scattered by randomly diluted impurities with short range potentials (interactions will be considered later),

$$\begin{aligned} \mathcal{H} &= \sum_i -\frac{\nabla_i^2}{2m} + V_0 \sum_{i,\ell} p_\ell \delta(\mathbf{r}_i - \mathbf{R}_\ell) \\ &= \sum_{\mathbf{k},\sigma} \epsilon_{\mathbf{k}} c_{\mathbf{k}\sigma}^\dagger c_{\mathbf{k}} + \frac{V_0}{\Omega} \sum_{\mathbf{R},\mathbf{R}'} \sum_{\sigma} p_\ell e^{-i(\mathbf{R}-\mathbf{R}')/\mathbf{R}_\ell} c_{\mathbf{R}'\sigma}^\dagger c_{\mathbf{R}\sigma} \end{aligned} \quad (4.1)$$

where p_ℓ is a random variable, taking values 1,0 with probabilities $p, 1-p$ where p is the atomic concentration of

impurities ($p \ll 1$). The volume of the sample is Ω , $\epsilon_{\mathbf{k}} = k^2/2m$ and \mathbf{R}_j are the positions of the sites of a lattice. The perturbation theory and Feynman diagrams for this Hamiltonian, first introduced by Edwards (1958), have been described in detail in several textbooks (AGD 1965, Doniach and Sondheimer 1974, Rickayzen 1980).

We assume that the scattering by a single impurity can be treated in the Born approximation. The final results expressed in terms of the lifetime of a momentum state τ or the mean free path $l = v_F \tau$ are still valid for strong single impurity potentials. This simplified model is most often used in this field and reveals the essential physics without unnecessary complicated algebra.

The basic vertex, after averaging over impurities, is drawn in Fig. 4.1 and corresponds to a factor $\mu^2 = c v_0^2$ where c is the volume concentration of impurities. It carries finite momentum but zero frequency.

The simplest self-energy diagram is shown in Fig. 4.2(a) (solid lines denote the impurity averaged Green's function) and gives,

$$\Sigma(\mathbf{k}, i\epsilon_m) = -\frac{i}{2\tau} \text{sgn } \epsilon_m \quad (4.2)$$

(an additional real constant is absorbed in the chemical potential). The lifetime of a momentum state, τ , is given by

$$\frac{1}{\tau} = 2\pi n_0 v^2 \quad (4.3)$$

where n_0 is the one-spin density of states per unit volume. The impurity averaged Green's function is

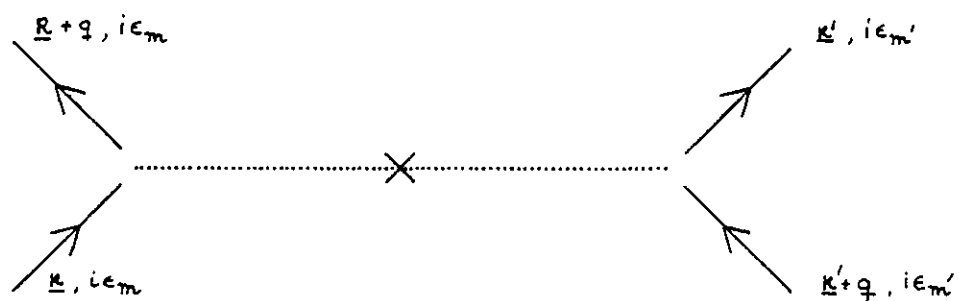
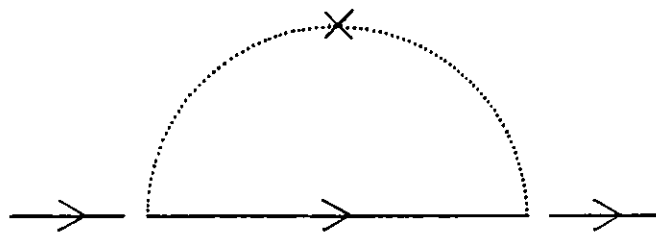
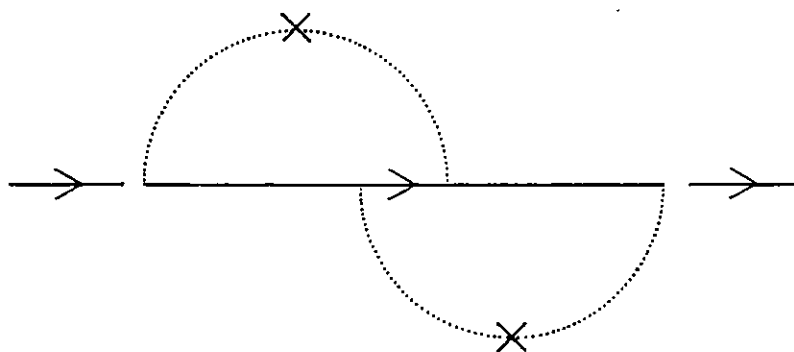


FIG 4.1

Basic impurity vertex after averaging over impurity configurations. It carries momentum, but no frequency.



(a)



(b)

FIG 4.2

- (a) Self-energy diagram to leading order
in $1/k_F \ell$
- (b) $1/k_F \ell$ correction to (a)

$$G_0(\underline{k}, i\epsilon_m) = \frac{1}{i\epsilon_m - \omega_{\underline{k}} + \frac{i}{2\tau} \operatorname{sgn}\epsilon_m} \quad (4.4)$$

with $\omega_{\underline{k}} \equiv \epsilon_{\underline{k}} - \mu$.

A first order correction to the diagram of Fig. 4.2(a) is shown in Fig. 4.2(b). Compared to the previous one, this diagram involves an additional factor

$$U^2 \int \frac{d^d \underline{k}'}{(2\pi)^d} G_0(\underline{k} + \underline{q}, i\epsilon_m) G_0(\underline{k}', i\epsilon_m) \quad (4.5)$$

The integral

$$I(\underline{q}; i\epsilon_m + i\omega_{\underline{q}}, i\epsilon_m) \equiv U^2 \int \frac{d^d \underline{k}}{(2\pi)^d} G_0(\underline{k} + \underline{q}, i\epsilon_m + i\omega_{\underline{q}}) G_0(\underline{k}, i\epsilon_m) \quad (4.6)$$

is studied in detail in Appendix C. In particular it is shown that for $\epsilon_m (\epsilon_m + \omega_{\underline{q}}) > 0$ it is at least of order $1/k_F \ell$ (eq. C8). Other corrections to the diagram of Fig. 4.2(a) can similarly be shown to be of order $1/k_F \ell$. Thus the self-energy is given by eqs. (4.2) and (4.3) to leading order in $1/k_F \ell$.

The recent developments in the theory of weakly disordered metals stem largely from the recognition of the importance of two singularities in the two particle Green's function which will now be described.

Consider the ladder diagram series shown in Fig. 4.3. Clearly D_0 is independent of \underline{k} and \underline{k}' and we have

$$D_0(\underline{q}; i\epsilon_m + i\omega_{\underline{q}}, i\epsilon_m) = U^2 + U^2 \int \frac{d^d \underline{k}}{(2\pi)^d} G_0(\underline{k} + \underline{q}, i\epsilon_m + i\omega_{\underline{q}}) G_0(\underline{k}, i\epsilon_m) \times D_0(\underline{q}; i\epsilon_m + i\omega_{\underline{q}}, i\epsilon_m)$$

which has the solution

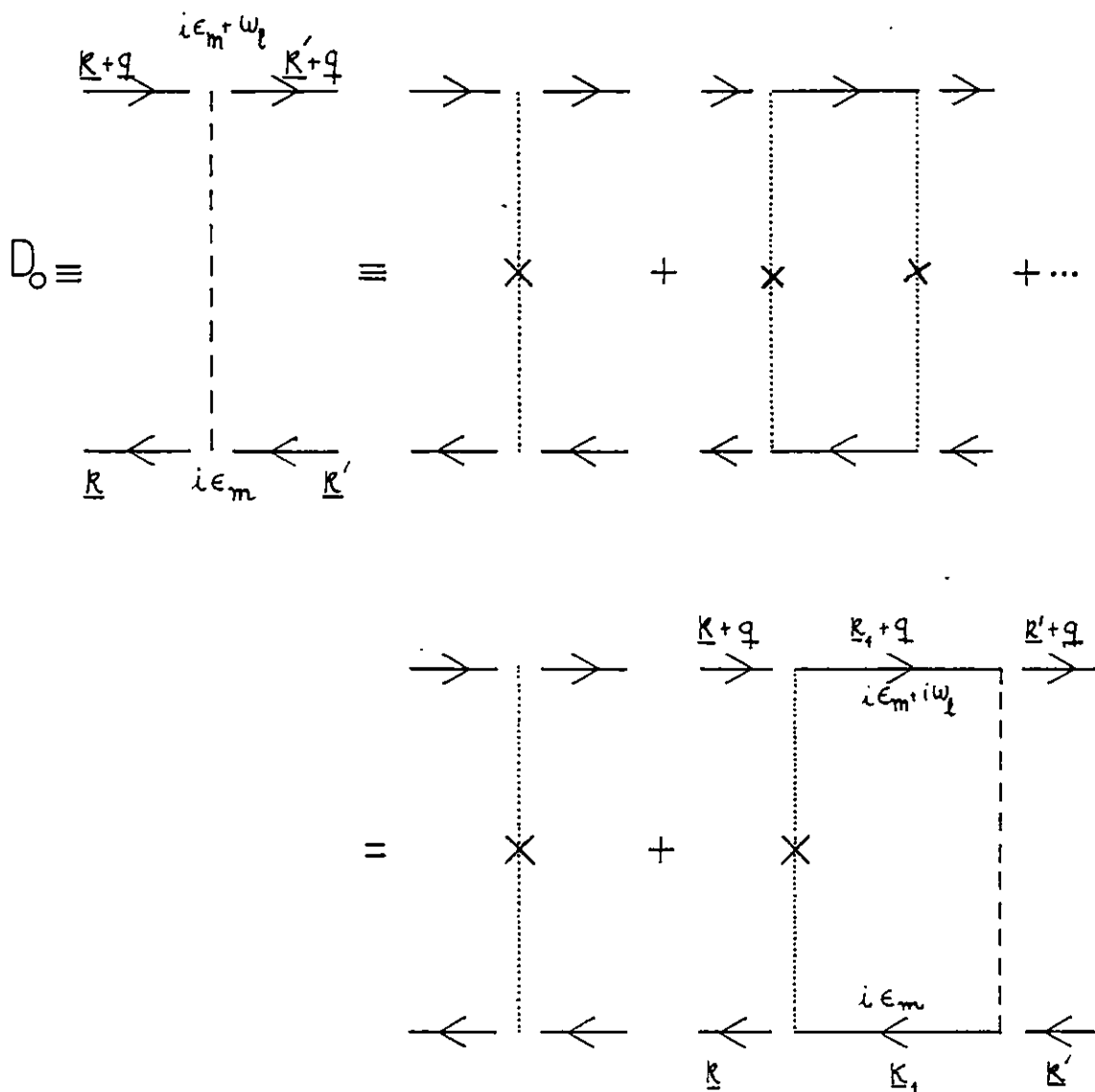


FIG 4.3

The particle-hole diffusion propagator D_0 .

$$\begin{aligned}
D_0(q; i\epsilon_m + i\omega_\ell, i\epsilon_m) &= \frac{\mu^2}{1 - \nu^2 \int \frac{d^d k}{(2\pi)^d} G_0(k+q, i\epsilon_m + i\omega_\ell) G_0(k, i\epsilon_m)} \\
&= \frac{\nu^2}{1 - I(q; i\epsilon_m + i\omega_\ell, i\epsilon_m)}
\end{aligned} \tag{4.7}$$

We have seen before that $I(q; i\epsilon_m + i\omega_\ell, i\epsilon_m)$ is of order $1/k_F \ell$ for $\epsilon_m(\epsilon_m + \omega_\ell) > 0$ (eq. (C8)). However, for $\epsilon_m(\epsilon_m + \omega_\ell) < 0$ and when the poles of the two Green's functions come together, i.e. when $q, \omega_\ell \rightarrow 0$ this integral tends to unity and D_0 diverges. More precisely, (eq. (C13b)), for $q\ell, \omega_\ell\tau \ll 1$

$$I(q; i\epsilon_m + i\omega_\ell, i\epsilon_m) \simeq 1 - i\omega_\ell\tau - Dq^2\tau$$

where $D \equiv v_F^2\tau/d = k_F\ell/dm$ is the diffusion constant, v_F the Fermi velocity and d the dimensionality.

Thus for $\epsilon_m(\epsilon_m + \omega_\ell) < 0$, $q\ell, \omega_\ell\tau \ll 1$

$$D_0(q; i\epsilon_m + i\omega_\ell, i\epsilon_m) = \frac{1}{2\pi n_0 \tau^2 [i\omega_\ell + Dq^2]} \tag{4.8}$$

(Equation (4.3) was used to express ν^2 in terms of τ).

This singularity is usually referred to as the particle-hole diffusive pole. The particle-particle pole is shown in Fig. 4.4. Clearly

$$\begin{aligned}
C_0(q; i\epsilon_m + i\omega_\ell, i\epsilon_m) &= \frac{\mu^2}{1 - \nu^2 \int \frac{d^d k}{(2\pi)^d} G_0(-k+q, i\epsilon_m + i\omega_\ell) G_0(k, i\epsilon_m)} \\
&= \frac{\nu^2}{1 - I(q; i\epsilon_m + i\omega_\ell, i\epsilon_m)}
\end{aligned} \tag{4.9}$$

Hence $C_0(q; i\epsilon_m + i\omega_\ell, i\epsilon_m)$ has a pole of exactly the same form as D_0 ,

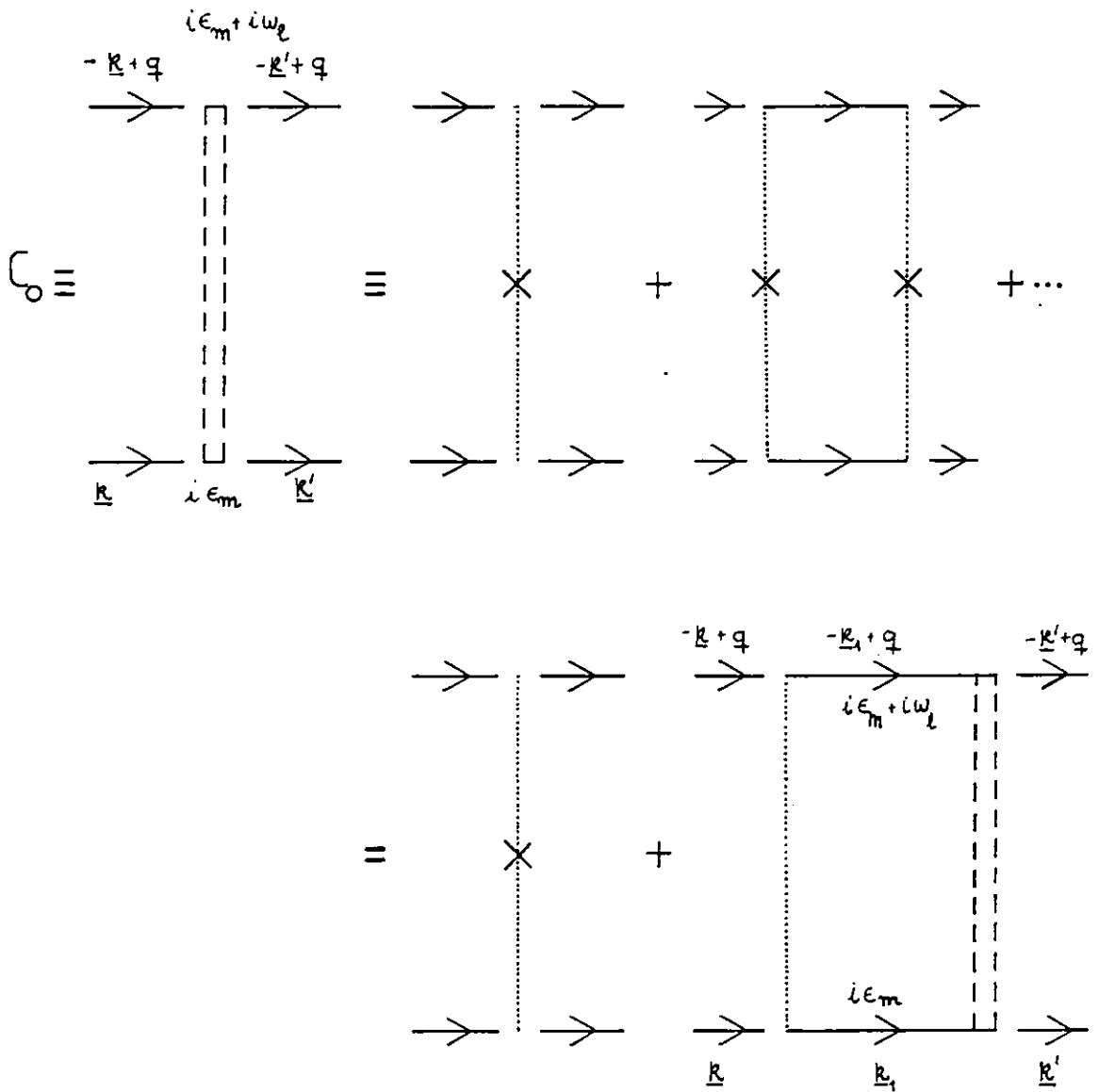


FIG 4.4

The particle-particle diffusion propagator C_0 .

$$C_0(q; i\epsilon_m + i\omega_\ell, i\epsilon_m) = \frac{1}{2\pi n_0 \tau^2 [|\omega_\ell| + Dq^2]} \quad ; \quad \epsilon_m(\epsilon_m + \omega_\ell) < 0 \quad (4.10)$$

$$q\ell, \omega_\ell \tau \ll 1.$$

We can redraw one of the ladder diagrams included in C_0 in the particle-hole channel (Fig. 4.6) and one easily sees, then, that C_0 corresponds to the series of maximally crossed diagrams. The particle-particle singularity occurs when the sum of the momenta of the two incoming particles is small, whereas the particle-hole singularity occurs when the incoming particle and hole states have a small momentum difference.

The way these singularities affect the transport properties is well illustrated by a calculation of the conductivity. Kubo has shown that (Kubo 1957)

$$\text{Re } \sigma(\omega) = - \text{Re} \frac{2e^2}{i\omega m^2} \frac{1}{\Omega} \sum_{\underline{k}, \underline{k}'} \kappa_x \kappa'_x \mathcal{N}^R(\underline{k}, \underline{k}'; \omega) \quad (4.11)$$

where $\mathcal{N}^R(\underline{k}, \underline{k}', i\omega_\ell)$ is the (imaginary) time fourier transform of the Green's function $\mathcal{N}^R(\underline{k}, \underline{k}', \tau) = - \langle T [\hat{n}_{\underline{k}}(\tau), \hat{n}_{\underline{k}'}^{(0)}] \rangle$ and $\hat{n}_{\underline{k}}$ is the number operator of the \underline{k} state.

Given an approximation for the self-energy, it is possible to derive a consistent approximation for any two particle Green's function, in the sense that particle conservation is respected, following the rules proposed by Baym and Kadanoff (1961) and Baym (1962). From the diagram of Fig. 4.2(a) we obtain for σ the diagrams of Fig. 4.6. In the case of delta-function impurity potentials only the first diagram contributes. The D_0 propagator does not depend on the external momenta \underline{k} , \underline{k}' and

$$\sum_{\underline{k}} \kappa_x G_0(\underline{k}, i\epsilon_m + i\omega_\ell) G_0(\underline{k}, i\epsilon_m) = 0$$

One obtains easily (AGD 1965, Rickayzen 1980)

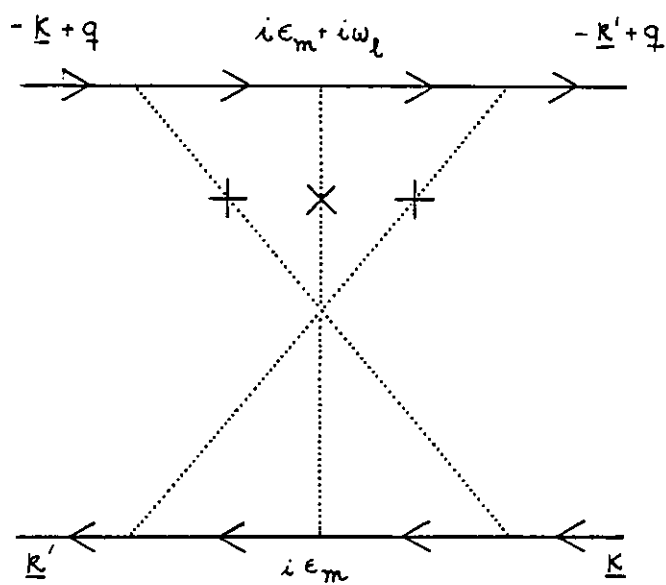


FIG 4.5

A diagram included in C_0 redrawn in the particle-hole channel

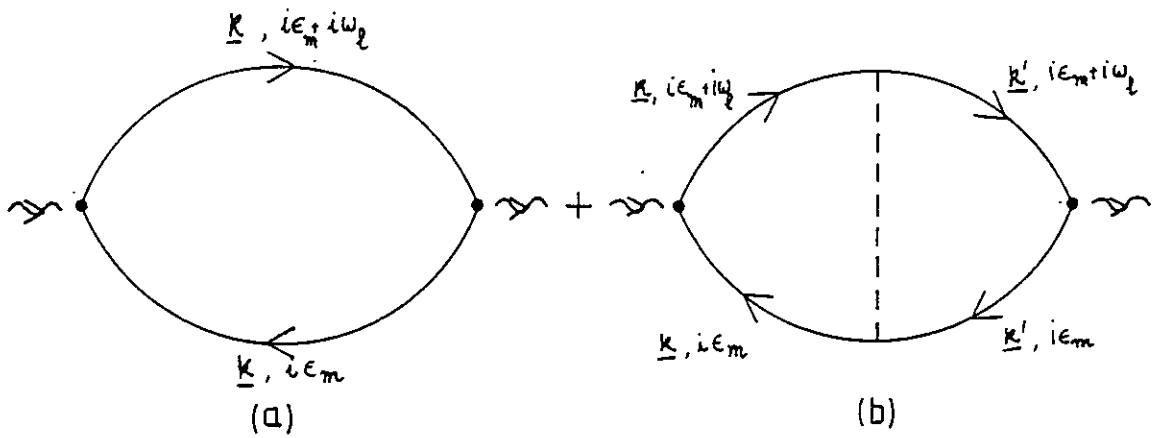


FIG 4.6

Conductivity diagrams consistent with the approximation of Fig. 4.2(a) for the self-energy. Only (a) contributes to delta-function impurity potentials.

$$\begin{aligned}\sigma_{DC} &= \frac{ne^2}{m} \tau \\ &= \frac{e^2 k_F}{3\pi^2} k_F \ell \quad \text{in 3D} \end{aligned} \quad (4.12a)$$

$$= \frac{e^2}{2\pi} k_F \ell \quad \text{in 2D} \quad (4.12b)$$

which is the classical result of Boltzmann's equation.

Consider, however, the effect of maximally crossed diagrams of Fig. 4.7 (Gorkov, Larkin and Khmel'nitzkii 1979, Abrahams and Ramakrishnan 1980)

$$\begin{aligned}\delta\sigma(\omega) &= -\frac{2e^2}{i\omega m^2} \int \frac{d^d q}{(2\pi)^d} \frac{d^d k}{(2\pi)^d} (-k+q)_x k_x \\ &\times \frac{1}{\beta} \sum_{\epsilon_m} G(-k+q, i\epsilon_m + i\omega_\ell) G(k, i\epsilon_m + i\omega_\ell) \\ &\times G(-k+q, i\epsilon_m) G(k, i\epsilon_m) C_0(q; i\epsilon_m + i\omega_\ell, i\epsilon_m) \end{aligned} \quad (4.13)$$

Strictly speaking, the Green's functions should be modified in order to ensure particle conservation. But we have seen that all corrections to τ are of order $1/k_F \ell$. Thus to leading order in $1/k_F \ell$ we can use the Green's functions given by eqs. (4.4) and (4.3). When $-\omega_\ell < \epsilon_m < 0$ the particle-particle propagator C_0 has a pole of the form $1/(\omega_\ell + Dq^2)$. In 2D the q integral will diverge logarithmically as $\omega_\ell \rightarrow 0$. The singular term is

$$\begin{aligned}\delta\sigma(\omega) &= -\frac{2e^2}{i\omega m^2} \int_{q \ll \ell^{-1}} \frac{d^2 q}{(2\pi)^2} \frac{1}{2\pi n_0 v^2} \frac{1}{\omega_\ell + Dq^2} \\ &\times \frac{1}{\beta} \sum_{-\omega_\ell < \epsilon_m < 0} \int \frac{d^2 k}{(2\pi)^2} (-k_x^2) \left[G^R(k, i\epsilon_m) \right]^2 \left[G^A(k, i\epsilon_m) \right]^2 \end{aligned} \quad (4.14)$$

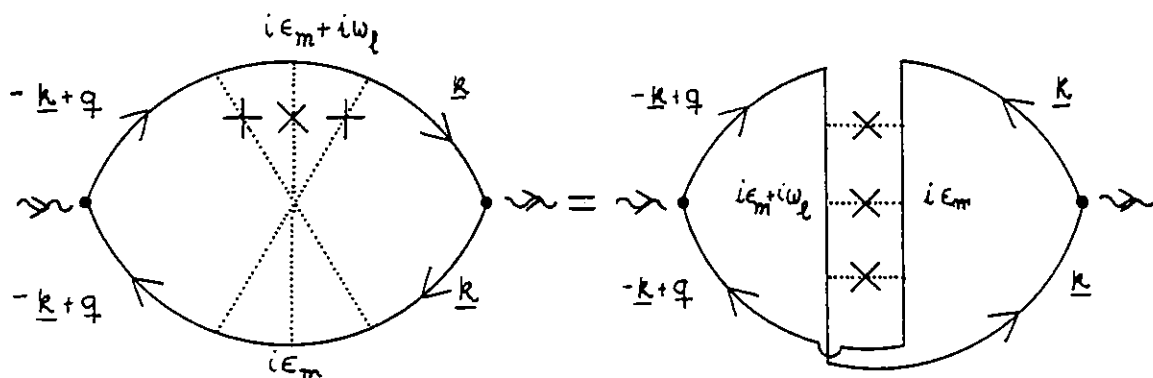


FIG 4.7

Contribution of maximally crossed diagrams to the conductivity.

where we have taken the limit $q, \omega \rightarrow 0$ everywhere except in C_0 . The k integral can easily be done by contour integration (see Appendix D) and we obtain after analytic continuation $i\omega \rightarrow \omega + i0^+$

$$\begin{aligned} \delta\sigma(\omega) &= - \frac{e^2}{\pi \pi} k_F \ell \int_{q < \ell^{-1}} \frac{d^2 q}{(2\pi)^2} \frac{1}{-i\omega + \mathcal{D}q^2} \\ &= \frac{e^2}{2\pi \pi^2} k_F \ell \int_0^{\ell^{-1}} dq q \frac{1}{-i\omega + \mathcal{D}q^2} \end{aligned} \quad (4.15)$$

The logarithmically divergent term is,

$$\delta\sigma(\omega) = - \frac{e^2}{2\pi^2} \ln \frac{1}{\omega \tau} \quad (4.16)$$

For a finite size system of linear dimension L the lower limit of the q integral in eq. (4.15) is L^{-1} and so, for $\omega \ll \mathcal{D}L^{-2}$

$$\delta\sigma(L) = - \frac{e^2}{\pi^2} \ln \frac{L}{\ell} \quad (4.17)$$

Quite obviously this logarithmic dependence cannot be valid for arbitrarily small frequencies or large lengths or σ would become negative. This point will be clarified in the next section. Here, however, we would like to stress some features of this calculation which will occur again in the calculations presented in the next chapter.

Notice that we isolated the term containing the diffusive singularity and ignored all other corrections. The diffusive pole leads to a more singular frequency dependence than that of the classical Boltzmann term and so, even when $k_F \ell \gg 1$, the diagrams of Fig. 4.7 must be taken into account. But non-singular corrections of order $1/k_F \ell$ can and have been neglected.

They would only alter the classical result or the coefficient of the logarithmic term by negligible amounts. Thus, when calculating any physical quantity, one must consider carefully the way in which the diffusive poles of eqs. (4.8) and (4.10) can affect the corresponding temperature or frequency dependences. But among the diagrams contributing to a term with a given frequency or temperature dependence, one need only consider the leading $1/k_F \ell$ contributions. These considerations will be amply illustrated in the following chapter.

4.3 Weak Localization and the Inelastic Scattering Time

The logarithmic length dependence of the conductivity of eq. (4.17) was anticipated by the scaling theory of localization of Abrahams, Anderson, Licciardello and Ramakrishnan (1979). They argued that in 2D all states are localized and for a large enough sample, $L \gg \xi$, where ξ is the localization length, the conductivity will always decay exponentially with length

$$\sigma(L) \sim e^{-L/\xi} \quad ; \quad L > \xi \quad (4.18)$$

For weak disorder the localization length can be extremely large though $\xi \sim \ell e^{K_F \ell}$. Hence, for shorter length scales, $L \ll \xi$, the system will have a metallic-like behaviour with high conductivity, which they found to have the form

$$\sigma(L)/e^2 \equiv g(L) = g(L_0) - g_a \ln\left(\frac{L}{L_0}\right) \quad (4.19)$$

where L_0 is the distance at which scaling begins to be valid and g_a is a constant of order unity. The perturbative result derived in the last section (eq. 4.17) should only be valid in

the regime where the conductivity is large, i.e. the weak localization regime. One has then, $L_0 = l$, $g(l_0) = k_F l / 2\pi$ and $g_a = 1/\pi^2$.

The inelastic scattering time comes in when we consider the system at finite temperatures. Thouless (1977) and Anderson, Abrahams and Ramakrishnan (1979) argued that between inelastic scattering events an electron diffuses a distance L_{in} given by

$$L_{in}^2 = D \tau_{in} \quad (4.20)$$

after which it can be scattered into another eigenstate and continue to propagate. So at finite temperatures the effective length scale of the system is L_{in} and

$$\delta\sigma(\tau) = -\frac{e^2}{\pi^2} \ln \frac{L_{in}}{l} = -\frac{e^2}{2\pi^2} \ln \frac{\tau_{in}}{\tau} \quad (4.21)$$

Normally $\tau_{in} \sim T^{-p}$ at low temperatures, and we get

$$\delta\sigma(\tau) = \frac{e^2}{2\pi^2} p \ln T \tau \quad (4.22)$$

We could then expect that a measurement of this logarithmic temperature correction to the Boltzmann conductivity would provide an experimental determination of τ_{in} . In practice, the situation is complicated by the fact that, when interactions are taken into account, there are other logarithmic corrections to the conductivity which do not depend on τ_{in} (Al'tschuler, Aronov and Lee 1980; Fukuyama 1980). They arise also from the diffusive poles described in section 4.2. (See Fukuyama 1983 for details). These two effects, localization and interactions, are found to co-exist experimentally (Pepper 1981). However, unlike the interaction effect, the localization one

is strongly affected by weak magnetic fields, and it turns out to be possible to obtain τ_{in} from magnetoresistance measurements (Kawaguchi and Kawaji 1980, Uren, Davies, Kaveh and Pepper 1981, Wheeler 1981, Bergmann 1982). These experimental results will be discussed in the following chapter.

4.4 Inelastic Scattering Time in Two Dimensions

Recently, Abrahams, Anderson, Lee and Ramakrishnan (AALR, 1981) calculated the inelastic scattering time in 2D using a method based on exact impurity eigenstates. This method does not require the derivation of a kinetic equation as in the previous calculations of Schmid (1973), Al'tschuler (1978) and Al'tschuler and Aronov (1979). The method used in this thesis is an extension of this one, so we shall now briefly describe the calculation of AALR.

In the absence of interactions the Hamiltonian of eq. (4.9) has a set of exact one electron eigenstates $\psi_{\alpha}(\mathbf{r})$. When interactions are present these states acquire a finite lifetime. If we describe the effect of interactions by a self-energy, which we assume to be dominated by the diagonal elements, $\sum_{\alpha} (i\epsilon_m)$, the quasiparticle energies $\tilde{\omega}_{\alpha}$ and inverse lifetimes Γ_{α} are given, as in normal Fermi liquid theory, by

$$\tilde{\omega}_{\alpha} = \omega_{\alpha} + \Delta_{\alpha}(\tilde{\omega}_{\alpha}) \quad (4.23a)$$

$$\Gamma_{\alpha} = z_{\alpha} \Gamma_{\alpha}(\tilde{\omega}_{\alpha}) \quad (4.23b)$$

where

$$\sum_{\alpha}(\omega \pm i0^{\pm}) = \Delta_{\alpha}(\omega) \mp i\Gamma_{\alpha}(\omega)$$

$$z_{\alpha} \equiv \left(1 - \left. \frac{\partial \Delta_{\alpha}}{\partial \omega} \right|_{\omega=\tilde{\omega}_{\alpha}} \right)^{-1} \quad (4.24)$$

However, these quantities depend on the particular configuration of impurities. The average inverse lifetime of a state with energy E with respect to the Fermi surface should then be

$$\Gamma(\epsilon, T) \equiv \frac{1}{\Omega n_0} \left\langle \sum_{\alpha} z_{\alpha} \Gamma_{\alpha}(\tilde{\omega}_{\alpha}) \delta(\tilde{\omega}_{\alpha} - \epsilon) \right\rangle_{av} \quad (4.25)$$

Or, to lowest order in the interactions, simply

$$\Gamma(\epsilon, T) = \frac{1}{\Omega n_0} \left\langle \sum_{\alpha} \Gamma_{\alpha}(\omega_{\alpha}) \delta(\omega_{\alpha} - \epsilon) \right\rangle_{av} \quad (4.26)$$

where $\langle \dots \rangle_{av}$ denotes an average over impurity configurations.

The inelastic scattering rate τ_{in}^{-1} is, strictly,

$$\frac{1}{\tau_{in}} = 2\Gamma \quad (4.27)$$

The reason for the factor two is that Γ , as defined in eq. (4.23b), is the rate of decay of the amplitude of finding a particle in state α whereas $1/\tau_{in}$ is the rate of decay of the corresponding probability, i.e. of the occupation number of state α . This difference is often overlooked in the literature (author included).

Abrahams, Anderson, Lee and Ramakrishnan work directly from this definition to calculate Γ to lowest order in the averaged screened Coulomb interaction (Fig. 4.8). One has

$$\Sigma_{\alpha}(i\epsilon_m) = \sum_{\beta} \frac{1}{\beta} \sum_{\omega_2} V_{\beta\alpha}^{\alpha\beta}(\omega_2) G_{0\beta}(i\epsilon_m + i\omega_2) \quad (4.28)$$

with $G_{0\beta}(i\epsilon_m)$ the unperturbed Green's function for state β ,

$$G_{0\beta}(i\epsilon_m) = \frac{1}{i\epsilon_m - \omega_{\beta}} \quad (4.29)$$

and the interaction $V_{\beta\alpha}^{\alpha\beta}(i\omega_2)$,

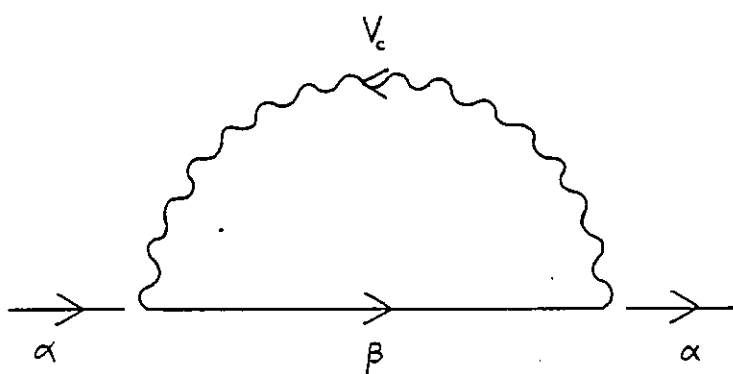


FIG 4.8

Self-energy diagram for an exact impurity eigenstate α to lowest order in the averaged screened Coulomb interaction .

$$V_{\beta\alpha}^{\alpha\beta}(i\omega_\ell) = \int d^d r d^d r' \psi_\alpha^*(\underline{r}) \psi_\beta^*(\underline{r}') \left[\int \frac{d^d q}{(2\pi)^d} e^{i\mathbf{q}(\underline{r}-\underline{r}')} V_c(\mathbf{q}, i\omega_\ell) \right] \\ \times \psi_\alpha(\underline{r}') \psi_\beta(\underline{r}) .$$

$V_c(\underline{q}, i\omega_\ell)$ is the averaged screened Coulomb interaction

$$V_c(\mathbf{q}, i\omega_\ell) = \frac{2\pi e^2/q}{1 - \frac{2\pi e^2}{q} \Pi(\mathbf{q}, i\omega_\ell)} \quad (4.30)$$

The polarization insertion $\Pi(\mathbf{q}, i\omega_\ell)$ is discussed in Appendix E. After performing the frequency sum and doing the analytic continuation $i\epsilon_m \rightarrow \omega - i0^+$ one obtains for the imaginary part of $\sum_\alpha \Gamma_\alpha(\omega - i0^+)$

$$\Gamma_\alpha(\omega) = \frac{1}{2} \sum_\beta \int \frac{d^d q}{(2\pi)^d} |f_{\alpha\beta}(\mathbf{q})|^2 \int_{-\omega}^{+\omega} d\eta [N(\eta) + f(\eta + \omega)] \\ \times 2 [\text{Im} V^A(\mathbf{q}, \eta)] \delta(\omega_\beta - \omega + \eta)$$

with

$$f_{\alpha\beta}(\mathbf{q}) = \int d^d r e^{i\mathbf{q}\cdot\mathbf{r}} \psi_\alpha^*(\underline{r}) \psi_\beta(\underline{r})$$

Averaging over impurity configurations

$$\Gamma(\mathbf{E}, \omega) = \frac{1}{\Omega n_0} \left\langle \sum_\alpha \Gamma_\alpha(\omega) \delta(\omega_\alpha - E) \right\rangle_{av} \\ = \frac{1}{2} \int \frac{d^d q}{(2\pi)^d} \int d\eta [N(\eta) + f(\eta + \omega)] 2 [\text{Im} V_c^A(\mathbf{q}, \eta)] \mathcal{D}(\mathbf{q}; E, \omega - \eta) \quad (4.31)$$

where $\mathcal{D}(\underline{q}; E, E')$ is the space fourier transform of the correlation function

$$\mathcal{D}(\underline{r}-\underline{r}'; \epsilon, \epsilon') \equiv \frac{1}{n_0} \left\langle \sum_{\alpha, \beta} \psi_{\alpha}^*(\underline{r}) \psi_{\beta}(\underline{r}) \psi_{\alpha}(\underline{r}') \psi_{\beta}^*(\underline{r}') \delta(\omega_{\alpha}-\epsilon) \delta(\omega_{\beta}-\epsilon') \right\rangle_{av} \quad (4.32)$$

This function, as defined, does not involve interactions and can be calculated by standard impurity perturbation techniques. In fact, AALR show that it is related to the spectral density of the density-density correlation function. In a disordered metal, density fluctuations decay by diffusion and from that alone one can show that, (Forster 1975)

$$\mathcal{D}(\underline{q}; \epsilon, \epsilon') = \mathcal{D}(\underline{q}, \epsilon-\epsilon') \sim \frac{\mathcal{D}q^2}{(\epsilon-\epsilon')^2 + (\mathcal{D}q^2)^2} \quad (4.33)$$

This divergence of $\mathcal{D}(\underline{q}, \eta)$ at low \underline{q} , low η causes $\Gamma(\epsilon, \omega)$ to diverge at $\omega = \epsilon$. (We shall later rederive eq. (4.31) and discuss it in greater detail). One gets

$$\Gamma(\epsilon, \omega) = \frac{k_B T}{2k_f \ell} \ln \frac{k_B T \epsilon}{(\omega - \epsilon)^2} \quad (4.34)$$

where $\epsilon = D\kappa^2$ and κ is the inverse screening radius $\kappa = 4\pi n_0 e^2 / 2m e^2$. To cure the divergence of eq. (4.34) on the energy shell, AALR state that in a higher order calculation one would have to take into account the quasiparticle energy shift which they claim to be

$$\Delta \approx \frac{k_B T}{2k_f \ell} \quad (4.35)$$

The result they obtain, in a way which is not clear to me, is

$$\Gamma = \frac{k_B T}{k_f \ell} \ln \frac{T_1}{T} \quad (4.36)$$

where $k_B T_1 = (k_F \ell)^2 \epsilon^{-1}$. One cannot obtain the logarithmic factor in eq. (4.36) from the kinetic equations of Schmid (1973) or Al'tschuler (1978) at least without substantial modification. One obtains a divergence with no obvious indication of how to renormalize it.

However, Fukuyama and Abrahams (1983) rightly pointed out that the inelastic scattering time that appears as a cutoff in weak localization is not, strictly, the single particle lifetime, but the lifetime of the particle-particle diffusion propagator, which for an interacting system will have the form,

$$(\epsilon_m (\epsilon_m + \omega_q) \langle 0 \rangle)$$

$$C(q; i\epsilon_m + i\omega_q, i\epsilon_m) = \frac{1}{2\pi n_0 \tau^2 [|\omega_q| + Dq^2 + \frac{1}{\tau_{loc}}]} \quad (4.37)$$

It is clear that inserting this expression in eq. (4.15) one obtains eq. (4.21), with τ_{in} replaced by τ_{loc} , in the limit $\omega \tau_{loc} \ll 1$. Fukuyama and Abrahams calculated τ_{loc} using the standard impurity perturbation technique in momentum space (This calculation will be further discussed in Chapter 5) and obtained exactly the same result as AALR for Γ

$$\frac{1}{\tau_{loc}} = \frac{k_B T}{k_F \ell} \ln \frac{T_1}{T} \quad (4.38)$$

As Fukuyama and Abrahams point out, this result is, in a sense, surprising. The two calculations have little in common and give little indication of why their results should be identical. In

¹ From the argument of AALR it would seem that the natural thing to do is to replace $\omega - E$ by Δ in which case one gets $\Gamma = (k_B T / 2 k_F \ell) \ln (T_2 / T)$ with $k_B T_2 = 4(k_F \ell)^2 \epsilon$. In the following chapter we shall present a self-consistent calculation of Γ in which we obtain this result. But the divergence is cut off by Γ , not the quasiparticle energy shift.

the next chapter we present a reformulation of the method of AALR in momentum space. We shall be able to do a self-consistent calculation of Γ where the divergence in eq. (4.34) is automatically renormalized without the need for additional arguments. The result we obtain is

$$\Gamma = \frac{k_B T}{2k_f \ell} \ln \frac{T_2}{T} \quad (4.39)$$

where $k_B T_1 = 4(k_f \ell)^2 \epsilon$ (see footnote 1). This calculation, in conjunction with the one by Fukuyama and Abrahams, also clarifies considerably the relation between Γ and τ_{loc} .

CHAPTER 5

SELF-CONSISTENT CALCULATION OF THE QUASIPARTICLE LIFETIME IN
TWO-DIMENSIONAL METALS

5.1 The Method of AALR in Momentum Space

The calculation of Abrahams, Anderson, Lee and Ramakrishnan (AALR, 1981) described in the previous chapter has the unsatisfying feature that the average imaginary self-energy diverges on the energy shell (eq. (4.34)). Such divergences often arise because the propagators which appear in the Feynman diagrams of the self-energy are not suitably renormalized. Renormalizing these propagators introduces an element of self-consistency into the calculation. We shall now present a reformulation of the calculation of AALR in momentum space which allows full use of diagrammatic techniques and accommodates, more easily than the original method, the self-consistent nature of the calculation.

It is useful, however, to introduce the method first in its simpler, non self-consistent version. We start from eq. (4.26) for the average, quasiparticle ^{inverse} lifetime, namely

$$\Gamma(E, T) = \frac{1}{\Omega n_0} \left\langle \sum_{\alpha} \Gamma_{\alpha}(E) \delta(\omega_{\alpha} - E) \right\rangle_{av} \quad (5.1)$$

The delta-function can be expressed in terms of the non-interacting Green's function for the impurity eigenstate α

$$\delta(\omega_{\alpha} - E) = \frac{1}{2\pi i} \left[G_{0\alpha}^A(E) - G_{0\alpha}^R(E) \right] \quad (5.2)$$

Also $\Gamma_{\alpha}(\omega)$, the imaginary part of the self-energy, is

$$\Gamma_{\alpha}(\omega) = \frac{1}{2i} [\sum_{\alpha}^A(\omega) - \sum_{\alpha}^R(\omega)] \quad (5.3)$$

One can then obtain the average inverse lifetime Γ by suitable analytic continuations of the function $\alpha(i\epsilon_{m'}, i\epsilon_m)$,

$$\alpha(i\epsilon_{m'}, i\epsilon_m) \equiv \frac{1}{\Omega} \langle \sum_{\alpha} \sum_{\alpha}(i\epsilon_{m'}) G_{o\alpha}(i\epsilon_m) \rangle_{av} \quad (5.4)$$

In fact,

$$\begin{aligned} \Gamma(E, T) &= - \frac{1}{4\pi\eta_0} \frac{1}{\Omega} \langle \sum_{\alpha} [\sum_{\alpha}^A(E) - \sum_{\alpha}^R(E)] [G_{o\alpha}^A(E) - G_{o\alpha}^R(E)] \rangle \\ &= - \frac{1}{4\pi\eta_0} [\alpha^{AA}(E, E) - \alpha^{AR}(E, E) + \alpha^{RR}(E, E) - \alpha^{RA}(E, E)] \\ &= \frac{1}{2\pi\eta_0} \text{Re} [\alpha^{RA}(E, E) - \alpha^{AA}(E, E)] \end{aligned} \quad (5.5)$$

The function $\alpha(i\epsilon_{m'}, i\epsilon_m)$ is a trace of a product of the matrices Σ and G_o (G_o is diagonal in the α representation and Σ is assumed to be dominated by diagonal elements) and, hence, it is invariant under change of basis. In the momentum representation,

$$\alpha(i\epsilon_{m'}, i\epsilon_m) = \frac{1}{\Omega} \langle \sum_{\substack{R, R'}} \Sigma(R, R'; i\epsilon_{m'}) G_o(R', R; i\epsilon_m) \rangle_{av} \quad (5.6)$$

This expression is easily given a diagrammatic representation. We choose for the self-energy the approximation of AALR, namely the lowest order term in the screened Coulomb interaction. Then the function $\alpha(i\epsilon_{m'}, i\epsilon_m)$ is just the average of the diagram of Fig. 5.1.

We shall see in the next sections that one easily recovers the result of AALR using this method. The divergence of (eq. (4.34)) disappears if the electron propagator which

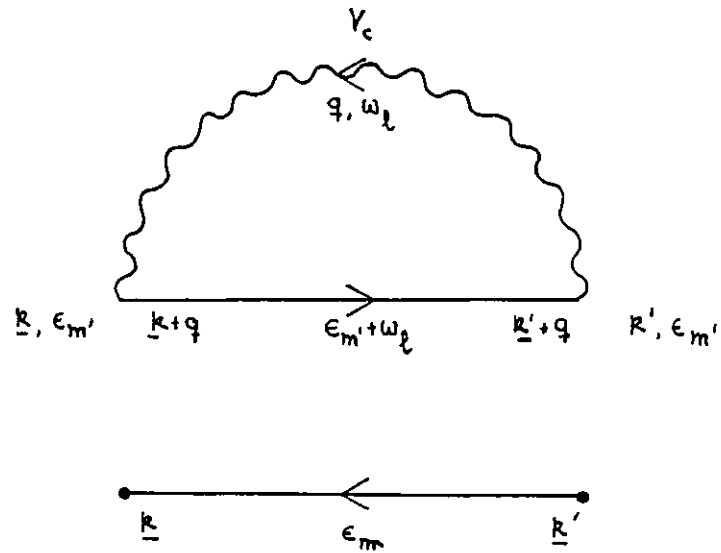


FIG 5.1

The function $\alpha(i\epsilon_{m'}, i\epsilon_m)$ defined in eq. (5.6), is the impurity average of this diagram.

appears in $\Sigma(\mathbf{k}, \mathbf{k}'; i\epsilon_m')$ is renormalized consistently. However, one cannot use eq. (5.1) as a starting definition. The renormalization of the propagator involves an energy shift as well as a lifetime. If the variable E is to be the real quasiparticle energy (and $E = 0$ the Fermi level) one must start from the definition of eq. (4.25), namely,

$$\Gamma(E, T) = \frac{1}{\Omega n_0} \left\langle \sum_{\alpha} z_{\alpha} \Gamma_{\alpha}(E) \delta(\tilde{\omega}_{\alpha} - E) \right\rangle_{av} \quad (5.7)$$

However, the delta function $\delta(\tilde{\omega}_{\alpha} - E)$ cannot be expressed in terms of G_0 . It is still possible, nevertheless, to formulate the calculation in momentum space, albeit at the cost of some extra complication.

Using eqs. (4.23), (4.24),

$$\begin{aligned} \delta(\tilde{\omega}_{\alpha} - E) &= \left(\frac{\partial \tilde{\omega}_{\alpha}}{\partial \omega_{\alpha}} \right)^{-1} \delta(\omega_{\alpha} - E + \Delta_{\alpha}(E)) \\ &= \left. \frac{\partial \omega_{\alpha}}{\partial \tilde{\omega}_{\alpha}} \right|_{\tilde{\omega}_{\alpha} = E} \delta(\omega_{\alpha} - E + \Delta_{\alpha}(E)) \\ &= z_{\alpha}^{-1} \delta(E - \omega_{\alpha} - \Delta_{\alpha}(E)) \end{aligned} \quad (5.8)$$

Thus,

$$\Gamma = \frac{1}{\Omega n_0} \left\langle \sum_{\alpha} \Gamma_{\alpha}(E) \delta(E - \omega_{\alpha} - \Delta_{\alpha}(E)) \right\rangle_{av} \quad (5.9)$$

The delta-function looks like the spectral function of the interacting Green's function except that the imaginary part of the self-energy is somehow ignored. Recall that the self-energy, in any basis, has the following analytical structure

$$\begin{aligned}\Sigma(z) &= \Sigma^R(z) & \text{Im}z > 0 \\ &= \Sigma^A(z) & \text{Im}z < 0\end{aligned}\quad (5.10)$$

where $\Sigma^A(z), \Sigma^R(z)$ are analytic functions. $\Sigma_\alpha(z)$ then has a branch cut on the real axis where

$$\Sigma_\alpha(\omega - i0^+) - \Sigma_\alpha(\omega + i0^+) = \Sigma^A(\omega) - \Sigma^R(\omega) = 2i \Gamma_\alpha(\omega) \quad (5.11a)$$

$$\Sigma_\alpha(\omega - i0^+) + \Sigma_\alpha(\omega + i0^+) = \Sigma^A(\omega) + \Sigma^R(\omega) = 2 \Delta_\alpha(\omega) \quad (5.11b)$$

We can define a somewhat unconventional Green's function

$$\tilde{G}_\alpha(z) = G_{0\alpha}(z) + G_{0\alpha}(z) \frac{1}{2} [\Sigma_\alpha^A(z) + \Sigma_\alpha^R(z)] \tilde{G}_\alpha(z) \quad (5.12)$$

which gives

$$\tilde{G}_\alpha(E \pm i0^+) = \frac{1}{E - \omega_\alpha - \Delta_\alpha(E) \pm i0^+} \quad (5.13)$$

Hence eq. (5.2) is replaced by

$$\delta(E - \omega_\alpha - \Delta_\alpha(E)) = \frac{1}{2\pi i} [\tilde{G}_\alpha^A(E) - \tilde{G}_\alpha^R(E)] \quad (5.14)$$

and the function $\alpha(i\epsilon_{m'}, i\epsilon_m)$ is

$$\alpha(i\epsilon_{m'}, i\epsilon_m) = \frac{1}{\Omega} \left\langle \sum_\alpha \Sigma_\alpha(i\epsilon_{m'}) \tilde{G}_\alpha(i\epsilon_m) \right\rangle_{av}. \quad (5.15)$$

Again $\alpha(i\epsilon_{m'}, i\epsilon_m)$ is independent of representation and

$$\alpha(i\epsilon_{m'}, i\epsilon_m) = \frac{1}{\Omega} \left\langle \sum_{\mathbf{k}, \mathbf{k}'} \Sigma(\mathbf{k}, \mathbf{k}'; i\epsilon_{m'}) \tilde{G}(\mathbf{k}', \mathbf{k}; i\epsilon_m) \right\rangle_{av} \quad (5.16)$$

Equation (5.12) in the momentum basis is

$$\tilde{G}(\underline{k}, \underline{k}'; z) = G_0(\underline{k}, \underline{k}'; z) + \sum_{\underline{k}_1, \underline{k}_2} G^0(\underline{k}, \underline{k}_1; z) \frac{1}{2} \left[\Sigma^A(\underline{k}_1, \underline{k}_2; z) + \Sigma^R(\underline{k}_2, \underline{k}_1; z) \right] \tilde{G}(\underline{k}_2, \underline{k}'; z) \quad (5.17)$$

and thus $\tilde{G}(\underline{k}, \underline{k}'; z)$ can be calculated using the same diagrams as the interacting Green's function, except that each self-energy insertion $\Sigma(\underline{k}, \underline{k}'; z)$ is to be interpreted as $(1/2) \left[\Sigma^A(\underline{k}, \underline{k}'; z) + \Sigma^R(\underline{k}, \underline{k}'; z) \right]$. The function $\alpha(i\epsilon_m, i\epsilon_m)$ is still given by the average of the diagram of Fig. 5.1, but now the upper Green's function is the fully renormalized one and the lower one is this unconventional \tilde{G} . This way we can still make full use of the apparatus of Feynman diagrams.

In section 5.2 we shall calculate the quasiparticle lifetime in the simplest approximation which consists of replacing the average of the product of the two Green's functions by the product of their averages. We shall use the simpler definition of $\alpha(i\epsilon_m, i\epsilon_m)$ (eq. (5.1)). We obtain in this approximation the same result as for the pure metal.

In sections 5.3 and 5.4 we consider the effect of the diffusive poles described in Chapter 4 (eqs. (4.8), (4.10)) in the quasiparticle lifetime. We shall recover the result of AALR and present the full self-consistent calculation. Finally, in section 5.5 we discuss some experimental results.

5.2 Clean Limit Contribution to the Quasiparticle Lifetime

The simplest diagram one can obtain from the average of the diagram of Fig. 5.1 is the one in which we replace the average of the product of the two Green's functions by the product of their averages. The diagram we obtain does not

contain explicitly any impurity lines. We can anticipate, then, that its leading $1/k_F^{\ell}$ contribution will be the result for the clean metal. We shall later consider corrections to this diagram which do contain impurity lines. Their contribution must then vanish when $k_F^{\ell} \rightarrow \infty$. We shall therefore refer to the contribution calculated in this section as the clean limit contribution.

We have

$$\alpha_0(i\epsilon_{m'}, i\epsilon_m) = - \int \frac{d^d k}{(2\pi)^d} G_0(\mathbf{k}, i\epsilon_m) \times \int \frac{d^d q}{(2\pi)^d} \frac{1}{\beta} \sum_{\omega_q} V_c(q, i\omega_q) G_0(\mathbf{k}+\mathbf{q}, i\epsilon_m + i\omega_q) \quad (5.18)$$

The frequency sum is calculated in the usual manner

$$\alpha_0(i\epsilon_{m'}, i\epsilon_m) = - \int \frac{d^d k}{(2\pi)^d} G_0(\mathbf{k}, i\epsilon_m) \times \int \frac{d^d q}{(2\pi)^d} \int_{-\infty}^{+\infty} \frac{d\eta}{2\pi i} \left\{ N(\eta) [V_c^R(q, \eta) - V_c^A(q, \eta)] G_0(\mathbf{k}+\mathbf{q}, \eta + i\epsilon_{m'}) + N(\eta - i\epsilon_{m'}) V_c(q, \eta - i\epsilon_{m'}) [G_0^R(\mathbf{k}+\mathbf{q}, \eta) - G_0^A(\mathbf{k}+\mathbf{q}, \eta)] \right\}$$

or, in terms of the spectral functions of the electron propagator $\rho_0(\mathbf{k}, \eta)$ and the Coulomb interaction $\sigma_c(q, \eta)$

$$\alpha_0(i\epsilon_{m'}, i\epsilon_m) = \int \frac{d^d k}{(2\pi)^d} G_0(\mathbf{k}, i\epsilon_m) \times \int \frac{d^d q}{(2\pi)^d} \int \frac{d\eta}{2\pi} \left[N(\eta) \sigma_c(q, \eta) G_0(\mathbf{k}+\mathbf{q}, \eta + i\epsilon_{m'}) - f(\eta) V_c(q, \eta - i\epsilon_{m'}) \rho_0(\mathbf{k}+\mathbf{q}, \eta) \right] \quad (5.19)$$

where

$$\rho_0(\mathbf{k}, \eta) \equiv \frac{1}{i} [G_0^A(\mathbf{k}, \eta) - G_0^R(\mathbf{k}, \eta)] = \frac{1/\tau}{(\eta - \omega_{\mathbf{k}})^2 + (1/2\tau)^2} \quad (5.20)$$

$$\sigma_c(q, \eta) \equiv \frac{1}{i} [V_c^A(q, \eta) - V_c^R(q, \eta)] = 2 \text{Im} V_c^A(q, \eta) \quad (5.21)$$

From eqn. (5.19) we get

$$\begin{aligned} \alpha_0^{RA}(\mathbf{k}, \mathbf{E}) &= \int \frac{d^d \mathbf{k}}{(2\pi)^d} G_0^A(\mathbf{k}, \mathbf{E}) \\ &\times \int \frac{d^d \mathbf{q}}{(2\pi)^d} \int \frac{d\eta}{2\pi} \left\{ N(\eta) \sigma_c(q, \eta) G_0^R(\mathbf{k}+\mathbf{q}, \eta+\mathbf{E}) \right. \\ &\quad \left. - f(\eta+\mathbf{E}) V_c^A(q, \eta) \rho_0(\mathbf{k}+\mathbf{q}, \eta+\mathbf{E}) \right\} \end{aligned} \quad (5.22a)$$

$$\begin{aligned} \alpha_0^{AA}(\mathbf{k}, \mathbf{E}) &= \int \frac{d^d \mathbf{k}}{(2\pi)^d} G_0^A(\mathbf{k}, \mathbf{E}) \\ &\times \int \frac{d^d \mathbf{q}}{(2\pi)^d} \int \frac{d\eta}{2\pi} \left\{ N(\eta) \sigma_c(q, \eta) G_0^A(\mathbf{k}+\mathbf{q}, \eta+\mathbf{E}) \right. \\ &\quad \left. - f(\eta+\mathbf{E}) V_c^R(q, \eta) \rho_0(\mathbf{k}+\mathbf{q}, \eta+\mathbf{E}) \right\} \end{aligned} \quad (5.22b)$$

The quasiparticle lifetime is then,

$$\Gamma_0 = \frac{1}{2\pi\eta_0} \int \frac{d^d \mathbf{k}}{(2\pi)^d} \rho_0(\mathbf{k}, \mathbf{E}) \Sigma_2(\mathbf{k}, \mathbf{E}) \quad (5.23)$$

where

$$\Sigma_2(\mathbf{k}, \mathbf{E}) = \frac{i}{4\pi} \int \frac{d^d \mathbf{q}}{(2\pi)^d} \int d\eta [N(\eta) + f(\eta+\mathbf{E})] \sigma_c(q, \eta) \rho_0(\mathbf{k}+\mathbf{q}, \eta+\mathbf{E}) \quad (5.24)$$

has exactly the form we would get for the imaginary part of the

self-energy in the pure system. Thus, in this approximation Γ_0 is just a momentum average of $Z_2(\underline{k}, \epsilon)$ weighted by a distribution $p_0(\underline{k}, \epsilon)$.

We shall in general calculate the temperature dependence of Γ_0 on the Fermi surface, i.e. put $E = 0$.

It is useful to make the change of variable $\underline{k} + \underline{q} \rightarrow \underline{k}'$ in eq. (5.24)

$$Z_2(\underline{k}, 0) = \frac{1}{4\pi} \int_{-\infty}^{+\infty} d\eta [N(\eta) + f(\eta)] \int \frac{d^d \underline{k}'}{(2\pi)^d} p_0(\underline{k}', \eta) \sigma_c(\underline{k} - \underline{k}', \eta). \quad (5.25)$$

The spectral function $\sigma_c(\underline{k} - \underline{k}', \eta)$ depends on the momenta via $|\underline{k} - \underline{k}'|$,

$$|\underline{k} - \underline{k}'|^2 = k^2 + k'^2 - 2kk' \cos \theta = (k - k')^2 + 4kk' \sin^2 \theta / 2 \quad (5.26)$$

The range of variation of $\omega_{\underline{k}}, \omega_{\underline{k}'}$ in eq. (5.23) is $|\omega_{\underline{k}}|, |\omega_{\underline{k}'}| \leq \text{Max} \{ k_B T, 1/2\tau \}$ because the electronic spectral functions are lorentzians peaked at $\omega_{\underline{k}} \approx 0$ $\omega_{\underline{k}'} \approx \eta$ with a width $1/2\tau$. So for $\sin \theta / 2 > \text{Max} \{ 1/k_F \ell, k_B T / \epsilon_F \}$ the second term of eq. (5.26) dominates and $\sigma_c(\underline{k} - \underline{k}', \eta)$ varies with $\omega_{\underline{k}}, \omega_{\underline{k}'}$ on a scale of order ϵ_F . We can then replace the electronic spectral functions by the corresponding delta functions

$$p_0(\underline{k}, \eta) \rightarrow 2\pi \delta(\omega_{\underline{k}} - \eta) \quad (5.27)$$

to get

$$\Gamma_0 = Z_2(k_F, 0) = \frac{n_0}{2} \int_{-\infty}^{+\infty} d\eta [N(\eta) + f(\eta)] \int_{R=k' \cdot k_F} d^d \Omega \sigma(\underline{k} - \underline{k}', \eta) \quad (5.28)$$

where $d^d \Omega$ is the element of angular integration in d

dimensions normalized to unity (eq. (C.3)).

The spectral density of the Coulomb interaction is discussed in detail in Appendix E. It is given exactly by

$$\sigma_c(q, \eta) = \frac{2 V_B^2(q) \Pi_2(q, \eta)}{[1 - V_B(q) \Pi_1(q, \eta)]^2 + [V_B(q) \Pi_2(q, \eta)]^2} \quad (5.29)$$

where $V_B(q)$ is the bare Coulomb interaction,

$$V_B(q) = \frac{4\pi e^2}{q^2} \quad ; \quad \text{in } 3D \quad (5.30a)$$

$$= \frac{2\pi e^2}{q} \quad ; \quad \text{in } 2D \quad (5.30b)$$

and $\Pi_1(q, \eta)$ and $\Pi_2(q, \eta)$ are the real and imaginary parts of the polarization function $\Pi(q, i\omega_2)$. At low frequencies $\Pi_2(q, \eta)$ is linear in η and $\Pi_1(q, \eta)$ tends to a constant. It is shown in Appendix E that for q not too close to 0 or $2k_F$, i.e.,

$$\delta \ll \frac{q}{2k_F} \ll 1 - \delta \quad (5.31)$$

where

$$\delta \approx \text{Max} \left\{ \frac{|\eta|}{\epsilon_F}, \frac{1}{k_F l} \right\} \ll 1 \quad (5.32)$$

we can approximate $\sigma_c(q, \eta)$ by

$$\sigma_c(q, \eta) = 2 V_{ss}^2(q) \Pi_2(q, \eta) \quad (5.33)$$

where $V_{SS}(q)$, the static screened Coulomb interaction, is

$$V_{SS}(q) \equiv \frac{V_B(q)}{1 - V_B(q) \Pi_1(q, 0)} \quad (5.34)$$

and

$$\Pi_2(q, \eta) = \pi n_0 \frac{\eta}{v_F q} \quad ; \quad \text{in 3D} \quad (5.35a)$$

$$= 2n_0 \frac{\eta}{v_F q \sqrt{1 - (q/2k_F)^2}} \quad ; \quad \text{in 2D} \quad (5.35b)$$

Using $q \approx 2k_F |\sin \theta/2|$ we can rewrite these results as

$$\Pi_2(q, \eta) = \frac{\pi n_0}{4 \epsilon_F} \frac{\eta}{\sin \theta/2} \quad ; \quad \text{in 3D} \quad (5.36a)$$

$$= \frac{n_0}{\epsilon_F} \frac{\eta}{|\sin \theta|} \quad \text{in 2D} \quad (5.36b)$$

In 3D then,

$$\Gamma_0 = \frac{\pi n_0^2}{4 \epsilon_F} \int_{-\infty}^{+\infty} d\eta \frac{\eta}{\sinh \beta \eta} \int d\Omega \frac{V_{SS}^2(\theta)}{\sin \theta/2}$$

The cutoff parameter δ in the angular integration can be ignored and

$$\Gamma_0 = \frac{\pi^3}{8} g^2 \frac{(k_B T)^2}{\epsilon_F} \quad (5.37)$$

with

$$g^2 \equiv 2n_0^2 \left\langle \frac{V_{SS}^2(\theta)}{\sin \theta/2} \right\rangle \quad (5.38)$$

The brackets denote an angular average over the Fermi surface.

This is the result one gets for clean metals using Boltzmann's equation with a scattering probability $2\pi V_{SS}^2(\theta)$ (Baym and Pethick 1978). Using the Thomas-Fermi approximation for $V_{SS}(q)$ one can show that $g^2 \rightarrow 1$ for short range effective interactions ($\kappa/k_F \gg 1$) where κ is the inverse screening radius) and $g^2 = \frac{\pi}{4}(\kappa/k_F)$ for long range interactions ($\kappa/k_F \ll 1$).

In 2D the cutoff parameter in the angular integration cannot be ignored because the angular integral diverges near $\theta \approx 0, \pi$. The restriction of eq. (5.31) is equivalent to

$$\delta \ll |\sin \theta/2| \ll 1 - \delta \iff \delta \ll |\theta| \ll \pi - \sqrt{\delta}$$

and so, using $V_{SS}(\theta) = V_{SS}(-\theta)$ to integrate θ between 0 and π ,

$$\Gamma_0 = \frac{2n_0^2}{\epsilon_F} \int_{-\infty}^{+\infty} d\eta \frac{\eta}{\sinh \beta \eta} \int_{\delta}^{\pi - \sqrt{\delta}} \frac{d\theta}{2\pi} \frac{V_{SS}^2(\theta)}{|\sin \theta|}$$

$$\approx \frac{2n_0^2}{\pi \epsilon_F} [V_{SS}^2(\theta=0) + \frac{1}{2} V_{SS}^2(\theta=\pi)] \int_0^{+\infty} d\eta \frac{\eta}{\sinh \beta \eta} \frac{d\eta}{\delta}$$

For $k_B T \gg \tau^{-1}$ $\delta = |\eta|/\epsilon_F$,

$$\Gamma_0(T) = \frac{\pi}{2} g^2 \frac{(k_B T)^2}{\epsilon_F} \ln \left[\frac{\epsilon_F}{k_B T} \right] \quad (5.39)$$

and for $k_B T \ll \tau^{-1}$ $\delta = 1/k_F \ell$

$$\Gamma_0(T) = \frac{\pi}{2} g^2 \frac{(k_B T)^2}{\epsilon_F} \ln k_F \ell \quad (5.40)$$

where

$$g^2 \equiv 2n_0^2 \left[V_{SS}^2(\theta=0) + \frac{1}{2} V_{SS}^2(\theta=\pi) \right]. \quad (5.41)$$

The $T^2 \ln(\epsilon_F/k_B T)$ temperature dependence of eq. (5.39) has been found previously by Guiliani and Quinn (1982) in a corresponding calculation for pure metals (first order in the screened Coulomb interaction). These authors, however, neglect the $\theta = \pm\pi$ singularity and obtain instead of eq. (5.41) $g^2 \propto n_0^2 V_{SS}^2(\theta=0)$. In a calculation of Γ_0 done with the Boltzmann electron-electron collision integral also in pure metals (unpublished) we found $g^2 = 2n_0^2 [V_{SS}^2(\theta=0) + V_{SS}^2(\theta=\pi)]$. The calculation presented here appears to be correct but the treatment of the logarithmic singularity is possibly oversimplified.

5.3 Contribution of the Particle-Hole Diffusion Pole to the Quasiparticle Lifetime

In the diagram of Fig. 5.1 we have to calculate an average of a product of two Green's functions. In the previous section we replaced that average by a product of the averaged Green's functions and obtained (eqs. (5.23), (5.24))

$$\Gamma(\tau) = \frac{1}{2} \int \frac{d^d q}{(2\pi)^d} \int_{-\infty}^{+\infty} d\eta [N(\eta) + f(\eta)] \sigma_c(q, \eta) A(q, \eta) \quad (5.42)$$

with

$$A(q, \eta) = \frac{1}{4\pi^2 n_0} \int \frac{d^d k}{(2\pi)^d} \rho_0(\mathbf{k}, 0) \rho_0(\mathbf{k} + \mathbf{q}, \eta) \quad (5.43)$$

This function $A(q, \eta)$ which arises from the product of the averaged Green's functions tends to a constant as $\eta \rightarrow 0$. The Coulomb spectral function $\sigma_c(q, \eta)$ is linear in η for

low η and therefore $\Gamma_0(T)$ varies as T^2 at low temperatures. But in Chapter 4 we saw that the two particle Green's function is singular at low frequency for certain values of the external momenta. We must then consider the effect of the particle-hole and particle-particle diffusion propagators (eqs. (4.8), (4.10)) in $\alpha(i\epsilon_{m'}, i\epsilon_m)$ (Fig. 5.2).

The Coulomb spectral function $\sigma_c(q, \eta)$ is large for small momentum q (see eq. E.19) and the diagram of Fig. 5.2(a), with the particle-hole propagator, gives the dominant contribution. In the diagram of Fig. 5.2(b) the momentum transferred by the interaction is of order $2k_F$ when the particle-particle propagator is large.

For the term of Fig. 5.2(a) we have

$$\begin{aligned} \alpha(i\epsilon_{m'}, i\epsilon_m) = & - \int \frac{d^d k}{(2\pi)^d} \frac{d^d k'}{(2\pi)^d} \int \frac{d^d q}{(2\pi)^d} \frac{1}{\beta} \sum_{\omega_2} V_c(q, i\omega_2) \\ & \times G_0(k, i\epsilon_m) G_0(k', i\epsilon_m) G_0(k'+q, i\epsilon_{m'}+i\omega_2) G_0(k+q, i\epsilon_{m'}+i\omega_2) \\ & \times D_0(q; i\epsilon_{m'}+i\omega_2, i\epsilon_m) . \end{aligned} \quad (5.44)$$

When $\epsilon_m(\epsilon_{m'}+i\omega_2) > 0$ or $q\ell \gg 1$ we have (see Appendix C), $I(q; i\epsilon_{m'}+i\omega_2, i\epsilon_m) \equiv \int \frac{d^d k}{(2\pi)^d} G_0(k+q, i\epsilon_{m'}+i\omega_2) G_0(k, i\epsilon_m) \ll 1$. It follows, then, from eq. (4.7) that D_0 becomes equal to the first term in the ladder series of Fig. 4.3, i.e.

$D_0 \approx (2\pi n_0 \tau)^{-1} \approx v^2$. The term of eq. (5.44) then becomes smaller than the one calculated in the previous section by the factor $I(q; i\epsilon_{m'}+i\omega_2, i\epsilon_m) \ll 1$. So, as before in the calculation of corrections to the Boltzmann result for the conductivity (see Chapter 4), we consider in eq. (5.44) only the terms in which the diffusion poles occur, i.e. terms with $\epsilon_m(\epsilon_{m'}+i\omega_2) < 0$ and $q\ell < 1$ (eq. (4.8)). For $\alpha^{RA}(i\epsilon_{m'}, i\epsilon_m)$

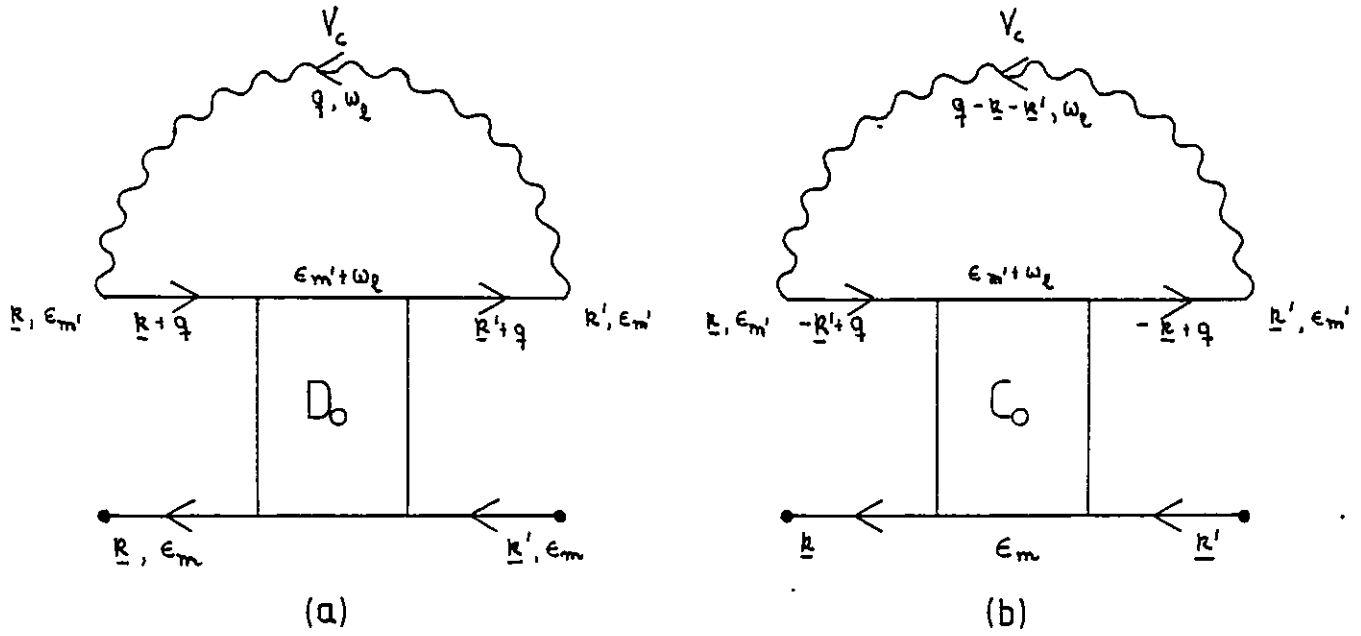


FIG 5.2

Contribution of particle-hole (a) and particle-particle (b) diffusion propagators to $\alpha(i\epsilon_m', i\epsilon_m)$

we have $\epsilon_m < 0$, so we consider only terms with $\epsilon_m + \omega_\ell > 0$,

$$\begin{aligned} \alpha^{RA}(\epsilon_{m'}, \epsilon_m) &= - \int \frac{d^d q}{(2\pi)^d} \frac{1}{\beta} \sum_{\omega_\ell > -\epsilon_{m'}} V_c(q, i\omega_\ell) \mathcal{D}_0^{RA}(q; \epsilon_{m'} + i\omega_\ell, \epsilon_m) \\ &\quad \times \int \frac{d^d k}{(2\pi)^d} \frac{d^d k'}{(2\pi)^d} G_0^A(\underline{k}, \epsilon_m) G_0^A(\underline{k}', \epsilon_m) G_0^A(\underline{k} + \underline{q}, \epsilon_{m'} + i\omega_\ell) \\ &\quad \times G_0^R(\underline{k}' + \underline{q}; \epsilon_{m'} + i\omega_\ell). \end{aligned}$$

The most singular term is obtained by expanding the Green's functions in powers of q and ω_ℓ . Recalling that, in the end, the frequencies $\epsilon_{m'}, \epsilon_m$ are continued to the same real value we may write

$$\begin{aligned} \alpha^{RA}(\epsilon_{m'}, \epsilon_m) &= - \int \frac{d^d q}{(2\pi)^d} \sum_{\omega_\ell > -\epsilon_{m'}} V_c(q, i\omega_\ell) \mathcal{D}_0^{RA}(q; \epsilon_{m'} + i\omega_\ell, \epsilon_m) \\ &\quad \times \left[\int \frac{d^d k}{(2\pi)^d} G_0^A(\underline{k}, \epsilon_m) G_0^R(\underline{k}, \epsilon_m) \right]^2 \\ &= - I_{11}^2 \int \frac{d^d q}{(2\pi)^d} \sum_{\omega_\ell > -\epsilon_{m'}} V_c(q, i\omega_\ell) \mathcal{D}_0^{RA}(q; \epsilon_{m'} + i\omega_\ell, \epsilon_m). \quad (5.46) \end{aligned}$$

The integrals I_{pq} are defined and calculated in Appendix D.

This gives, after doing the frequency summations,

$$\begin{aligned} \alpha^{RA}(\epsilon_{m'}, \epsilon_m) &= (2\pi n_0 \tau)^2 \int \frac{d^d q}{(2\pi)^d} \int_{-\infty}^{+\infty} \frac{d\eta}{2\pi} \left\{ N(\eta) \sigma_c(q, \eta) \mathcal{D}_0^{RA}(q; \eta + i\epsilon_{m'}, \epsilon_m) \right. \\ &\quad \left. + \frac{1}{i} f(\eta) V_c(q, \eta - i\epsilon_{m'}) \mathcal{D}_0^{RA}(q; \eta + i0^+, \epsilon_m) \right\} \quad (5.47) \end{aligned}$$

which, after the analytic continuations $\epsilon_{m'} \rightarrow E + i0^+$, $\epsilon_m \rightarrow E - i0^+$ is

$$\begin{aligned} \alpha^{RA}(\epsilon, \epsilon) &= 2\pi n_0^2 \tau^2 \int \frac{d^d q}{(2\pi)^d} \int_{-\infty}^{+\infty} d\eta [N(\eta) + f(\eta + \epsilon)] \sigma_c(q, \eta) \mathcal{D}_0^{RA}(q; \epsilon + \eta, \epsilon) \\ &\quad - 2\pi i n_0^2 \tau^2 \int \frac{d^d q}{(2\pi)^d} \int_{-\infty}^{+\infty} d\eta f(\eta + \epsilon) V_c^R(q, \eta) \mathcal{D}_0^{RA}(q; \epsilon + \eta, \epsilon) \end{aligned} \quad (5.48)$$

We can calculate $\alpha^{AA}(i\epsilon_m', i\epsilon_m)$ in a similar fashion,

$$\alpha^{AA}(i\epsilon_m', i\epsilon_m) = -(2\pi n_0 \tau)^2 \int \frac{d^d q}{(2\pi)^d} \frac{1}{\beta} \sum_{\omega_p > -\epsilon_m'} V_c(q, i\omega_p) \mathcal{D}_0^{RA}(q; i\epsilon_m' + i\omega_p, i\epsilon_m) \quad (5.49)$$

which gives

$$\alpha^{AA}(\epsilon, \epsilon) = -2\pi i n_0 \tau^2 \int \frac{d^d q}{(2\pi)^d} \int_{-\infty}^{+\infty} d\eta f(\eta + \epsilon) V_c^R(q, \eta) \mathcal{D}_0^{RA}(q; \epsilon + \eta, \epsilon) \quad (5.50)$$

Therefore the quasiparticle inverse lifetime is,

$$\begin{aligned} \Gamma(\epsilon, T) &= n_0 \tau^2 \int \frac{d^d q}{(2\pi)^d} \int_{-\infty}^{+\infty} d\eta [N(\eta) + f(\eta + \epsilon)] \sigma_c(q, \eta) \text{Re} \mathcal{D}_0^{RA}(q, \epsilon + \eta, \epsilon) \\ &= \frac{1}{2\pi} \int_{q < \ell'} \frac{d^d q}{(2\pi)^d} \int_{-\infty}^{+\infty} d\eta [N(\eta) + f(\eta + \epsilon)] \sigma_c(q, \eta) \text{Re} \frac{i}{\eta + i\mathcal{D}q^2} \end{aligned} \quad (5.51)$$

This is exactly the result of AALR (c.f. eqs. (4.31), (4.33)

with $\omega = \epsilon$). In 3D an explicit evaluation recovers the result of Schmid (1974). From eq. (E.19),

$$\sigma_c(q, \eta) = \frac{8\pi e^2}{q^2} \frac{\eta \epsilon}{\eta^2 + \epsilon^2} \quad q\ell, \eta\tau \ll 1, 3D$$

where $\epsilon = \mathcal{D}k_F^2 \gg \epsilon_F$ and ℓ the inverse screening radius is $k_F^2 = 8\pi n_0 e^2 = 4me^2 k_F / \pi$. Hence, for $k_B T \ll \tau^{-1} \ll \epsilon$

$$\Gamma(\tau) = \frac{4e^2}{\pi^2 \epsilon} \int_0^\infty d\eta \frac{\eta}{\sinh \beta \eta} \int_0^{\ell^{-1}} dq \frac{Dq^2}{\eta^2 + (Dq^2)^2}$$

The upper limit of the q integral can be put equal to $+\infty$ because the integral is dominated by $q \sim \sqrt{D/\eta} \ll \ell^{-1}$ for $\eta \ll \tau^{-1}$. We obtain,

$$\begin{aligned} \Gamma(\tau) &= \frac{4e^2}{\pi^2 \epsilon \sqrt{D}} \int_0^\infty d\eta \frac{\eta^{1/2}}{\sinh \beta \eta} \int_0^\infty du \frac{u^2}{1+u^4} \\ &= \frac{\alpha}{(k_F \ell)^{3/2}} \frac{(k_B T)^{3/2}}{\epsilon_F^{1/2}} \end{aligned} \quad (5.52)$$

where

$$\alpha = \frac{3\sqrt{3}}{4} \int_0^\infty dx \frac{x^{1/2}}{\sinh x}.$$

This is the result obtained by Schmid.

In 2D we have (eq. (E.19))

$$\sigma_c(q, \eta) = 4\pi e^2 \frac{D\kappa}{\eta^2 + \epsilon Dq^2} \quad ; \quad q\ell, \eta\tau \ll 1, \quad 2D \quad (5.53)$$

where κ is the inverse screening radius in 2D $\kappa = 4\pi e^2 \eta_0 = 2me^2$ and $\epsilon = D\kappa^2$ again. For $k_B T \ll \tau^{-1}$

$$\Gamma(\tau) = \frac{2e^2 \kappa}{\pi \epsilon} \int_0^\infty d\eta \frac{\eta}{\sinh \beta \eta} \int_0^{\ell^{-1}} dq \frac{Dq}{\eta^2 + Dq^2} \frac{Dq^2}{\eta^2 + (Dq^2)^2} \quad (5.54)$$

If we make a change of variable $u^2 = Dq^2/|\eta|$ in the q integral we find that, at low η , it varies as $1/|\eta|$. The η integral then diverges near $\eta = 0$. This is the divergence we mentioned in Chapter 4 (eq. (4.34)). We now show that this divergence is cured by renormalizing the electron propagator which appears in

the interaction self-energy. As we saw in section 5.1, we must then use the definition of $\alpha(i\epsilon_m', i\epsilon_m)$ given in eq. (5.15). This function is still given by the average of the diagram of Fig. 5.1 except that now the upper Green's function is the fully renormalized $G(\underline{k}+q, \underline{r}'+q; i\epsilon_m' + i\omega_2)$ and the lower one is $\tilde{G}(\underline{k}', \underline{k}; i\epsilon_m)$ defined in eq. (5.17). After averaging over impurity configurations we again generate a clean limit contribution, in which the average of the product of the Green's functions is replaced by the product of their averages, and a correction to that term involving the particle-hole diffusion propagator D (Fig. 5.2(a)). Both the averaged Green's function and the particle-hole propagator are modified by the interactions. The Green's functions are well behaved at low frequencies and, at low temperatures, elastic scattering dominates the lifetime of a momentum state. We may then assume that the averaged Green's functions may be replaced by their noninteracting value $G_0(\underline{k}, i\epsilon_m)$. The only change in the calculation lies, then, in the renormalization of the particle-hole propagator, D .

As it was defined in Chapter 4 (Fig. 4.3), the unrenormalized particle-hole propagator D_0 was a true two particle Green's function for the noninteracting system. As is shown in Appendix E, its diffusive pole gives for the density-density correlation function the diffusive, low momentum and low frequency, behaviour that one expects from macroscopic hydrodynamic arguments (Forster 1975). The renormalized version of this propagator with which we now deal, D , is no longer a true two particle Green's function for the interacting system. It is generated from an average of $G(\underline{k}+q, \underline{k}'+q; i\epsilon_m' + i\omega_2)$ and $\tilde{G}(\underline{k}', \underline{k}; i\epsilon_m)$ and therefore has no interaction lines going between the upper

and lower Green's function. We shall soon find that the diffusive singularity in D will be cut off by a finite lifetime. The true interacting two particle Green's function, however, still shows a diffusive singularity as one expects from the macroscopic hydrodynamic arguments.

The propagator D , to which we shall refer simply as the renormalized particle-hole propagator, bearing in mind, however, the comments made above, obeys the equation represented in Fig. 5.3, where D_0 is the unrenormalized propagator defined in Chapter 4, and the block T contains the interactions. From the comments made above it follows that the interaction vertex T does not contain Coulomb lines going between the upper and lower Green's functions. By including the integration over external momenta in the definition of T the equation of Fig. 5.3 becomes an algebraic one,

$$\begin{aligned} D(q; i\epsilon_{m'}, i\epsilon_m) &= D_0(q; i\epsilon_{m'}, i\epsilon_m) \\ &+ D_0(q; i\epsilon_{m'}, i\epsilon_m) T(q; i\epsilon_{m'}, i\epsilon_m) D(q; i\epsilon_{m'}, i\epsilon_m) \quad (5.55) \\ &= \frac{1}{D_0^{-1}(q; i\epsilon_{m'}, i\epsilon_m) - T(q; i\epsilon_{m'}, i\epsilon_m)} \end{aligned}$$

We are interested in the singular term which occurs for $\epsilon_{m'} \epsilon_m < 0$,

$$D(q; i\epsilon_{m'}, i\epsilon_m) = \frac{1}{2\pi n_0 \tau^2 [|\Omega_\lambda| + Dq^2 + \frac{1}{\tau_D}]} \quad ; \epsilon_{m'} \epsilon_m < 0 \quad (5.56)$$

where $\Omega_\lambda \equiv \epsilon_{m'} - \epsilon_m$ and

$$\frac{1}{\tau_D(i\epsilon_{m'}, i\epsilon_m)} = - \frac{1}{2\pi n_0 \tau^2} T(q=0; i\epsilon_{m'}, i\epsilon_m) \quad (5.57)$$

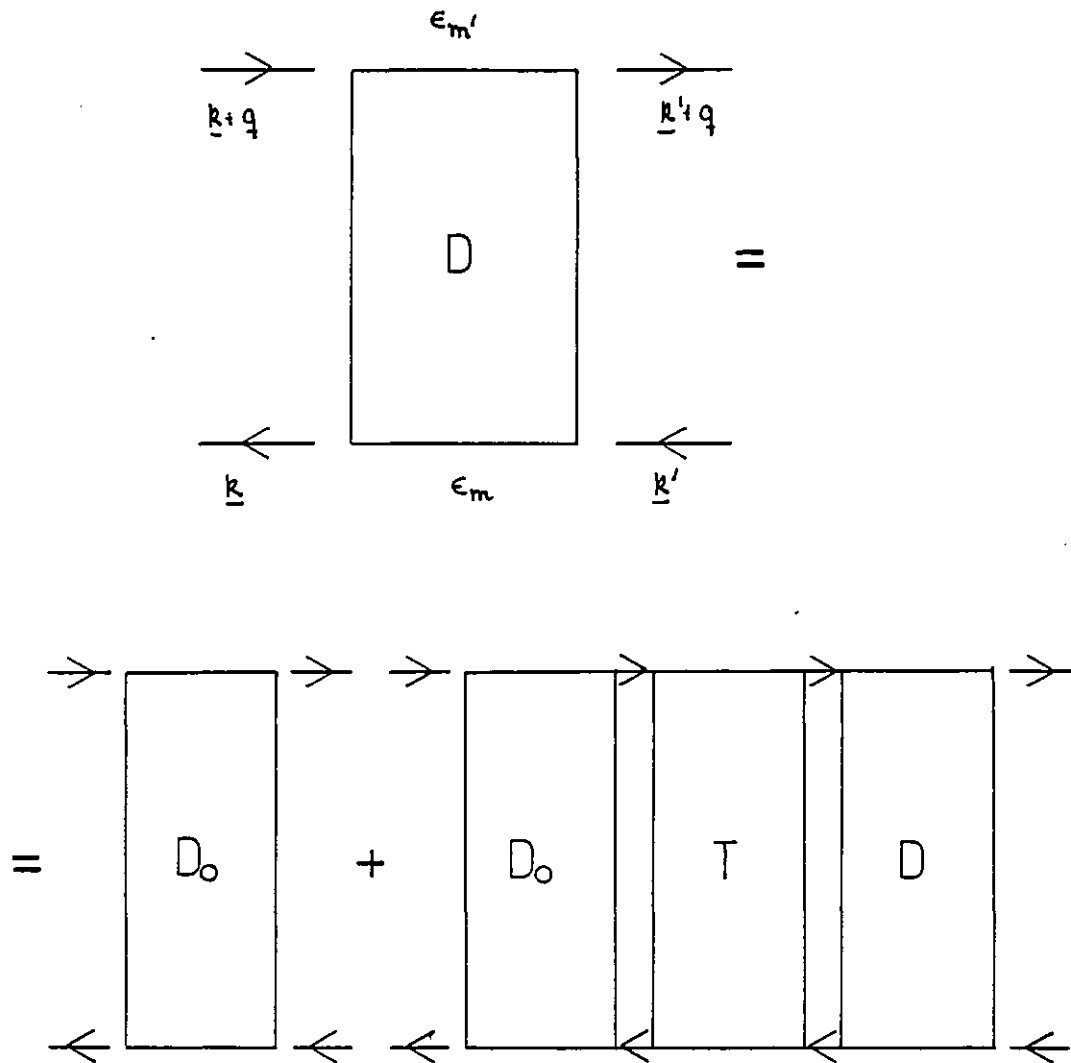


FIG 5.3

Equation for the renormalized particle-hole propagator D .
The block T contains the interactions.

We have taken the limit $q \rightarrow 0$ in T because we only need the leading q, Ω_λ term in the denominator of D . We shall eventually make the analytic continuations $i\epsilon_m \rightarrow \epsilon + \eta \pm i0^+$ and $i\epsilon_m \rightarrow \epsilon \mp i0^+$ and we may again put $\eta = 0$ in $1/\tau_D$,

$$\frac{1}{\tau(\epsilon, T)} \equiv \frac{1}{\tau_D^{RA}(\epsilon, \epsilon)} = - \frac{1}{2\pi n_0 \tau^2} T(q=0; \epsilon + i0^+, \epsilon - i0^+) \quad (5.58)$$

(We shall see that τ_D is real; so $\tau_D^{RA} = \tau_D^{AR}$).

In the next section we shall calculate τ_D the lifetime of the D propagator. For the moment let us return to the quasiparticle lifetime.

As we have said, renormalizing the ^{Green's} function in the self-energy and using the exact definition of quasiparticle lifetime of eq. (5.7) instead of the lowest order expression of eq. (5.1) amounts to replacing, in eq. (5.51), the bare particle-hole propagator D_0 given in eq. (4.8) by its renormalized version D given in eq. (5.56). Instead of eq. (5.51), then, we have,

$$\begin{aligned} \Gamma(\epsilon, T) = & \frac{1}{2\pi} \int \frac{d^d q}{(2\pi)^d} \int_{-\infty}^{+\infty} d\eta [N(\eta) + f(\eta + \epsilon)] \\ & \times \sigma_c(q, \eta) \operatorname{Re} \frac{i}{\eta + i D q^2 + \frac{i}{\tau_D}} \end{aligned} \quad (5.59)$$

which in 2D for $E \ll k_B T \ll \tau^{-1}$ is

$$\begin{aligned} \Gamma(T) = & \frac{2 e^2 \kappa}{\pi \epsilon} \int_0^\infty d\eta \frac{\eta}{\sinh \beta \eta} \\ & \times \int_0^\infty dq \frac{D q}{(\eta^2/\epsilon) + D q^2} \operatorname{Re} \frac{1}{i\eta + D q^2 + i/\tau_D} \end{aligned} \quad (5.60)$$

where we used the result of eq. (5.53) for the spectral function of the Coulomb interaction in the diffusive limit.

Defining a new variable of integration $v \equiv D q^2$ we can

do the q integral exactly,

$$\Gamma(\tau) = \frac{e^2 k}{\pi \epsilon} \int_0^{\infty} d\eta \frac{\eta}{\sinh \beta \eta} \operatorname{Re} \frac{1}{i\eta + \frac{1}{\tau_D} - \frac{\eta^2}{\epsilon}} \ln \frac{\epsilon [i\eta + 1/\tau_D]}{\eta^2} \quad (5.61)$$

For $\eta \ll \tau^{-1}$ we have $\eta^2/\epsilon \ll \eta$ and we can drop η^2/ϵ in the denominator of this equation. The η integral is divergent when $1/\tau_D \rightarrow 0$. The divergent term is, for $\tau_D k_B T \gg 1$

$$\begin{aligned} \Gamma(\tau) &= \frac{e^2 k}{2\epsilon} k_B T \ln [k_B T \epsilon \tau_D^2] \\ &= \frac{k_B T}{2k_F l} \ln [k_B T \epsilon \tau_D^2]. \end{aligned} \quad (5.62)$$

In the next section we shall see that $1/\tau_D$ is given by (eq. (5.89))

$$\frac{1}{\tau_D} = \frac{k_B T}{2k_F l} \ln \frac{T_2}{T} \quad (5.63)$$

Therefore to leading order in temperature

$$\Gamma(\tau) = \frac{1}{\tau_D(\tau)} = \frac{k_B T}{2k_F l} \ln \frac{T_2}{T} \quad (5.64)$$

with $k_B T_2 = 4(k_F l)^2 \epsilon$. This expression is valid for temperatures greater than $T^* \sim T_2 e^{-2k_F l} (1/\tau_D \ll k_B T)$.

We recall that the result obtained by AALR (eq. (4.36)) differs from this one both in the prefactor (they have an extra factor of 2) and in the temperature T_2 which, in their case, is $(k_F l)^2 \epsilon$. In the following we discuss the evaluation of τ_D and prove eq. (5.63).

5.4 The Lifetime of the Particle-hole Propagator D

The evaluation of the lifetime of the particle-hole propagator D , given in eq. (5.57) in terms of the interaction vertex V , is considerably more complicated than that of Γ in the previous section. The underlying principles, though, are the same, as we shall soon see. And in the end Γ and $1/\tau_D$ turn out to be equal. We shall restrict ourselves to the diagrams which are of first order in the screened Coulomb interaction. The simplest diagram for Γ is given in Fig. 5.4. It differs from the diagram which gives the clean limit contribution to Γ in that it has two extra Green's functions at the ends of the self-energy insertion. There is a corresponding diagram with the interaction line on the lower Green's function which must be treated according to the prescription of section 5.1. Note that the singular behaviour in the propagator $D(q; i\epsilon_{m'}, i\epsilon_m)$ only occurs for $\epsilon_{m'}\epsilon_m < 0$ (eq. (5.56)). We shall calculate τ_D for $\epsilon_{m'} > 0, \epsilon_m < 0$. In the other case of interest, $\epsilon_{m'} < 0, \epsilon_m > 0$ we would get the same result. The contribution of the diagram of Fig. (5.4) and its counterpart with the interaction line in the lower Green's function is

$$\frac{1}{\tau_D^0} = - \frac{1}{2\pi n_0 \tau^2} \left\{ \int \frac{d^d k}{(2\pi)^d} [G_0^R(k, i\epsilon_{m'})]^2 G_0^A(k, i\epsilon_m) \Sigma^R(k, i\epsilon_{m'}) \right. \\ \left. + \int \frac{d^d k}{(2\pi)^d} G_0^R(k, i\epsilon_{m'}) [G_0^A(k, i\epsilon_m)]^2 \frac{1}{2} [\Sigma^A(k, i\epsilon_m) + \Sigma^R(k, i\epsilon_m)] \right\} \quad (5.65)$$

where

$$\Sigma(k, i\epsilon_{m'}) = - \int \frac{d^d q}{(2\pi)^d} \frac{1}{\beta} \sum_{\omega_2} V_c(q, i\omega_2) G_0(k+q, i\epsilon_{m'} + i\omega_2) \quad (5.66)$$

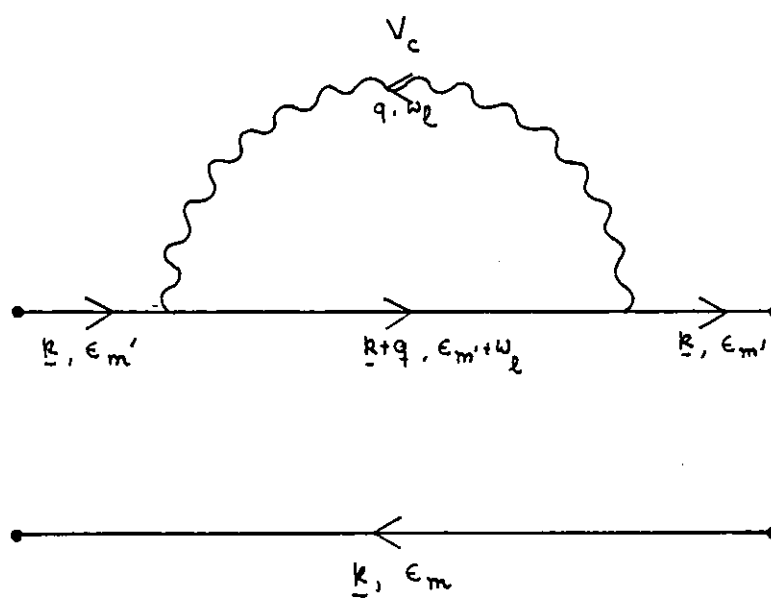


FIG 5.4

Clean limit contribution to $1/\tau_D$

The term in the second line of (5.65) corresponds to the diagram with the interaction line in the lower Green's functions. So, following the prescription of section 5.1, we have replaced the self-energy (which would be $\Sigma^A(\underline{k}, i\epsilon_m)$ because $\epsilon_m < 0$) by $(1/2) [\Sigma^A(\underline{k}, i\epsilon_m) + \Sigma^R(\underline{k}, i\epsilon_m)]$.

After the analytic continuations $i\epsilon_m \rightarrow E + i0^+$ and $i\epsilon_m \rightarrow E - i0^+$ (see eq. 5.58) we get from eq. (5.65)

$$\frac{1}{\tau_D^0} = - \frac{1}{2\pi\eta_0\tau^2} \int \frac{d^d k}{(2\pi)^d} \left\{ [G^R(\underline{k}, E)]^2 G^A(\underline{k}, E) \Sigma^R(\underline{k}, E) + G^R(\underline{k}, E) [G^A(\underline{k}, E)]^2 \frac{1}{2} [\Sigma^A(\underline{k}, E) + \Sigma^R(\underline{k}, E)] \right\}. \quad (5.67)$$

The imaginary part of $\Sigma^A(\underline{k}, E)$ was calculated in section (5.2) (eq. 5.24). It was shown that it is a weakly varying function of $\omega_{\underline{k}}$ (on a scale of order ϵ_F). The real part, $\Sigma_1(\underline{k}, E)$ is related to the imaginary part, $\Sigma_2(\underline{k}, E)$ by a Kramers-Krönig relation, therefore the same applies to it. Hence we can put $k = k_F$ in the self-energy functions in eq. (5.67) to get

$$\begin{aligned} \frac{1}{\tau_D^0} &= - \frac{I_{21}}{2\pi\eta_0\tau^2} \Sigma^R(k_F, E) - \frac{I_{12}}{2\pi\eta_0\tau^2} \frac{1}{2} [\Sigma^A(k_F, E) + \Sigma^R(k_F, E)] \\ &= - \frac{1}{2i} [\Sigma^R(k_F, E) - \Sigma^A(k_F, E)] = \Sigma_2(k_F, E) \\ &= \Gamma_0(\epsilon, T). \end{aligned} \quad (5.68)$$

Thus τ_D^0 is just the quasiparticle lifetime in the clean limit.

We shall consider the effect of the diffusion poles in the evaluation of τ_D . We shall soon see that τ_D is going to depend itself on the renormalized particle-hole propagator defined in eq. (5.56) and this will eventually lead to a self-

consistent equation for τ_D . Unfortunately the calculation is considerably complicated. The leading $1/k_F^2$ contributions to the interaction vertex T are shown in Fig. 5.5. Again, there is a similar set of diagrams with interaction lines in the lower Green's function which have to be treated according to the prescription of section 5.1.

Strictly speaking, the particle-hole propagators appearing in Figs. 5.5(a) - (c) are different from the one in Fig. 5.5(d). The particle-hole propagator appearing in Fig. 5.5(d) is the renormalized D propagator defined in the previous section (eq. 5.56) because it originates from the average of a product of the renormalized Green's function G and \tilde{G} . The particle-hole propagators in Figs. 5.5(a) - (c) originate from the average of a product of two G 's. For the moment, though, we shall replace them by the unrenormalized D_0 propagator defined in Chapter 4. Later we shall see that the only term in which we need to renormalize the D_0 propagator is that of Fig. 5.5(d).

The appearance of the diagrams of Figs. 5.5(a) and (d) is easy enough to understand. They represent the possible ways of inserting the particle-hole propagator in Fig. 5.4. In the diagram of Fig. 5.5(a) the diffusive poles occur when

$\epsilon_{m'} + \omega_\ell < 0$ (remember $\epsilon_{m'} > 0$) and $q\ell, \omega_\ell \tau \ll 1$. Hence the Green's function inside the self-energy insertion is essentially $G^A(\mathbf{k}, i\epsilon_{m'})$ which is of order τ for $|\omega_\ell|, |\epsilon_{m'}| \ll \tau^{-1}$. The diagram of Fig. 5.5(b) gives a contribution similar to that of Fig. 5.5(a) except that $G^A(\mathbf{k}, i\epsilon_{m'})$ is replaced by

$$u^2 \int \frac{d^d k}{(2\pi)^d} [G^R(\mathbf{k}, i\epsilon_{m'})]^2 G^A(\mathbf{k}, i\epsilon_{m'}) = \frac{I_{21}}{2\pi n_0 \tau}$$

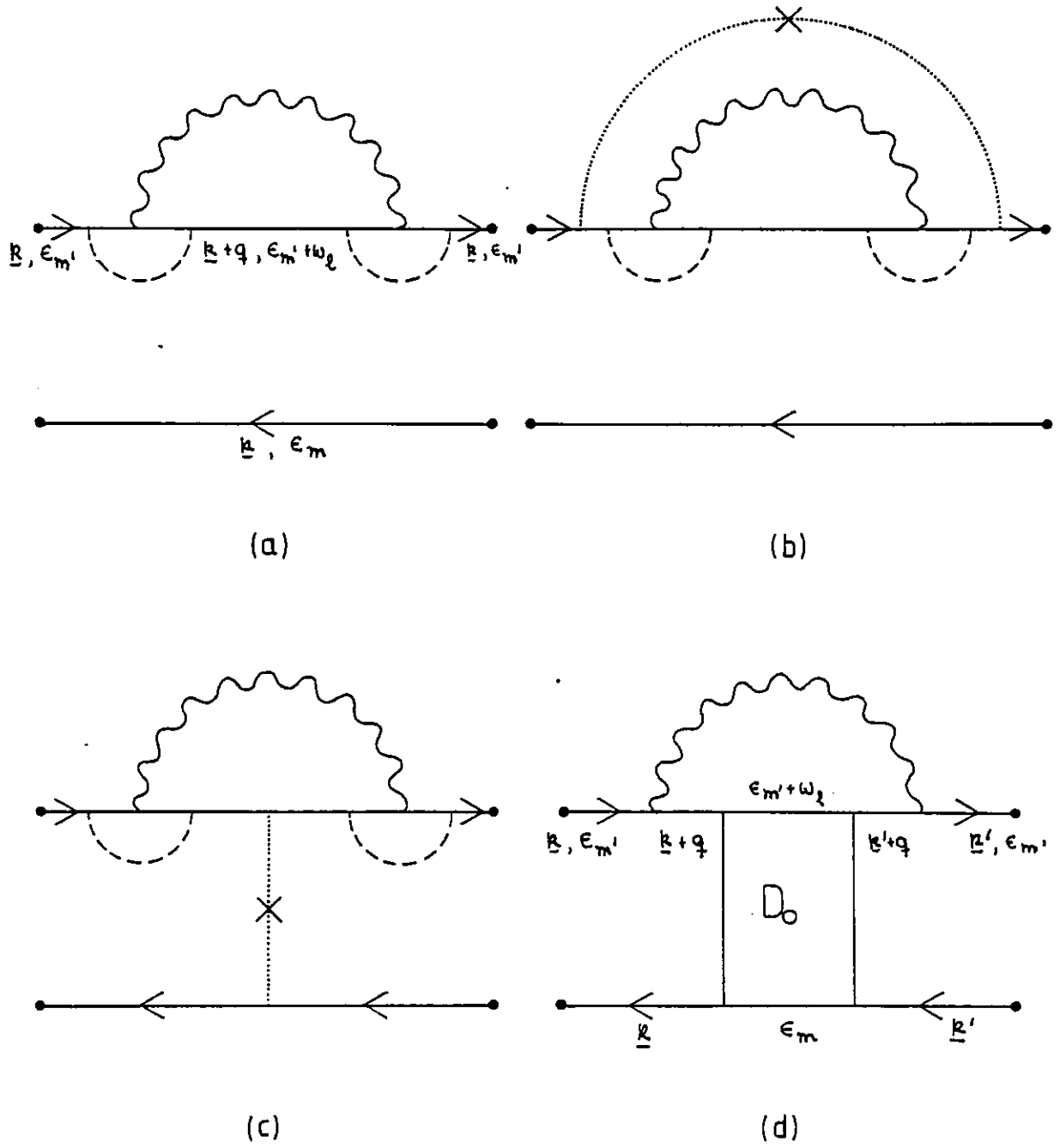


FIG 5.5

Contributions to the inverse lifetime of the renormalized D propagator.

which is also of order τ . The contribution of the diagram of Fig. 5.5(c) can be shown to be of the same order as the previous two in a similar way.

It is not easy to prove that all diagrams, other than these four, give smaller contributions. But the reader can easily convince himself that this is so if he keeps in mind the region of momentum and frequency in which the singular diffusive poles appear and the results of Appendix C for the integral $I(q; i\epsilon_m, i\epsilon_m)$. As an example consider inserting an impurity line in one of the interaction vertices in Fig. 5.5(d). This diagram is large for $\epsilon_{m'} + \omega_\ell > 0$, hence $\epsilon_{m'}(\epsilon_{m'} + \omega_\ell) > 0$ and such an insertion reduces the contribution of the diagram by a factor $I(q; i\epsilon_{m'} + i\omega_\ell, i\epsilon_{m'}) \sim 1/k_F\ell$.

The reader is warned that the following pages are a bit heavy with calculations and is well advised to skip a few pages (to eq. (5.87)) if he/she feels that his/her patience is dwindling!

We consider first the diagrams of Figs. 5.5(a) - (c). We denote their contribution by S_{a-c} ,

$$\begin{aligned}
 S_{a-c} = & \frac{1}{2\pi n_0 z^2} \int \frac{d^d q}{(2\pi)^d} \frac{1}{\beta} \sum_{\omega_\ell < -\epsilon_{m'}} V_c(q, i\omega_\ell) [\Gamma^{AR}(q; i\epsilon_{m'} + i\omega_\ell, i\epsilon_{m'})]^2 \\
 & \times \left\{ \int \frac{d^d k}{(2\pi)^d} [G_o^R(k, i\epsilon_{m'})]^2 G_o^R(k, i\epsilon_m) G_o^A(k+q, i\epsilon_{m'} + i\omega_\ell) \right. \\
 & + U^2 \int \frac{d^d k}{(2\pi)^d} \int \frac{d^d k'}{(2\pi)^d} [G_o^R(k, i\epsilon_{m'})]^2 G_o^A(k, i\epsilon_m) [G_o^R(k', i\epsilon_{m'})]^2 \\
 & \quad \left. \times G_o^A(k'+q, i\epsilon_{m'} + i\omega_\ell) \right. \\
 & \left. + U^2 \left[\int \frac{d^d k}{(2\pi)^d} G_o^R(k, i\epsilon_{m'}) G_o^A(k, i\epsilon_m) G_o^A(k+q, i\epsilon_{m'} + i\omega_\ell) \right]^2 \right\}
 \end{aligned}$$

where $\Gamma(q; i\epsilon_m + i\omega_\ell, i\epsilon_m)$ is defined by

$$\Gamma(q; i\epsilon_m + i\omega_\ell, i\epsilon_m) = \int \frac{d^d k}{(2\pi)^d} G_o(\underline{k} + q, i\epsilon_m + i\omega_\ell) G_o(\underline{k}, i\epsilon_m) \times D_o(q; i\epsilon_m + i\omega_\ell, i\epsilon_m) \quad (5.70)$$

which for $\epsilon_m(\epsilon_m + \omega_\ell) < 0$ and $q\ell, \omega_\ell\tau \ll 1$ is

$$\Gamma(q; i\epsilon_m + i\omega_\ell, i\epsilon_m) = \frac{I_{11}}{2\pi n_0 z^2 [|\omega_\ell| + Dq^2]} = \frac{1}{|\omega_\ell|\tau + Dq^2\tau} \quad (5.71)$$

As usual we expand the Green's functions inside the curly brackets of eq. (5.69) in powers of \underline{q} and ω_ℓ . We can also put $\epsilon_{m'} = \epsilon_m$ inside the curly brackets because we shall later continue $i\epsilon_{m'}$ and $i\epsilon_m$ to the same real value. For the first line of eq. (5.69) we get

$$\begin{aligned} & \int \frac{d^d k}{(2\pi)^d} [G^R(\underline{k}, i\epsilon_{m'})]^2 G^R(\underline{k}, i\epsilon_m) G^R(\underline{k} + q, i\epsilon_{m'} + i\omega_\ell) \\ & \approx \int \frac{d^d k}{(2\pi)^d} [G^R(\underline{k}, i\epsilon_m)]^2 [G^R(\underline{k}, i\epsilon_m)]^2 \{1 - i\omega_\ell G^R(\underline{k}, i\epsilon_m) + v_F^2 q^2 \cos^2\theta [G^R(\underline{k}, i\epsilon_m)]^2\} \\ & \approx I_{22} - i\omega_\ell I_{23} + \frac{v_F^2 q^2}{d} I_{24} \end{aligned}$$

where we used

$$\int d^d \Omega \cos^2\theta = \frac{1}{d} \quad (5.72)$$

Proceeding similarly for the other terms inside the curly brackets and using the results of Appendix D for the integrals I_{pq} one finds that the leading $\underline{q}, \omega_\ell$ term cancels and,

$$\begin{aligned} \{ \dots \} &= 2\pi n_0 \tau^3 [-\omega_\ell \tau + Dq^2 \tau] \\ &= 2\pi n_0 \tau^3 [\Gamma^{AR}(q; i\epsilon_{m'} + i\omega_\ell, i\epsilon_m)]^{-1} \end{aligned} \quad (5.73)$$

Therefore the leading contribution from the diagrams of Figs. 5.5(a) - (c) is

$$\begin{aligned} S_{a-c} &= \tau \int \frac{d^d q}{(2\pi)^d} \frac{1}{\beta} \sum_{\omega_\ell < -\epsilon_{m'}} V_c(q, i\omega_\ell) \Gamma^{AR}(q; i\epsilon_{m'} + i\omega_\ell, i\epsilon_m) \\ &= 2\pi n_0 \tau^2 \int \frac{d^d q}{(2\pi)^d} \frac{1}{\beta} \sum_{\omega_\ell < -\epsilon_{m'}} V_c(q, i\omega_\ell) D_0^{AR}(q; i\epsilon_{m'} + i\omega_\ell, i\epsilon_m). \end{aligned} \quad (5.74)$$

This gives, after doing the frequency sums and performing the analytic continuations $i\epsilon_{m'} \rightarrow \epsilon + i0^+$, $i\epsilon_m \rightarrow \epsilon - i0^+$

$$S_{a-c} = -i n_0 \tau^2 \int \frac{d^d q}{(2\pi)^d} \int_{-\infty}^{+\infty} d\eta f(\eta + \epsilon) V_c^A(q, \eta) D_0^{AR}(q; \epsilon, \eta, \epsilon). \quad (5.75)$$

The contribution of the corresponding diagrams with self-energy insertions in the lower Green's functions can be calculated in a similar way. Denoting it by $S_{a'-c'}$,

$$\begin{aligned} S_{a'-c'} &= \frac{1}{2\pi n_0 \tau^2} \int \frac{d^d q}{(2\pi)^d} \frac{1}{\beta} \sum_{\omega_\ell > -\tilde{\epsilon}_m} V_c(q, i\omega_\ell) [\Gamma^{RA}(q; i\tilde{\epsilon}_m + i\omega_\ell, i\epsilon_m)]^2 \\ &\times \left\{ \int \frac{d^d k}{(2\pi)^d} G^R(k, i\epsilon_{m'}) [G^A(k, i\epsilon_m)]^2 G^R(k+q, i\tilde{\epsilon}_m + i\omega_\ell) \right. \\ &+ U^2 \int \frac{d^d k}{(2\pi)^d} \int \frac{d^d k'}{(2\pi)^d} G^R(k, i\epsilon_{m'}) [G^A(k, i\epsilon_m)]^2 [G^A(k', i\epsilon_m)]^2 \\ &\quad \times G^R(k+q; i\tilde{\epsilon}_m + i\omega_\ell) \\ &\left. + U^2 \left[\int \frac{d^d k}{(2\pi)^d} G^R(k, i\epsilon_{m'}) G^A(k, i\epsilon_m) G^R(k+q, i\tilde{\epsilon}_m + i\omega_\ell) \right]^2 \right\} \end{aligned} \quad (5.76)$$

Note now that the frequency of the self-energy insertion $\tilde{\epsilon}_m$ is treated as different from the frequency of the Green's function, ϵ_m . According to the prescription of section 5.1 we must calculate half the sum of two terms, one with $\tilde{\epsilon}_m > 0$ the other with $\tilde{\epsilon}_m < 0$, even though ϵ_m is always less than zero. But the term in curly brackets is the same in both cases and we calculate it in the same way as in S_{a-c} to get,

$$S_{a'-c'} = 2\pi n_0 \tau^2 \int \frac{d^d q}{(2\pi)^d} \frac{1}{\beta} \sum_{\omega_2 > -\tilde{\epsilon}_m} V_c(q, i\omega_2) D_0^{RA}(q; i\tilde{\epsilon}_m + i\omega_2, i\epsilon_m). \quad (5.77)$$

For $\tilde{\epsilon}_m < 0$ this gives

$$S_{a'-c'}^{(-)} = i n_0 \tau^2 \int \frac{d^d q}{(2\pi)^d} \int_{-\infty}^{+\infty} d\eta f(\eta + \epsilon) V^R(q, \eta) D_0^{RA}(q; \epsilon + \eta, \epsilon) \quad (5.78)$$

and for $\tilde{\epsilon}_m > 0$

$$S_{a'-c'}^{(+)} = -n_0 \tau^2 \int \frac{d^d q}{(2\pi)^d} \int_{-\infty}^{+\infty} d\eta N(\eta) \sigma_c(q, \eta) D_0^{RA}(q; \epsilon + \eta, \epsilon) \\ + i n_0 \tau^2 \int \frac{d^d q}{(2\pi)^d} \int_{-\infty}^{+\infty} d\eta f(\eta + \epsilon) V_c^A(q, \eta) D_0^{RA}(q; \epsilon + \eta, \epsilon). \quad (5.79)$$

The total contribution of these diagrams is, then,

$$S'_{a-c} \equiv \frac{1}{2} [S_{a'-c'}^{(-)} + S_{a'-c'}^{(+)}] \\ = -\frac{n_0 \tau^2}{2} \int \frac{d^d q}{(2\pi)^d} \int_{-\infty}^{+\infty} d\eta N(\eta) \sigma_c(q, \eta) D_0^{RA}(q; \epsilon + \eta, \epsilon) \\ + i n_0 \tau^2 \int \frac{d^d q}{(2\pi)^d} \int_{-\infty}^{+\infty} d\eta f(\eta + \epsilon) [\text{Re} V^A(q, \eta)] D_0^{RA}(q; \epsilon + \eta, \epsilon) \quad (5.80)$$

The calculation of the contribution of the diagrams of Fig. 5.5(d) and its counterpart presents no novel features,

$$S_d = -2\pi n_0 \tau^2 \int \frac{d^d q}{(2\pi)^d} \frac{1}{\beta} \sum_{\omega_2 > -\epsilon_m} V_c(q, i\omega_2) D_0^{RA}(q; i\epsilon_m + i\omega_2, i\epsilon_m) \quad (5.81)$$

$$S_d' = -2\pi n_0 \tau^2 \int \frac{d^d q}{(2\pi)^d} \frac{1}{\beta} \sum_{\omega_2 < -\tilde{\epsilon}_m} Y_c(q, i\omega_2) \mathcal{D}^{AR}(q; i\tilde{\epsilon}_m + i\omega_2, i\epsilon_m') \quad (5.82)$$

which give

$$S_d = n_0 \tau^2 \int \frac{d^d q}{(2\pi)^d} \int_{-\infty}^{+\infty} d\eta [N(\eta) + f(\eta + \epsilon)] \sigma_c(q, \eta) \mathcal{D}_0^{RA}(q; \epsilon + \eta, \epsilon) \\ - i n_0 \tau^2 \int \frac{d^d q}{(2\pi)^d} \int_{-\infty}^{+\infty} d\eta f(\eta + \epsilon) V_c^R(q, \eta) \mathcal{D}_0^{RA}(q; \epsilon + \eta, \epsilon) \quad (5.83)$$

$$S_d' = \frac{n_0 \tau^2}{2} \int \frac{d^d q}{(2\pi)^d} \int_{-\infty}^{+\infty} d\eta N(\eta) \sigma_c(q, \eta) \mathcal{D}_0^{AR}(q; \epsilon + \eta, \epsilon) \\ + i n_0 \tau^2 \int \frac{d^d q}{(2\pi)^d} \int_{-\infty}^{+\infty} d\eta f(\eta + \epsilon) [\text{Re } V_c(q, \eta)] \mathcal{D}_0^{AR}(q; \epsilon + \eta, \epsilon) \quad (5.84)$$

Adding eqs. (5.75), (5.80), (5.83), (5.84) we get an interesting result,

$$\frac{1}{\tau_D} = n_0 \tau^2 \int \frac{d^d q}{(2\pi)^d} \int_{-\infty}^{+\infty} d\eta [N(\eta) + f(\eta + \epsilon)] \sigma_c(q, \eta) \mathcal{D}_0^{RA}(q; \epsilon + \eta, \epsilon) \\ - i n_0 \tau^2 \int \frac{d^d q}{(2\pi)^d} \int_{-\infty}^{+\infty} d\eta f(\eta + \epsilon) [V_c^R(q, \eta) \mathcal{D}_0^{RA}(q; \epsilon + \eta, \epsilon) \\ + V_c^A(q, \eta) \mathcal{D}_0^{AR}(q; \epsilon + \eta, \epsilon)] \\ + \frac{n_0 \tau^2}{2} \int \frac{d^d q}{(2\pi)^d} \int_{-\infty}^{+\infty} d\eta N(\eta) \sigma_c(q, \eta) \\ \times [\mathcal{D}_0^{AR}(q; \epsilon + \eta, \epsilon) - \mathcal{D}_0^{RA}(q; \epsilon + \eta, \epsilon)] \\ + i n_0 \tau^2 \int \frac{d^d q}{(2\pi)^d} \int_{-\infty}^{+\infty} d\eta f(\eta + \epsilon) \text{Re } V_c(q, \eta) \\ \times [\mathcal{D}_0^{RA}(q; \epsilon + \eta, \epsilon) + \mathcal{D}_0^{AR}(q; \epsilon + \eta, \epsilon)] \quad (5.85)$$

Using the fact that $\mathcal{D}^{RA}(q; \epsilon, \epsilon') = [\mathcal{D}^{AR}(q; \epsilon, \epsilon')]^*$ and $\sigma_c(q, \eta) = 2 \text{Im } V^A(q, \eta)$ these terms can be combined to give

$$\begin{aligned} \frac{1}{\tau_D} &= n_0 \tau^2 \int \frac{d^d q}{(2\pi)^d} \int_{-\infty}^{+\infty} d\eta [N(\eta) + f(\eta + \epsilon)] \sigma_c(q, \eta) \mathcal{D}_0^{RA}(q; \epsilon + \eta, \epsilon) \\ &\quad - i n_0 \tau^2 \int \frac{d^d q}{(2\pi)^d} \int_{-\infty}^{+\infty} d\eta [N(\eta) + f(\eta + \epsilon)] \sigma_c(q, \eta) \text{Im} \mathcal{D}_0^{RA}(q; \epsilon + \eta, \epsilon) \end{aligned} \quad (5.86)$$

or, finally,

$$\frac{1}{\tau_D} = n_0 \tau^2 \int \frac{d^d q}{(2\pi)^d} \int_{-\infty}^{+\infty} d\eta [N(\eta) + f(\eta + \epsilon)] \sigma_c(q, \eta) \text{Re} \mathcal{D}_0^{RA}(q; \epsilon + \eta, \epsilon) \quad (5.87)$$

which has exactly the same right hand side as eq. (5.51) for the quasiparticle inverse lifetime! However, we can now cure the divergence by replacing \mathcal{D}_0 in this equation by the renormalized propagator D given in eq. (5.56), thus obtaining a self-consistent equation for τ_D .

The reader may worry at this point about the fact that the diffusion propagators which appear in the other terms should be similarly renormalized and then their contribution would not cancel out. The important point is, however, that whereas the term in eq. (5.87) diverges as the inverse lifetime of the diffusion propagator goes to zero, the sum of all the other terms vanishes. Therefore the term of eq. (5.87) is the dominant one.

So, finally, replacing \mathcal{D}_0 in eq. (5.87) by the renormalized particle-hole propagator D defined in eq. (5.56), we obtain

($E \ll k_B T$)

$$\frac{1}{\tau_D} = \frac{1}{2\pi} \int \frac{d^d q}{(2\pi)^d} \int d\eta [N(\eta) + f(\eta)] \sigma_c(q, \eta) \text{Re} \frac{i}{\eta + i D q^2 + i/\tau_D} \quad (5.88)$$

We already calculated the right hand side of this equation in 2D (eq. (5.59) and obtained

$$\frac{1}{\tau_D} = \frac{k_B T}{2 k_F \ell} \ln [k_B T \epsilon \tau_D^2] \quad (5.89)$$

which to leading order in temperature is

$$\frac{1}{\tau_D} = \frac{k_B T}{2 k_F \ell} \ln \frac{T_2}{T} \quad (5.90)$$

where again $k_B T_2 = 4(k_F \ell)^2 \epsilon$. This is the result we quoted in section 5.3 (eq. (5.63)).

It is in a sense surprising that we end up with the same expression for $1/\tau_D$ that we had for Γ , the quasiparticle inverse lifetime, if we consider the complexity of the calculation of τ_D compared to that of Γ . The important point is, however, that the dominant term in $1/\tau_D$ is that arising from the diagram of Fig. 5.5(d) which is remarkably similar to the diagram which gives the dominant contribution to Γ (Fig. 5.2(a)).

We have mentioned in Chapter 4 that the cutoff of weak localization, the quantity which is obtained experimentally in magnetoresistance measurements, is, strictly speaking, the lifetime of the particle-particle diffusion propagator (eq. (4.37)), τ_{loc} . This quantity was calculated by Fukuyama and Abrahams (1983), who obtained

$$\frac{1}{\tau_{loc}} = \frac{k_B T}{k_F \ell} \ln \frac{T_1}{T} \quad (5.91)$$

with $k_B T_1 = (k_F \ell)^2 \epsilon$. It is enlightening to compare our calculations with theirs.

The particle-particle diffusion propagator obeys an equation similar to that of Fig. 5.4. This propagator, which enters in the calculation of the conductivity (see Chapter 4) is a true two particle interacting Green's function. So, in principle, the corresponding interaction vertex \mathcal{T}' , would

have diagrams with interaction lines going between the upper and lower Green's functions, in addition to those with self-energy insertions in either of the Green's functions (see Fig. 5.6). In these latter diagrams there is no frequency transferred between the upper and lower Green's functions, hence the two particle-particle propagators on either side of have the same frequency difference $\Omega_\lambda = \epsilon_m - \epsilon_m$. In the diagrams with interaction lines going between the two Green's functions, the frequency difference of these two particle-particle propagators is no longer the same, it differs by $2\omega_\ell$ where ω_ℓ is the frequency transferred by the interaction line. If we recall that the particle-particle propagators (eq. 4.10) are singular when $\Omega_\lambda \rightarrow 0$ we see that these latter terms are less singular than the ones with self-energy insertion on either Green's function, provided the interaction itself is not singular as $\omega_\ell \rightarrow 0$.

The result is that the equation for the renormalized particle-particle propagator reduces to an algebraic equation as the one we had for the D propagator (eq. 5.55) with the solution

$$C(q; i\epsilon_m', i\epsilon_m) = \frac{1}{C_0(q; i\epsilon_m', i\epsilon_m) - T'(q; i\epsilon_m', i\epsilon_m)}$$

$$= \frac{1}{2\pi n_0 \tau^2 \left[i\Omega_\lambda + Dq^2 + \frac{1}{\tau_{loc}} \right]} \quad (5.92)$$

where

$$\frac{1}{\tau_{loc}} = - \frac{1}{2\pi n_0 \tau^2} T'(q=0; i\epsilon_m', i\epsilon_m) \quad (5.93)$$

The interaction vertex T' is given by a set of diagrams similar to those of T , the interaction vertex of the particle-

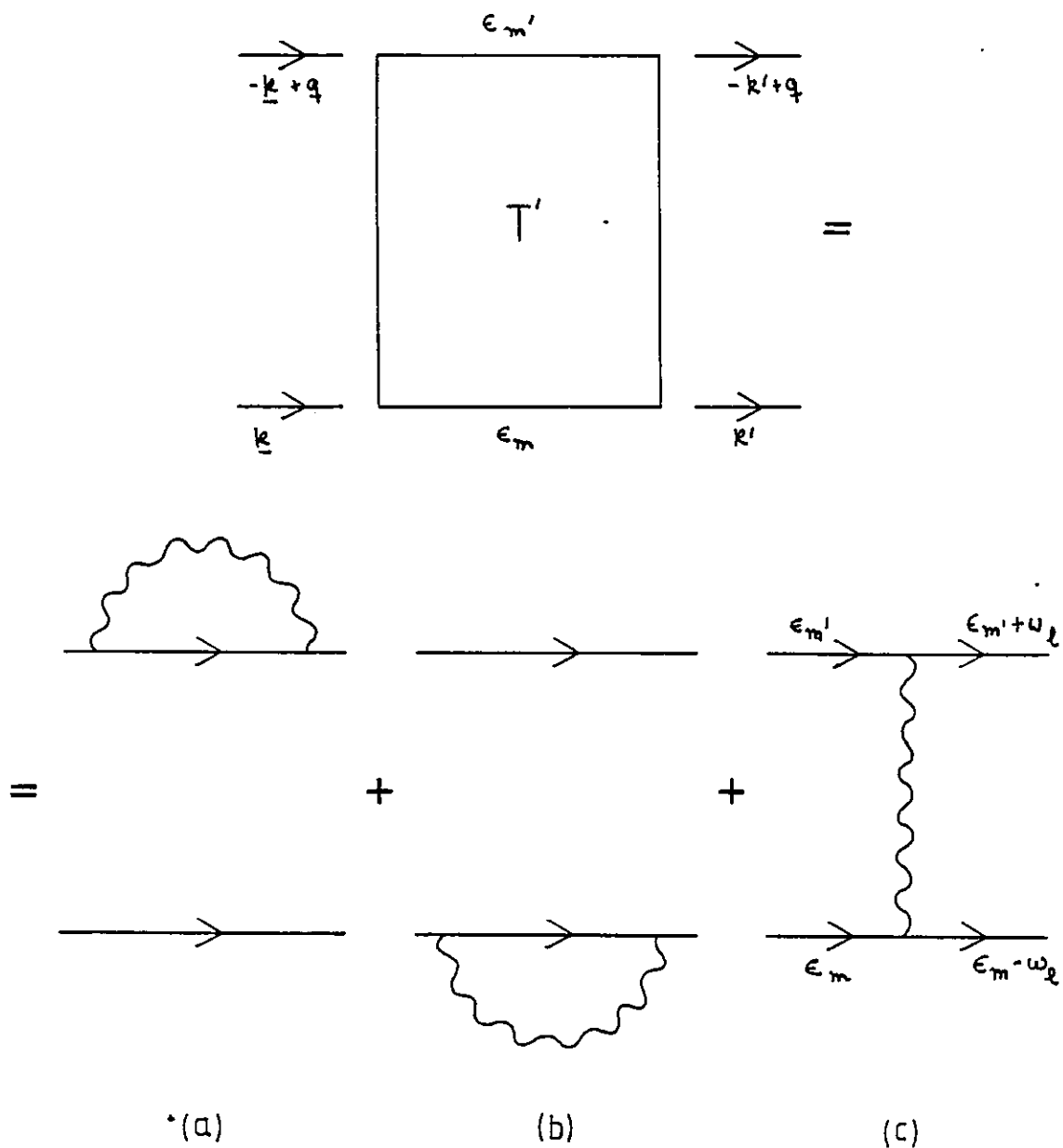


FIG 5.6

Contributions to the interaction vertex of the particle-particle propagator before averaging over impurities.

hole propagator D . The diagrams in \mathcal{T}' , however, have the upper and lower electron lines running in the same direction and q is their momentum sum (Fig. 5.6; see also the definition of the particle-particle propagator in Chapter 4, Fig. 4.4). For this reason the diagram corresponding to the one of Fig. 5.5(d) has a particle-particle propagator instead of a particle-hole one.

Also, in \mathcal{T}' the diagrams with self-energy insertions in the lower Green's functions are treated in the standard way without the prescription we had to use in calculating \mathcal{T} . The dominant contribution to $1/\tau_{loc}$ comes again from the diagram similar to that of Fig. 5.5(d). However, its counterpart, with the self-energy in the lower Green's function, gives now an identical contribution. Therefore the self-consistent equation for τ_{loc} is

$$\frac{1}{\tau_{loc}} = \frac{k_B T}{k_F l} \ln [k_B T \epsilon \tau_{loc}^2] \quad (5.94)$$

which has the solution of eq. (5.91). The extra factor of two that appears in this equation as compared to that of (eq. 5.89) for $1/\tau_D$ is due to the contribution of the diagram with a self-energy insertion in the lower Green's function.

In conclusion the dominant contribution to $1/\tau_{loc}$ comes then from a diagram similar to that of Fig. 5.5(d) and its counterpart with self-energy insertions in the lower Green's functions. The dominant contribution to Γ , the quasiparticle lifetime, comes from the diagram of Fig. 5.2(a), which virtually is identical to that of Fig. 5.5(d). This explains, then, why $1/\tau_{loc}$ is essentially 2Γ apart from the difference in temperatures T_1 and T_2 (which is due to the same factor 2).

This simple relation between $1/\tau_{loc}$ and Γ is, in the

end, due to the fact that diagrams of the type of Fig. 5.6(c) can be neglected in the calculation of $1/\tau_{loc}$. If the interaction is singular at $\omega_f = 0$ these diagrams are important and this relation between $1/\tau_{loc}$ and Γ may not apply.

5.5 Experimental Results

There is now a variety of experimental determinations of τ_{loc} obtained from magnetoresistance measurements, both in silicon inversion layers and in thin metallic films.

In silicon inversion layers the results indicate that the dominant scattering mechanism is electron-electron in nature. One observes for $1/\tau_{loc}$ the T^2 term characteristic of clean metals (Kawaguchi and Kawaji, 198) and at lower temperatures, typically a few kelvin, the linear T dependence induced by disorder. (Wheeler 1981, Uren, Davies, Kaveh and Pepper 1981, Bishop, Tsui and Dynes 1982, Davies and Pepper 1983). The variation of the prefactor of the linear term with disorder is consistent with a $1/k_F \ell$ behaviour. The existence of the extra logarithmic factor $\ln(T_1/T)$ is still controversial, though. Because T_1 is much larger than T in the range of temperatures in which these experiments are conducted, the variation of the logarithmic factor is quite negligible. However, it does appear as an enhancement of the prefactor of the linear term which will then be ($T \sim 1^\circ\text{K}$)

$$A = \frac{k_B \ln T_1}{k_F \ell} \quad ; \quad T_1 \text{ in } ^\circ\text{K}$$

Bishop, Tsui and Dynes (1982) claim to obtain a large enough scattering rate $1/\tau_{loc}$ to be consistent with this enhancement. However, Davies and Pepper (1983) and Poole, Pepper and Hughes (1982) point out that even for $T \sim 1^\circ\text{K}$ the

T^2 term is still important and any attempt to fit $1/\tau_{loc}$ to a simple linear variation in temperature leads to erroneous results. They fit $1/\tau_{loc}$ to a law $A_1T + A_2T^2$ and obtain for the coefficient A_1

$$A_1 = a \frac{k_B}{k_F \ell}$$

where 'a' is a constant of order unity. They also find that A_2 varies as $1/E_F$ as the theory predicts (eq. 5.40).

In thin films the results are, if anything, less clear. In Mg films Bergmann (1982) finds only a T^2 temperature dependence with a coefficient which is independent of disorder. In noble metal films (Au, Ag, Cu) he obtains a $T^{1.65}$ law again with a coefficient which is only weakly dependent on the mean free path. These results seem to indicate that the clean limit contribution is dominating the scattering rate in the Mg measurement and is still present, together with the linear term, in the noble metal measurements. However, Bergmann claims that an estimate of the clean limit contribution to τ_{loc} gives a result three orders of magnitude smaller than the observed values.

In conclusion, although the experiments in silicon inversion layers have established clearly the existence of a disorder induced linear T term in the electron-electron scattering rate, the existence of the extra logarithmic factor, first predicted by Abrahams, Anderson, Lee and Ramakrishnan (1981), is in doubt. In the following chapter we present a similar calculation of the quasiparticle lifetime due to phonon mediated interactions and show that this extra logarithmic term does not occur. This indicates that the form of the dynamically screened Coulomb interaction in the diffusive limit (eq. E.19) is an essential ingredient of the calculation. It could then be possible that averaging ab initio the Coulomb interaction

is not a valid approximation and in a better calculation this logarithmic term might disappear. This is a question for future investigation.

CHAPTER 6PHONON MEDIATED INTERACTIONS IN DISORDERED METALS. A MODEL
CALCULATION6.1 Introduction

In this chapter we address ourselves to the question of electron-phonon scattering rates in disordered systems.

In view of the previous results for electron-electron interactions one may expect that electron-phonon scattering rates will also be affected by the presence of elastic impurity scattering.

This problem has been considered by several authors (Schmid 1973, Takayama 1973, Keck and Schmid 1976, Al'tschuler 1978) using different model Hamiltonians. All these calculations, however, have neglected phonon renormalization effects.

The results obtained in Chapter 2 indicate that, by suitably renormalizing the phonons we should obtain, in the low temperature regime, inelastic scattering rates with temperature dependences similar to those found in Chapter 5 for electron-electron interactions.

We shall consider only a very simple model in which the electron-phonon interaction is taken to be the same as in the ordered metal and given, as in Chapter 2, by a Frölich type Hamiltonian

$$\mathcal{H} = \frac{1}{\sqrt{\Omega}} \sum_{\mathbf{k}, \mathbf{q}} M_{\mathbf{q}}^{\circ} c_{\mathbf{k}+\mathbf{q}}^{\dagger} c_{\mathbf{k}} \phi_{\mathbf{q}} \quad (6.1)$$

with

$$|M_{\mathbf{q}}^{\circ}|^2 = \frac{\lambda_{\circ} v_{\mathbf{q}}^{\circ}}{2n_{\circ}} \quad ; \quad q \ll k_F \quad (6.2)$$

where λ_0 is a dimensionless coupling constant which is typically of order one. Impurities are assumed to couple only to electrons in the way described in Chapter 4.

This Hamiltonian was the one used by Al'tschuler, who obtained for the inelastic scattering rate in 3D,

$$\begin{aligned} \frac{1}{\tau_{in}} &\sim \lambda_0 k_B T_1 \frac{T^4}{\theta_D^2 T_2^2} && T \ll T_2 \\ &\sim \lambda_0 k_B T_1 \left(\frac{T}{\theta_D}\right)^2 && T_2 \ll T \ll T_1 \\ &\sim \lambda_0 k_B \frac{T^3}{\theta_D^2} && T_1 \ll T \ll \theta_D \end{aligned} \quad (6.3)$$

with $k_B T_2 = 3(c_s/v_F)^2/\tau$ and $k_B T_1 = c_s/v_F \tau$. We shall see that for $T \ll T_2$ we obtain a $T^{3/2}$ dependence if phonon renormalization is taken into account. In 2D we obtain a linear temperature dependence without the extra logarithmic factor which occurs for dynamically screened Coulomb interactions (see Chapter 5).

It should be stressed, at this point, that the Hamiltonian of eq. (6.1) involves a number of important simplifications. When a phonon is present in the system the impurity atoms move, and this gives rise to additional impurity dynamical scattering. Schmid (1973) and Keck and Schmid (1976) calculated $1/\tau_{in}$ using a model Hamiltonian, originally due to Tsuneto (1960), which includes these effects. They found a T^4 dependence for $T < T_1$ and T^2 and T^3 terms above (the first one being due to transverse phonons). An additional difficulty for low dimensional electron systems is that the phonon dimensionality can be different from the electronic one, in general higher. This is the case, for instance of silicon inversion layers (Ando, Fowler and Stern 1982).

Our results should then be regarded as a preliminary indication of the need to take phonon mediated interactions into account when discussing the magnitude of electron-electron scattering rates in disordered systems. But any comparisons with experiment would be, at this point, out of place.

The expressions for the quasiparticle lifetime derived in the previous chapter remain valid provided we make the replacement

$$\sigma_c(q, \eta) \rightarrow |M_q^0|^2 \sigma(q, \eta) \quad (6.4)$$

where $\sigma(q, \eta)$ is the phonon spectral function which will be discussed in detail in section 2.

6.2 The Phonon Spectral Function

The averaged renormalized phonon propagator obeys a Dyson equation similar to that of the screened Coulomb interaction $V_c(q, i\omega_\ell)$. We have

$$D(q, i\omega_\ell) = \frac{1}{D_0^{-1}(q, i\omega_\ell) - S(q, i\omega_\ell)} \quad (6.5)$$

where the bare propagator D_0 and the self-energy $S(q, i\omega_\ell)$ are

$$D_0(q, i\omega_\ell) = \frac{-2\gamma_q^0}{\omega_\ell^2 + \gamma_q^{0^2}} \quad (6.6)$$

$$S(q, i\omega_\ell) = |M_q^0|^2 \Pi(q, i\omega_\ell) \quad (6.7)$$

For $q\ell \gg 1$ the impurity vertex corrections may be ignored in $\Pi(q, i\omega_\ell)$ and $\Pi(q, i\omega_\ell) \approx \Pi_0(q, i\omega_\ell)$ (eq. (E.20)) where $\Pi_0(q, i\omega_\ell)$ is the bare polarization bubble. For

frequencies $\eta \lesssim v_q^0 \ll v_F q$ we can use the clean limit result for $\pi_2^0(q, \eta)$ (eqs. (E.24)) and replace $\pi_1^0(q, \eta)$ by its zero frequency value. The spectral function $\sigma(q, \eta)$ defined by eq. (A.12) then has exactly the same form as in the pure case (see Appendix A).

For $q\ell \ll 1$ we have $v_q \ll k_B T_1 \ll \tau^{-1}$ where $k_B T_1 = c_s/v_F \tau$. We shall see that the important values of η are $\eta \lesssim v_q \ll \tau^{-1}$. We are then in the diffusive limit for $\pi(q, i\omega_\ell)$ and we have (eqs. (E.16))

$$\pi_1(q, \eta) = \frac{-2n_0(Dq^2)^2}{\eta^2 + (Dq^2)^2} \quad (6.8a)$$

$$\pi_2(q, \eta) = \frac{2n_0\eta Dq^2}{\eta^2 + (Dq^2)^2} \quad (6.8b)$$

We consider separately the limits $v_q^0 \gg k_B T_2$ and $v_q^0 \ll k_B T_2$ with $k_B T_2 \equiv c_s^2/D = d(c_s/v_F)^2/\tau$

i) $v_q^0 \gg k_B T_2$

Note that $Dq^2 = v_q^0/k_B T_2$ and hence $v_q^0 = (k_B T_2/v_q^0) Dq^2 \ll Dq^2$. So for $|\eta| \lesssim v_q^0$,

$$\pi_1(q, \eta) \approx -2n_0 \quad (6.9a)$$

$$\pi_2(q, \eta) = \frac{2n_0\eta}{Dq^2} \quad (6.9b)$$

The spectral function becomes, using eq. (6.2)

$$\begin{aligned} \sigma(q, \eta) &= \frac{8\lambda_0 v_q^0{}^3 \eta / Dq^2}{(\eta^2 - v_q^0{}^2 + 2\lambda_0 v_q^0{}^2)^2 + (2\lambda_0 v_q^0{}^2 \eta / Dq^2)^2} \\ &= \frac{8\lambda_0 v_q^0 k_B T_2 \eta}{[\eta^2 - v_q^0{}^2 (1 - 2\lambda_0)]^2 + [2\lambda_0 T_2 \eta]^2} \end{aligned} \quad (6.10)$$

The renormalized phonon energy and inverse lifetime are given by (c.f. eq. (A.13))

$$\nu_q^2 + \gamma_q^2 = \nu_q^{o2} (1 - 2\lambda_0) \quad (6.11a)$$

$$\gamma_q = 2\lambda_0 k_B T_2 \ll \nu_q \quad (6.11b)$$

We see, then, that the phonon modes are well defined and we can rewrite eq. (6.10) as

$$\sigma(q, \eta) = \frac{\nu_q^o}{\nu_q} \left[\frac{2\gamma_q}{(\eta - \nu_q)^2 + \gamma_q^2} - \frac{2\gamma_q}{(\eta + \nu_q)^2 + \gamma_q^2} \right] ; \quad \begin{array}{l} |\eta| \leq \nu_q^o \\ \nu_q^o \gg k_B T_2 \end{array} \quad (6.12)$$

which, again, is a form identical to that of the pure case. (Eq. A.14).

ii) $\nu_q^o \ll k_B T_2$

In this case the full frequency dependence of the self-energy (eqs. (6.8)) cannot be ignored. It is useful to define the variable $u^2 = \mathfrak{D}q^2/|\eta|$. We have,

$$\pi_1(q, \eta) = -2n_0 \frac{u^4}{1 + u^4} \quad (6.13a)$$

$$\pi_2(q, \eta) = 2n_0 \frac{u^2}{1 + u^2} \operatorname{sgn} \eta \quad (6.13b)$$

and for the spectral function, noting that $\nu_q^{o2} = k_B T_2 |\eta| u^2$,

$$\sigma(q, \eta) = \frac{8\lambda_0}{(k_B T_2 |\eta|)^{1/2}} \frac{u^5 (1+u^4) \operatorname{sgn} \eta}{\left[\left(\frac{|\eta|}{k_B T_2} - u^2 \right) (1+u^4) + 2\lambda_0 u^6 \right]^2 + [2\lambda_0 u^4]^2} \quad (6.14)$$

Using

$$|M_q^o|^2 = \frac{\lambda_0}{2n_0} \nu_q^o = \frac{\lambda_0}{2n_0} (k_B T_2 |\eta|)^{1/2} u \quad (6.15)$$

we get

$$|M_q^0|^2 \sigma(q, \eta) = \frac{4\lambda_0^2}{n_0} \frac{v^6 (1+v^4)}{\left[\left(\frac{|\eta|}{k_B T_2} - v^2 \right) (1+v^4) + 2\lambda_0 v^6 \right]^2 + [2\lambda_0 v^4]^2} \quad (6.16)$$

We shall see later that for $T \ll T_2$ the values of q that dominate the scattering are $q \sim (k_B T/D)^{\frac{1}{2}}$, i.e. $v \sim 1$ and we can set $|\eta|/k_B T_2 = 0$ in this expression.

6.3 Clean Limit Contribution

The clean limit contribution for the quasiparticle inverse lifetime can be written by analogy with the case of Coulomb interactions (eq. (5.28)) as

$$\Gamma_0 = \frac{n_0}{Z} \int d\eta [N(\eta) + f(\eta + E)] \int_{R=K'=R_F} d^d \Omega |M_{K'-K}^0|^2 \sigma(K'-K, \eta) \quad (6.17)$$

with the restriction

$$\frac{|K'-K|}{2R_F} = \sin \theta/2 > \text{Max} \left\{ \frac{k_B T}{E_F}, \frac{1}{k_F l} \right\} \quad (6.18)$$

As usual we consider $E \ll k_B T$. We saw in the previous section that for $q l \gg 1$, i.e. $v_q^0 \gg k_B T_1$ the phonon spectral function is the same as in pure metals. Therefore, for $T_1 \ll T \ll \theta_D$ we get a real phonon scattering term from the modes with $v_q \lesssim k_B T$ and a virtual phonon term from those with $v_q \gg k_B T$ which can be calculated as in Chapter 2. The restriction $|K'-K|/2R_F > \text{Max} \left\{ \frac{k_B T}{E_F}, \frac{1}{k_F l} \right\}$ can be waived because in either case the integral is dominated by phonon modes with energies of the order or larger than $k_B T$ i.e.

$$|K'-K|/2R_F \gtrsim k_B T/\theta_D \gg \text{Max} \left\{ \frac{k_B T}{E_F}, \frac{1}{k_F l} \right\}$$

One obtains in 3D ,

$$\Gamma_0(\tau) = \alpha \lambda_0 \frac{(k_B T)^3}{\theta_D} + \frac{\pi^3}{8} \lambda^2 \frac{(k_B T)^2}{\epsilon_F} \quad \begin{array}{l} T \gg T_1 \\ \text{in 3D} \end{array} \quad (6.19)$$

where θ_D is defined as $\theta_D = 2 \kappa_F c_s$ and

$$\lambda^2 \equiv 2 n_0^2 \left\langle \frac{(2 |M_{\mathbf{k}'-\mathbf{k}}|^2 / v_{\mathbf{k}'-\mathbf{k}})^2}{\sin \theta/2} \right\rangle \quad (6.20)$$

$$\alpha = 2\pi \int_0^\infty dx \frac{x^2}{\sinh x} \quad (6.21)$$

The virtual phonon term has exactly the same form as that of eq. (5.36) with $V_{ss}(\mathbf{q})$ replaced $2 |M_{\mathbf{q}}|^2 / v_{\mathbf{q}}$ (see Chapter 2). In 2D the real phonon scattering contribution also has a T^2 dependence and dominates the virtual phonon contribution in this temperature range, $T \gg T_1$

$$\Gamma_0(\tau) = \frac{\pi^2}{2} \lambda_0 \frac{(k_B T)^2}{\theta_D} \quad \begin{array}{l} T \gg T_1 \\ \text{in 2D} \end{array} \quad (6.22)$$

For $T \ll T_1$ only the virtual phonon contribution from the phonon modes with $q\ell > 1$ remains.

We have ignored the clean limit contribution of the modes with $q\ell < 1$. One can show that their contribution is either dominated by the terms we have just calculated (for $T \gg T_1$) or by the contribution of the diagram Fig. 5.2(a) with the particle-hole diffusive pole, to which we now turn.

6.4 Contribution of Particle-Hole Diffusion Pole

For temperatures below T_1 the thermal phonon wavevector is

$q = v_q/c_s < l^{-1}$. We therefore expect to find an electron-phonon scattering rate modified by impurities in this temperature range. As before, the most important contribution is that of the diagram of Fig. 5.2(a). By analogy with the Coulomb interaction case (c.f. eq. (5.51))

$$\Gamma = n_0 \tau^2 \int d\eta [N(\eta) + f(\eta + \epsilon)] \int_{q < l^{-1}} \frac{d^d q}{(2\pi)^d} |M_q^0|^2 \sigma(q, \eta) \text{Re } D_o^{RA}(q; \epsilon, \eta, \epsilon) \quad (6.23)$$

The phonon spectral function limits the range of important values of η to $|\eta| \lesssim v_q < k_B T_1$. Hence for $T > T_1$ the contribution of this term becomes temperature independent. We shall limit ourselves to the temperature range $T \ll T_1$. We shall have to distinguish the regions $T \gg T_2$ and $T \ll T_2$.

i) $T_2 \ll T \ll T_1$

We saw in section 6.2 that for phonon wavevectors with $k_B T_2 \ll v_q \ll k_B T_1$ the phonon modes are well defined, i.e. the spectral function has a double Lorentzian form with a small width γ_q at the peaks $\pm v_q$. As $\gamma_q \sim k_B T_2 \ll k_B T$ and $\gamma_q \ll \mathcal{D}q^2$ we can perform the η integration by replacing the phonon-spectral function by the corresponding delta-function (eq. (2.11)),

$$\begin{aligned} \Gamma(T) &= 2 \int_{k_B T_2 < v_q < k_B T_1} \frac{d^d q}{(2\pi)^d} [N(v_q) + f(v_q)] |M_q|^2 \frac{\mathcal{D}q^2}{v_q^2 + (\mathcal{D}q^2)^2} \\ &= 2 \int_{k_B T_2 < v_q < k_B T_1} \frac{d^d q}{(2\pi)^d} [N(v_q) + f(v_q)] |M_q|^2 \frac{1}{k_B T_2 + \mathcal{D}q^2} \end{aligned} \quad (6.24)$$

As in Chapter 2, the factor (v_q^0/v_q) is absorbed in the electron-phonon matrix element, so that $|M_q|^2 = \lambda_0 v_q / 2\pi_0$. In 3D we have,

$$\Gamma(T) = \frac{\lambda_0 k_B T_2}{2\pi^2 n_0 C_s^3} \int_{k_B T_2}^{\infty} d\nu_q \frac{\nu_q}{\sinh \beta \nu_q} \frac{1}{1 + \left(\frac{k_B T_2}{\nu_q}\right)^2} \quad ; \quad T_2 \ll T \ll T_1$$

in 3D

$$= \frac{3\pi^2 \lambda_0}{2 k_F \ell} \left(\frac{k_B T}{\nu_D}\right)^2 \quad (6.25)$$

This is the result obtained by Al'tschuler (1978) (eq. (6.3)).

In 2D,

$$\Gamma(T) = \frac{1}{2\pi} \frac{\lambda_0}{n_0 C_s^2} (k_B T_2) \int_{k_B T_2}^{\infty} d\nu_q \frac{\nu_q^2}{\sinh \beta \nu_q} \frac{1}{\nu_q^2 + k_B T_2}$$

which gives for $T \gg T_2$

$$\Gamma(T) = \frac{2\lambda_0}{k_F \ell} k_B T \ln \frac{T}{T_2} \quad ; \quad T_2 \ll T \ll T_1$$

in 2D

ii) $T \ll T_2$

For $\nu_q < k_B T_2$ we have $\nu_q > \mathcal{D}q^2$. We cannot then ignore the full frequency dependence of the phonon self-energy as we did for $T > T_1$. We saw in section 6.2 that in terms of the variable $u^2 \equiv \mathcal{D}q^2/|\eta|$ we had ,

$$|M_q^0|^2 \sigma(q, \eta) = \frac{4\lambda_0}{n_0} \frac{u^6 (1+u^4) \operatorname{sgn} \eta}{\left[\left(\frac{|\eta|}{k_B T_2} - u^2\right)(1+u^4) + 2\lambda_0 u^6\right]^2 + [2\lambda_0 u^4]^2}$$

and

$$\int \frac{d^d q}{(2\pi)^d} (\dots) = \frac{\Omega_d}{(2\pi)^d} \left(\frac{|\eta|}{D}\right)^{d/2} \int_0^{u_{\max}} u^{d-4} du (\dots) \quad (6.27)$$

where Ω_d is the full solid angle in d dimensions and

$u_{\max} \equiv \left(1/d|\eta|\tau\right)^{1/2} \gg 1$. The equation for $\Gamma(E, T)$ becomes

$$\Gamma(\epsilon, T) = \frac{\Omega d}{(2\pi)^{d+1}} \frac{4\lambda_0^2}{n_0 D^{d/2}} \int_{-\infty}^{\infty} d\eta [N(\eta) + f(\eta + \epsilon)] \operatorname{sgn} \eta |\eta|^{d/2-1} \times \int_0^{u_{\max}} du \frac{u^{d+3} (1+u^4)}{[(\frac{|\eta|}{k_B T_2} - u^2)(1+u^4) + 2\lambda_0 u^6]^2 + [2\lambda_0 u^4]^2} \frac{u^2}{1+u^4} \quad (6.28)$$

We consider separately the cases of 3D and 2D.

i) 3D

The u integral is dominated by $u \sim 1$ for $|\eta|/(k_B T_2) < 1$.

So we write

$$\Gamma(T) = \frac{\lambda_0^2}{\pi^3} \frac{1}{n_0 D^{d/2}} \int_{-\infty}^{\infty} d\eta \operatorname{sgn} \eta [N(\eta) + f(\eta)] |\eta|^{1/2} I_{\lambda_0} \quad (6.29)$$

with

$$I_{\lambda_0} = \int_0^{\infty} du \frac{u^{10}}{[(2\lambda_0 - 1)u^6 - u^2]^2 + [2\lambda_0 u^4]^2} = \int_0^{\infty} du \frac{u^6}{[(1 - 2\lambda_0)u^4 + 1]^2 + [2\lambda_0 u^2]^2} \quad (6.30)$$

Using $n_0 = m k_F / 2\pi^2$ and $D = k_F \ell / 3m$

$$\Gamma(T) = \alpha \frac{\lambda_0^2 I_{\lambda_0}}{(k_F \ell)^{3/2}} \frac{(k_B T)^{3/2}}{\epsilon_F^{1/2}} \quad (6.31)$$

with

$$\alpha = \frac{6\sqrt{6}}{\pi} \int_0^{\infty} dx \frac{x^{1/2}}{\sinh x}$$

This result has exactly the same form as the result found

by Schmid for Coulomb interaction (see eq. (5.52)). We are clearly dealing with the phonon-mediated interaction we discussed in Chapter 2.

ii) 2D

If we replace the ν integral in eq. (6.28) by its value at $|\eta|/\kappa_3\tau_2 = 0$ we obtain an η integral that diverges logarithmically near $\eta \sim 0$. We found the same problem when dealing with Coulomb interaction in Chapter 5. This divergence can be cured exactly in the same way. In a self-consistent calculation the only change in the expression for the quasiparticle inverse lifetime lies in the particle-hole propagator which acquires a finite lifetime given exactly by the same equation as the quasiparticle one. So we write,

$$\Gamma(T) = \frac{2}{\pi^2} \frac{\lambda_0^2}{\eta_0 \mathcal{D}} \int_0^\infty d\eta \frac{1}{\sinh \beta \eta} \mathcal{I}_{\lambda_0} \left(\frac{1}{\tau_2 |\eta|} \right) \quad (6.32)$$

with

$$\begin{aligned} \mathcal{I}_{\lambda_0} \left(\frac{1}{\tau_2 |\eta|} \right) &= \int_0^\infty du \frac{u^3 (1+u^4)}{[(1-2\lambda_0)u^4+1]^2 + [2\lambda_0 u^2]^2} \frac{(u^2 + (1/\tau_2 |\eta|))}{1 + (u^2 + (1/\tau_2 |\eta|))^2} \\ &= \frac{1}{2} \int_0^\infty dy \frac{y(1+y^2)}{[(1-2\lambda_0)y^2+1]^2 + [2\lambda_0 y]^2} \operatorname{Re} \frac{1}{i + y + (1/\tau_2 |\eta|)} \end{aligned} \quad (6.33)$$

We can invert the y and η integration,

$$\begin{aligned} \Gamma(T) &= \frac{\lambda_0^2}{\pi^2 \eta_0 \mathcal{D}} \int_0^\infty dy \frac{y(1+y^2)}{[(1-2\lambda_0)y^2+1]^2 + (2\lambda_0 y)^2} \\ &\times \operatorname{Re} \int_0^\infty d\eta \frac{1}{\sinh \beta \eta} \frac{1}{i + y + \frac{1}{\tau_2 |\eta|}} \end{aligned} \quad (6.34)$$

We now isolate the divergent term in the η integral

$$\begin{aligned}
\text{Re} \int_0^{\infty} d\eta \frac{1}{\sinh \eta} \frac{1}{i + \gamma + \frac{1}{\tau_D \eta}} &\approx k_B T \text{Re} \int_0^1 dx \frac{1}{ix + x\gamma + \frac{1}{k_B T \tau_D}} \\
&\approx k_B T \frac{\gamma}{1 + \gamma^2} \ln [k_B T \tau_D] \quad (6.35)
\end{aligned}$$

Therefore $\Gamma(T)$ is

$$\begin{aligned}
\Gamma(T) &= \frac{\lambda_0^2 I_{\lambda_0}}{\pi^2 n_0 D} k_B T \ln [k_B T \tau_D] \\
&= \frac{4 \lambda_0^2 I_{\lambda_0}}{\pi k_F \ell} k_B T \ln [k_B T \tau_D] \quad (6.36)
\end{aligned}$$

with

$$I_{\lambda_0} \equiv \int_0^{\infty} d\gamma \frac{\gamma^2}{[(1-2\lambda_0)\gamma^2+1]^2 + [2\lambda_0\gamma]^2} \quad (6.37)$$

We know from Chapter 5 that $\Gamma = \tau_D^{-1}$ and therefore to leading order in temperature

$$\Gamma(T) = \frac{g^2 k_B T}{k_F \ell} \ln \left[\frac{k_F \ell}{g^2} \right] ; \quad T \ll T_2, \text{ in } 2D \quad (6.38)$$

where

$$g^2 \equiv \frac{4}{\pi} \lambda_0^2 I_{\lambda_0} \quad (6.39)$$

is taken to be of order one.

We find then a different temperature dependence from the one found for Coulomb interactions. The singularity at low η and low q in the scattering rate leads only to an enhancement of the coefficient of the linear temperature term by a factor

$\ln k_F t$. This shows that the $T \ln (T_1/T)$ dependence found in Chapter 5 is closely related to the form of the Coulomb interaction in the diffusive limit.

Appendix A

The Phonon Self-Energy and Spectral Function in Pure Metals

A.1 Self-energy

The phonon self-energy given by the diagram of Fig. 2.2(b) is

$$S(q, i\nu_n) = |M_q^0|^2 \Pi^0(q, i\nu_n) \quad (\text{A.1})$$

where $\Pi^0(q, i\nu_n)$ is the simple polarization bubble

$$\Pi^0(q, i\nu_n) = \frac{1}{\beta} \sum_{\epsilon_m} \int \frac{d^3k}{(2\pi)^3} G(\underline{k}, i\epsilon_m) G(\underline{k}+q, i\epsilon_m + i\nu_n) .$$

The imaginary part of the corresponding advanced function is

$$\Pi_2^0(q, \eta) = \int \frac{d^3k}{(2\pi)^3} \frac{d\xi}{2\pi} \rho(\underline{k}, \xi) \rho(\underline{k}+q, \xi+\eta) [f(\xi) - f(\xi+\eta)] \quad (\text{A.2})$$

and the real part is given by a Kramers-Krönig relation

$$\Pi_1^0(q, \eta) = \rho \int \frac{d\eta'}{\pi} \frac{\Pi_2^0(q, \eta')}{\eta - \eta'} \quad (\text{A.3})$$

Changing variables

$$\begin{aligned} \xi + \eta &\rightarrow \xi \\ \underline{k} + q &\rightarrow \underline{k} \end{aligned}$$

one obtains

$$\Pi_2^0(q, \eta) = -\Pi_2^0(-q, \eta)$$

and for a system with a centre of symmetry

$$\Pi_2^\circ(q, \eta) = -\Pi_2^\circ(q, -\eta) \quad (\text{A.4a})$$

$$\Pi_1^\circ(q, \eta) = \Pi_1^\circ(q, -\eta) \quad (\text{A.4b})$$

This is a general property of the phonon self-energy which is valid beyond this approximation. In the following we consider $\eta > 0$.

The thermal occupation factors in eq. (A.2) restrict the values of ξ to $|\xi|, |\xi + \eta| \lesssim \text{Max}\{\eta, k_B T\}$. If we have $\text{Max}\{\eta, k_B T\} \ll v_D$ the widths of the electronic spectral functions $\Gamma_{\underline{k}}, \Gamma_{\underline{k}+q}$ (see eq. (2.7)) become vanishingly small. Using arguments similar to those involved in Chapter 2, one can then show that the leading contribution to $\Pi_2^\circ(q, \eta)$ comes from the region of momentum integration, such that

$$|\epsilon_{\underline{k}}| \lesssim \text{Max}\{\eta, k_B T\} \quad (\text{A.5a})$$

$$|\epsilon_{\underline{k}+q} - \epsilon_{\underline{k}} - \eta| \lesssim \Gamma_{\underline{k}+q} \ll \text{Max}\{\eta, k_B T\} \quad (\text{A.5b})$$

so that both peaks of the spectral functions occur at the same value of ξ , namely $\xi \simeq \epsilon_{\underline{k}}, \xi + \eta \simeq \epsilon_{\underline{k}+q}$. As

$$-v_F q \left(1 - \frac{q}{2k_F}\right) \lesssim \epsilon_{\underline{k}+q} - \epsilon_{\underline{k}} \lesssim v_F q \left(1 + \frac{q}{2k_F}\right)$$

this requires also that $\eta \ll v_F q \left(1 + q/2k_F\right)$. The integral over ξ is then dominated by the peaks of the spectral functions and, because the thermal factors vary on a scale of order

$\text{Max}\{\eta, k_B T\} \gg \Gamma_{\underline{k}}, \Gamma_{\underline{k}+q}$ we have

$$\pi_2^0(q, \eta) = \int \frac{d^3 k}{(2\pi)^3} [f(\epsilon_{\underline{k}}) - f(\epsilon_{\underline{k}+q})] \\ \times z_{\underline{k}} z_{\underline{k}+q} \int \frac{d\xi}{2\pi} \frac{2\Gamma_{\underline{k}}}{(\xi - \epsilon_{\underline{k}})^2 + \Gamma_{\underline{k}}^2} \frac{2\Gamma_{\underline{k}+q}}{(\xi + \eta - \epsilon_{\underline{k}+q})^2 + \Gamma_{\underline{k}+q}^2}$$

The integral over ξ can be performed by contour integration,

$$\pi_2^0(q, \eta) = \int \frac{d^3 k}{(2\pi)^3} [f(\epsilon_{\underline{k}}) - f(\epsilon_{\underline{k}+q})] \\ \times \frac{2 z_{\underline{k}} z_{\underline{k}+q} (\Gamma_{\underline{k}} + \Gamma_{\underline{k}+q})}{(\epsilon_{\underline{k}+q} - \epsilon_{\underline{k}} - \eta)^2 + (\Gamma_{\underline{k}} + \Gamma_{\underline{k}+q})^2}$$

The angular integration is dominated by the values of $\epsilon_{\underline{k}+q}$ such that

$$|\epsilon_{\underline{k}+q} - \epsilon_{\underline{k}} - \eta| \lesssim \Gamma_{\underline{k}} + \Gamma_{\underline{k}+q} \ll \text{Max}\{\eta, k_B T\} \quad (\text{A.6})$$

Hence, we can ignore the restriction of eq. (A.5b) and make the replacement

$$z_{\underline{k}} z_{\underline{k}+q} \frac{2(\Gamma_{\underline{k}} + \Gamma_{\underline{k}+q})}{(\epsilon_{\underline{k}+q} - \epsilon_{\underline{k}} - \eta)^2 + (\Gamma_{\underline{k}} + \Gamma_{\underline{k}+q})^2} \rightarrow 2\pi z_{\underline{k}} z_{\underline{k}+q} \delta(\epsilon_{\underline{k}+q} - \epsilon_{\underline{k}} - \eta)$$

to obtain

$$\pi_2^0(q, \eta) = 2\pi \int \frac{d^3 k}{(2\pi)^3} z_{\underline{k}} z_{\underline{k}+q} [f(\epsilon_{\underline{k}}) - f(\epsilon_{\underline{k}+q})] \\ \times \delta(\epsilon_{\underline{k}+q} - \epsilon_{\underline{k}} - \eta) \quad (\text{A.7})$$

The values of $\epsilon_{\underline{k}}$ in this integral are restricted by the thermal factors and the delta function to the interval

$|\epsilon_{\underline{k}}| < \text{Max}\{\eta, k_B T\}$ so we can also ignore the restriction of eq. (A.5a) and sum freely over momentum.

A straightforward calculation gives

$$\pi_2^0(q, \eta) = \pi n_0 \frac{\eta}{v_F q} \quad ; \quad \eta < v_F q \left(1 - \frac{q}{2k_F}\right) \quad (\text{A.8})$$

where n_0 and v_F are the unrenormalized density of states at fermi level and fermi velocity.

In general we need values of $\eta \lesssim v_q$ and for $q \sim k_F$, $v_q \sim v_D$ and the derivation presented above fails because we can no longer assume that $\Gamma_k, \Gamma_{k+q} \ll \text{Max}\{\eta, k_B T\}$. In fact $\Sigma(k_F, \eta) \sim v_D$ for $\eta \gtrsim v_D$ (see AGD). Nevertheless, the result of eq. (A.8) remains valid as we now show.

We can rewrite eq. (A.1) as

$$\begin{aligned} \pi_2^0(q, \eta) = & \int \frac{d\xi}{2\pi} [f(\xi) - f(\xi + \eta)] \\ & \times \int d\omega_k \frac{n(\omega_k)}{2v_k q} \rho(k, \xi) \int_{e_-}^{e_+} d\omega_{k+q} \rho(k+q, \xi + \eta) \end{aligned} \quad (\text{A.9})$$

where $e_{\pm} = \omega_k \pm v_{k+q} (1 \pm q/2k)$. The spectral functions - as functions of ω_k and ω_{k+q} - are also lorentzians, with widths $\Sigma_2(k_F, \xi), \Sigma_2(k_F, \xi + \eta) \lesssim v_D$. The scale of variation of $n(\omega_k)$ or v_k with ω_k is of order ϵ_F . If we have $v_D \ll v_F q (1 - q/2k_F)$ the integrals of ω_k and ω_{k+q} are dominated by $|\omega_k|, |\omega_{k+q}| \lesssim v_D$ and the limits e_{\pm} can be replaced by $\pm \infty$. We get, then, to lowest order in v_D/ϵ_F ,

$$\pi_2^0(q, \eta) = \pi n_0 \frac{1}{v_F q} \int d\xi [f(\xi) - f(\xi + \eta)]$$

which for either $k_B T \gg \eta$ or $k_B T \ll \eta$ is

$$\pi_2^0 = \pi n_0 \frac{\eta}{v_F q} \quad ; \quad \eta \lesssim v_D \ll v_F q \left(1 - \frac{q}{2k_F}\right) \quad (\text{A.10})$$

The integral in eq. (A.2) is dominated by values of $\eta' \sim v_F q (1 - q/2k_F)$. Hence for $\eta \ll v_F q (1 - q/2k_F)$ we can approximate $\Pi_1^0(q, \eta)$ by $\Pi_1^0(q, 0)$. In conclusion, for all but the very high momentum phonons $q \sim 2k_F$ we have

$$S_2(q, \eta) = \pi n_0 |M_q^0|^2 \frac{\eta}{v_F q} \quad (\text{A.11a})$$

$$\eta \lesssim v_q^0 \ll v_F q$$

$$S_1(q, \eta) = |M_q^0|^2 \Pi_1(q, 0) \quad (\text{A.11b})$$

A.2 The Spectral Function

The phonon spectral function $\sigma(q, \eta)$ is given in terms of $S_1(q, \eta)$ and $S_2(q, \eta)$ by

$$\begin{aligned} \sigma(q, \eta) &= \frac{1}{i} (\mathcal{D}^A(q, \eta) - \mathcal{D}^R(q, \eta)) \\ &= \frac{8 v_q^{02} S_2(q, \eta)}{[\eta^2 - v_q^{02} - 2 v_q^0 S_1(q, \eta)]^2 + [2 v_q^0 S_2(q, \eta)]^2} \end{aligned} \quad (\text{A.12})$$

This function has poles at $\pm v_q \pm i \gamma_q$ where v_q and γ_q are the renormalized energy and inverse lifetime of the q -phonon state. As $v_q \ll v_F q$ we can use eqs. (A.11) for all but the very high q phonons to get,

$$v_q^2 + \gamma_q^2 = v_q^{02} + 2 v_q^0 S_1(q, 0) \quad (\text{A.13a})$$

$$\gamma_q = \frac{v_q^0}{v_q} S_2(q, v_q) \quad (\text{A.13b})$$

Using eqs. (A.11) and (A.13) we can write, for $|\eta| \lesssim v_q$

$$\sigma(q, \eta) = \frac{v_q^0}{v_q} \left(\frac{2 \gamma_q}{(\eta - v_q)^2 + \gamma_q^2} - \frac{2 \gamma_q}{(\eta + v_q)^2 + \gamma_q^2} \right) \quad (\text{A.14})$$

For most metals the factor $n_0 |m_q^0|^2 / v_q$ is of order one, hence

$$\frac{\sigma_q}{v_q} \approx \frac{\pi n_0}{v_q} \frac{|M_q^0|^2 v_q^0}{v_F q} \sim \frac{C_J^0}{v_F} \sim \frac{v_D}{v_F} \ll 1 \quad (\text{A.15})$$

For $\eta \ll v_q$, $\sigma(q, \eta)$ is well represented by the first term of its power expansion about $\eta = 0$ which can be obtained by setting $\eta = 0$ in the denominator of the right hand side of eq. (A.12)

$$\begin{aligned} \sigma(q, \eta) &= \frac{8 v_q^{\circ 2} S_2(q, \eta)}{[v_q^{\circ 2} + 2 v_q^{\circ} S_1(q, 0)]^2} = \frac{8 v_q^{\circ 2} S_2(q, \eta)}{[v_q^{\circ 2} + v_q^{\circ 2}]^2} \\ &\approx \frac{8 v_q^{\circ 2} S_2(q, \eta)}{v_q^4} \end{aligned} \quad (\text{A.16})$$

Appendix B

Intermediate States and the Imaginary Part of the Self-Energy

We define as "intermediate state" in a self-energy diagram any set of propagators which has the property that, when the propagators are cut, the diagram falls into only two parts, each linked to one external vertex (Fig. B.1).

We shall show that the contribution of any diagram to the imaginary part of the self energy $\Sigma_2(\mathbf{p}, \omega)$ is given by a sum of terms corresponding to each of these intermediate states. These terms can be identified by a delta function conserving energy between the initial state, one electron plus background, and the intermediate state. For the state of Fig. B.1 we would have

$$\delta(\omega - \xi_1 - \xi_2 + \xi_3 - \eta_1 + \eta_2)$$

where the ξ and η denote the spectral frequencies corresponding to each propagator.

A general diagram will have r propagators and p ($p < r$) independent frequencies to be summed. The remaining $r-p$ are determined by frequency conservation at each vertex. Using spectral representations for the propagators, the frequency sum has the following structure,

$$\left(\frac{1}{\beta}\right)^p \sum_{\{\epsilon_1, \dots, \epsilon_p\}} \frac{1}{i\Omega_1 - \xi_1} \dots \frac{1}{i\Omega_r - \xi_r}$$

where Ω_i is a linear combination of the external frequency and the p independent frequencies $\epsilon_1, \dots, \epsilon_p$, with coefficients $\pm 1, 0$. For the purpose of this discussion it is not necessary to distinguish between boson and fermion frequencies.

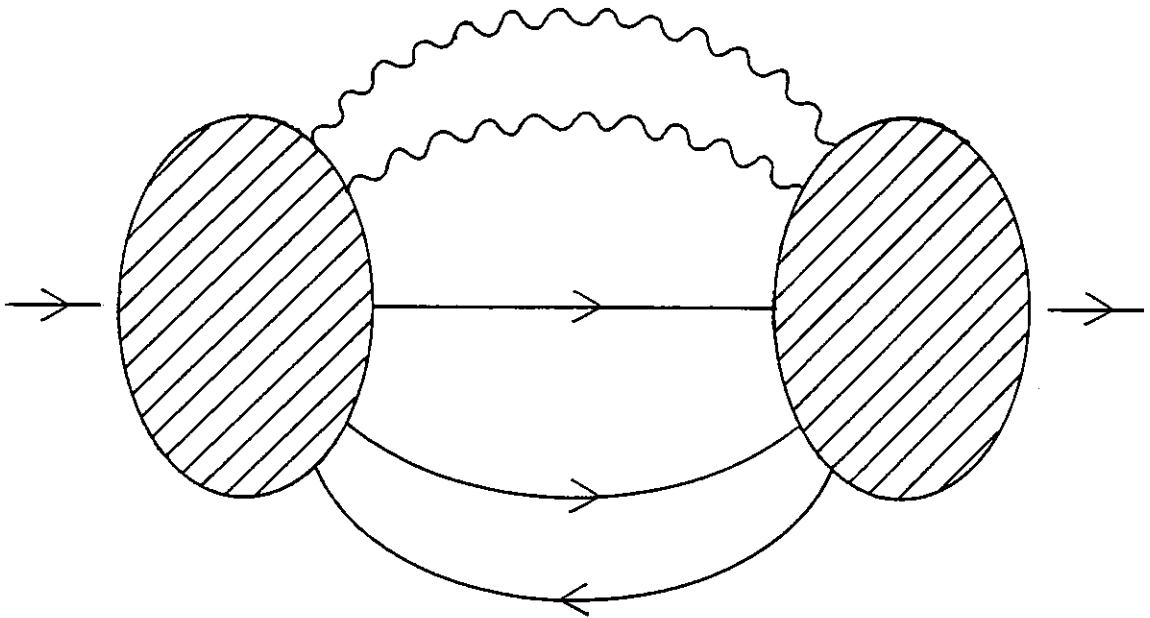


FIG B.1

A self-energy diagram with an intermediate state with one electron, an electron-hole pair and two phonons.

All other factors in the self-energy contribution are real.

The sum over $\epsilon_1, \dots, \epsilon_p$ can be performed by the usual method of contour integration. Each frequency appears in several energy denominators. Summing over the first frequency ϵ_j , we obtain a sum of terms corresponding to each of the poles, $i\Omega_j = \xi_j$, in which ϵ_j appears. Summing over the p frequencies, we then obtain a sum of terms with $r-p$ energy denominators, each corresponding to p different poles. In each of these contributions we can relabel the propagators in such a way that the p independent frequencies correspond to the p poles which determine that term. In doing the frequency summation, then, all we do is replace $\epsilon_1, \dots, \epsilon_p$, in the remaining $r-p$ denominators by the corresponding spectral densities ξ_1, \dots, ξ_p . These denominators can only have two possible forms

$$\frac{1}{i\omega_n - \Omega_j(\xi_1, \dots, \xi_p, \xi_j)} \quad \text{or} \quad \frac{1}{\Omega_j(\xi_1, \dots, \xi_p, \xi_j)}$$

where Ω_j is a linear combination (coefficients $\pm 1, 0$) of the p spectral frequencies and ξ_j the spectral frequency of this energy denominator. Using the identities

$$\begin{aligned} \frac{1}{i\omega_n - \Omega_1} \frac{1}{i\omega_n - \Omega_2} \dots &= \frac{1}{\Omega_2 - \Omega_1} \frac{1}{\Omega_3 - \Omega_1} \dots \frac{1}{i\omega_n - \Omega_1} \\ &+ \frac{1}{\Omega_1 - \Omega_2} \frac{1}{\Omega_3 - \Omega_2} \dots \frac{1}{i\omega_n - \Omega_2} \\ &+ \dots \end{aligned}$$

we can write the self-energy as a sum of terms in which the

external frequency appears only in a single energy denominator of the form

$$\frac{1}{i\omega_n - \Omega_j(\xi_1, \dots, \xi_p, \xi_j)}$$

all other factors in the term being real.

Doing the analytic continuation $i\omega_n \rightarrow \omega - i0^+$ each of these contributions to $\Sigma_2(\underline{k}, \omega)$ will have a single delta function conserving energy

$$\pi \delta(\omega - \Omega_j(\xi_1, \dots, \xi_p, \xi_j))$$

The important point to stress is that the Matsubara frequency of the j 'th propagator is determined by the external frequency and a number α ($\alpha < p$) of the independent frequencies. Hence each term in the imaginary part of the self-energy can be associated with $\alpha + 1$ propagators whose Matsubara frequencies are restricted by a single frequency conserving condition

$$\omega_n - \Omega'_j(\epsilon_1, \dots, \epsilon_{\alpha+1}) = 0$$

These $\alpha + 1$ propagators clearly define an intermediate state of the type defined in the beginning.

Appendix C

The Integral $I(q; i\epsilon_m + i\omega_\ell, i\epsilon_m)$

The integral $I(q; i\epsilon_m + i\omega_\ell, i\epsilon_m)$,

$$I(q; i\epsilon_m + i\omega_\ell, i\epsilon_m) \equiv u^2 \int \frac{d^d k}{(2\pi)^d} G(\underline{k} + q, i\epsilon_m + i\omega_\ell) G(\underline{k}, i\epsilon_m) \quad (C.1a)$$

$$= u^2 \int \frac{d^d k}{(2\pi)^d} G(-\underline{k} + q, i\epsilon_m + i\omega_\ell) G(\underline{k}, i\epsilon_m) \quad (C.1b)$$

occurs in the calculation of the particle-hole and particle-particle propagators $D_o(q; i\epsilon_m + i\omega_\ell, i\epsilon_m)$ and $C_o(q; i\epsilon_m + i\omega_\ell, i\epsilon_m)$. Also, because impurity lines do not carry frequency, one frequently ends up just with an extra factor $I(q; i\epsilon_m + i\omega_\ell, i\epsilon_m)$ or a similar integral. As we shall see, this integral is much smaller than unity except when $(\epsilon_m + \omega_\ell)\epsilon_m < 0$ and $q\ell, \omega_\ell\tau < 1$. We will restrict ourselves to $|\epsilon_m|, |\omega_\ell| \ll \epsilon_F$ as that is certainly where I is largest.

A. $\epsilon_m(\epsilon_m + \omega_\ell) > 0$

For simplicity take $\epsilon_m, \epsilon_m + \omega_\ell > 0$. The case of negative frequencies is similar. We can write

$$I = u^2 \int d^d \Omega d\omega_{\underline{k}} n(\omega_{\underline{k}}) \frac{1}{i\epsilon_m - \omega_{\underline{k}} + i/2\tau} \frac{1}{i(\epsilon_m + \omega_\ell) - \omega_{\underline{k} + q} + i/2\tau}$$

where $d^d \Omega$ is the angular integration in d dimensions normalized to unity

$$\int d^3 \Omega (\dots) \equiv \frac{1}{4\pi} \int_0^{2\pi} d\phi \int_0^\pi d\theta \sin\theta (\dots) \quad (C.3a)$$

$$\int d^2 \Omega (\dots) \equiv \frac{1}{2\pi} \int_{-\pi}^{\pi} d\theta (\dots) \quad (C.3b)$$

The density of states $n(\omega_{\underline{k}})$ has the form

$$n(\omega_{\underline{k}}) = n_0 f\left(\frac{\omega_{\underline{k}}}{\epsilon_F}\right) \quad (\text{C.4})$$

where n_0 is the density of states at the Fermi level and the function $f(x)$ is

$$f(x) = \begin{cases} \sqrt{1+x} & 3\text{D} \\ 1 & 2\text{D} \\ 0 & \end{cases} \quad \left. \begin{array}{l} x > -1 \\ \\ x < -1 \end{array} \right\} \quad (\text{C.5})$$

We can analytically continue $f(x)$ to the complex plane as $f(z) = (1+z)^{\frac{1}{2}}$ in 3D and $f(z) = 1$ in 2D if we exclude the real axis for $\text{Re } z < -1$.

Thus we can write

$$I = n_0 u^2 \int_{-\mu}^{\infty} d^d \Omega \int_{-\mu}^{\infty} f\left(\frac{\omega_{\underline{k}}}{\epsilon_F}\right) \frac{1}{i\epsilon_m - \omega_{\underline{k}} + i/2\tau} \frac{1}{i\epsilon_m + i\omega_{\underline{k}} - \omega_{\underline{k}+\underline{q}} + i/2\tau} \quad (\text{C.6})$$

We can perform the $\omega_{\underline{k}}$ integral by contour integration by closing the contour in the lower half plane, thus excluding the poles of the Green's functions (Fig. C.1). We get

$$I = -n_0 u^2 \int_{-\mu}^{\infty} d^d \Omega \int_{-\mu-i\infty}^{-\mu} d\omega_{\underline{k}} f\left(\frac{\omega_{\underline{k}}}{\epsilon_F}\right) \frac{1}{i\epsilon_m - \omega_{\underline{k}} + i/2\tau} \frac{1}{i\epsilon_m + i\omega_{\underline{k}} - \omega_{\underline{k}+\underline{q}} + i/2\tau} \quad (\text{C.7})$$

Consider the limit $q \ll k_F$. We have $|\omega_{\underline{k}}|, |\omega_{\underline{k}+\underline{q}}| \sim \mu$. As $|\epsilon_m|, |\omega_{\underline{k}}|, 1/\tau \ll \mu$ the only remaining energy scale in the integral is of order ϵ_F . Thus, by dimensional analysis we must have

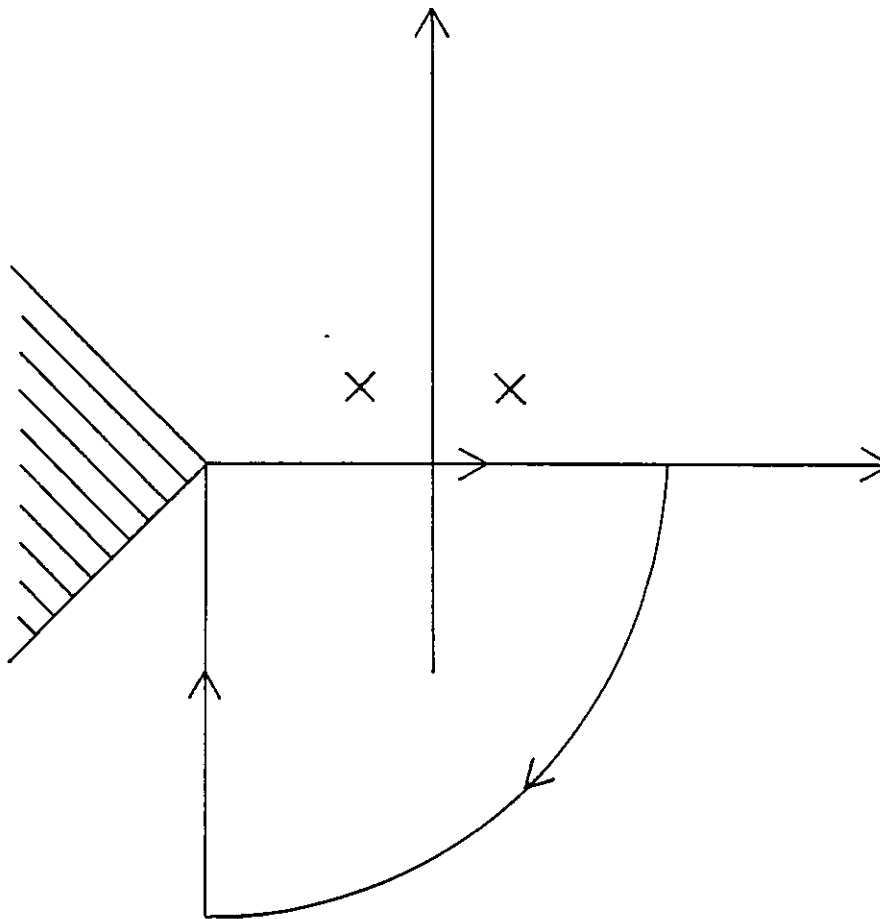


FIG C.1

Contour chosen to calculate the $\omega_{\underline{k}}$ integral in eq. (C.6). The crosses denote the positions of the poles of the Green's functions. Outside the shaded region $f(z) = (1 + z)^{1/2}$ in 3D and $f(z) = 1$ in 2D.

$$I \sim -n_0 v^2 \frac{1}{\epsilon_F} \sim \frac{1}{v \epsilon_F} \sim \frac{1}{k_F \ell} \quad (\text{C.8})$$

Having $q \sim k_F$ does not change this estimate.

$$\text{B. } \epsilon_m (\epsilon_m + \omega_\ell) < 0$$

We carry out the same analysis as in the previous case. However, when closing the contour in the complex plane, we always enclose the pole of one of the Green's functions. The integral between $-\mu \pm i\infty$ and $-\mu$ is still of order $1/k_F \ell$. But we have now another contribution from one of the poles of the Green's function. To be explicit, assume $\epsilon_m < 0$ and $\epsilon_m + \omega_\ell > 0$ and close the contour in the lower half-plane.

$$\begin{aligned} I &= n_0 \mu^2 \int d^d \Omega \frac{2\pi i}{i\omega_\ell - v_F q \cos \theta - (q^2/2m) + i/\tau} + \mathcal{O}\left(\frac{1}{k_F \ell}\right) \\ &= 2\pi n_0 v^2 \int d^d \Omega \frac{1}{\frac{1}{\tau} + \omega_\ell + i v_F q \cos \theta + i \frac{q^2}{2m}} + \mathcal{O}\left(\frac{1}{k_F \ell}\right) \end{aligned} \quad (\text{C.9})$$

where we used $f(x) \approx 1$ for $|x| \ll 1$. Using $1/\tau = 2\pi n_0 \mu^2$,

$$I = \int d^d \Omega \frac{1}{1 + \omega_\ell \tau + i v_F q \cos \theta + i (q^2/2m) \tau} \quad (\text{C.10})$$

Again, for $q \ell \gg 1$ or $\omega_\ell \tau \gg 1$ we have $I \ll 1$. But for $q \ell, \omega_\ell \tau \ll 1$ we can expand the denominator of eq. (C.10) in powers of ω_ℓ and q to get

$$\begin{aligned} I &= \int d^d \Omega \left[1 - \omega_\ell \tau - (q \ell)^2 \cos^2 \theta \right] \\ &= 1 - \omega_\ell \tau - \frac{v_F^2 \tau^2}{d} q^2 = 1 - \omega_\ell \tau - \mathcal{D} q^2 \tau \end{aligned} \quad (\text{C.11})$$

where $\mathcal{D} = v_F^2 \tau / d = k_F \ell / d m$ is the diffusion constant in d

dimensions. For $\epsilon_m > 0$, $\epsilon_m + \omega_\ell < 0$ we would get, through a similar procedure,

$$I \approx 1 + \omega_\ell \tau - \mathcal{D}q^2 \tau \quad ; \quad q\ell, \omega_\ell \tau \ll 1 \quad (\text{C.12})$$

In conclusion, for $\epsilon_m(\epsilon_m + \omega_\ell) < 0$

$$I(q; i\epsilon_m + i\omega_\ell, i\epsilon_m) \ll 1 \quad , \quad \text{if } q\ell \text{ or } \omega_\ell \tau \gg 1 \quad (\text{C.13a})$$

$$\approx 1 - |\omega_\ell| \tau - \mathcal{D}q^2 \tau \quad , \quad \text{if } q\ell, \omega_\ell \tau \ll 1 \quad (\text{C.13b})$$

Appendix D

The Momentum Integrals I_{pq}

The momentum integrals I_{pq} ,

$$I_{pq} \equiv \int \frac{d^d \underline{k}}{(2\pi)^d} [G^R(\underline{k}, i\epsilon_m)]^p [G^A(\underline{k}, i\epsilon_m)]^q \quad (D.1)$$

occur repeatedly in the theory of weakly disordered metals. One is generally interested in $|\epsilon_m| \ll \mu$. As long as $p, q > 1$ the integral over $\omega_{\underline{k}}$ is dominated by the vicinity of the Fermi surface and we may write

$$I_{pq} = n_0 \int_{-\infty}^{+\infty} d\omega_{\underline{k}} \left(\frac{1}{i\epsilon_m - \omega_{\underline{k}} + i/2\tau} \right)^p \left(\frac{1}{i\epsilon_m - \omega_{\underline{k}} - i/2\tau} \right)^q \quad (D.2)$$

Using the following identities, easily proved by induction,

$$z^{-p} = \frac{(-)^{p-1}}{(p-1)!} \frac{d^{p-1}}{dz^{p-1}} z^{-1} \quad (D.3a)$$

$$\frac{d^p}{dz^p} z^{-q} = (-)^p \frac{(p+q-1)!}{(q-1)!} z^{-(p+q)} \quad (D.3b)$$

one obtains from eq. (D.2), integrating by parts,

$$I_{pq} = (-)^{p-1} \frac{(p+q-2)!}{(p-1)!(q-1)!} n_0 \int_{-\infty}^{+\infty} d\omega_{\underline{k}} \frac{1}{i\epsilon_m - \omega_{\underline{k}} + i/2\tau} \left(\frac{1}{i\epsilon_m - \omega_{\underline{k}} - i/2\tau} \right)^{q+p-1} \quad (D.4)$$

The $\omega_{\underline{k}}$ integral can be done by contour integration by closing the contour in the upper half plane,

$$I_{pq} = -2\pi i (-)^{p-1} \frac{(p+q-2)!}{(p-1)!(q-1)!} n_0 \left(\frac{1}{-i/\tau} \right)^{p+q-1}$$

and finally

$$I_{pq} = 2\pi n_0 \tau (-)^{q-1} \frac{(p+q-2)!}{(p-1)!(q-1)!} \left(\frac{\tau}{i} \right)^{p+q-2} \quad (\text{D.5})$$

Some examples:

$$I_{11} = 2\pi n_0 \tau \quad (\text{D.6a})$$

$$I_{21} = -I_{12} = 2\pi n_0 \frac{\tau^2}{i} \quad (\text{D.6b})$$

$$I_{22} = 4\pi n_0 \tau^3 \quad (\text{D.6c})$$

Appendix E

The Polarization Insertion $\Pi(q, i\omega_\ell)$ and the Screened Coulomb Interaction

The averaged screened Coulomb interaction $V_c(q, i\omega_\ell)$ is given by the diagram of Fig. E1,

$$V_c(q, i\omega_\ell) = \frac{V_B(q)}{1 - V_B(q) \Pi(q, i\omega_\ell)} \quad (\text{E.1})$$

where the bare interaction $V_B(q)$ is

$$V_B(q, i\omega_\ell) = \frac{4\pi e^2}{q^2} \quad \text{in } 3D \quad (\text{E.2a})$$

$$= \frac{2\pi e^2}{q} \quad \text{in } 2D \quad (\text{E.2b})$$

The polarization insertion $\Pi(q, i\omega_\ell)$ which is also the density-density correlation function for the non-interacting system, is given by the same diagrams as the conductivity $\sigma(q, \omega)$ (see Fig. 4.7) but without the factors k_x, k'_x in the external vertices. For this reason the contribution of the diagram of Fig. 4.7(b) does not vanish. One has

$$\begin{aligned} \Pi(q, i\omega_\ell) = & \Pi_0(q, i\omega_\ell) + \frac{2}{\beta} \sum_{\epsilon_m} \int \frac{d^d k}{(2\pi)^d} \int \frac{d^d k'}{(2\pi)^d} G(k+q, i\epsilon_m+i\omega_\ell) \\ & \times G(k, i\epsilon_m) G(k'+q, i\epsilon_m+i\omega_\ell) G(k', i\epsilon_m) \mathcal{D}_0(q; i\epsilon_m+i\omega_\ell, i\epsilon_m). \end{aligned} \quad (\text{E.3})$$

The bare polarization, $\Pi_0(q, i\omega_\ell)$, is

$$\Pi_0(q, i\omega_\ell) = \frac{2}{\beta} \sum_{\epsilon_m} \int \frac{d^d k}{(2\pi)^d} G(k+q, i\epsilon_m+i\omega_\ell) G(k, i\epsilon_m) \quad (\text{E.4})$$

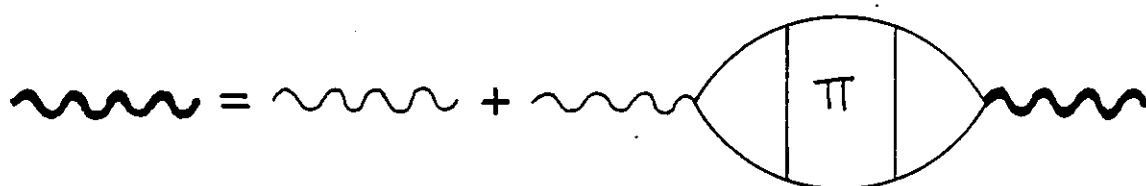


FIG E.1

The screened Coulomb interaction

We shall consider separately the case $q\ell, \omega_\ell \tau \ll 1$ (diffusive regime) and $q\ell \gg 1$.

A. Diffusive Regime

It is easily proven from eqs. (E.3), (E.4) that

$$\Pi(q, i\omega_\ell) = \Pi(q, -i\omega_\ell) \quad . \quad \text{We take } \omega_\ell > 0 \text{ for simplicity.}$$

When, in the second term of eq. (E.3) we have $\epsilon_m(\epsilon_m + \omega_\ell) > 0$ the propagator D_0 is (eqs. (4.7), (C.8)),

$$D_0(q, i\epsilon_m + i\omega_\ell, i\epsilon_m) \approx (2\pi n_0 \tau)^{-1} \equiv v^2 \quad ; \quad \epsilon_m(\epsilon_m + \omega_\ell) > 0 \quad (\text{E.5})$$

Each term in the frequency sum of the second term of eq. (E.3) is smaller than the corresponding term in $\Pi_0(q, i\omega_\ell)$ by a factor (eq. (C.8)),

$$\begin{aligned} I(q, i\epsilon_m + i\omega_\ell, i\epsilon_m) &\equiv v^2 \int \frac{d^d k}{(2\pi)^d} G(\underline{k} + \underline{q}, i\epsilon_m + i\omega_\ell) G(\underline{k}, i\epsilon_m) \\ &\sim \frac{1}{k_F \ell} \quad ; \quad \epsilon_m(\epsilon_m + \omega_\ell) > 0 \end{aligned} \quad (\text{E.6})$$

Thus to leading order in $1/k_F \ell$

$$\begin{aligned} \Pi(q, i\omega_\ell) &= \Pi_0(q, i\omega_\ell) + \frac{2}{2\pi n_0 \tau^2 [\omega_\ell + Dq^2]} \\ &\times \frac{1}{\beta} \sum_{-\omega_\ell < \epsilon_m < 0} \left[\int \frac{d^d k}{(2\pi)^d} G^R(\underline{k} + \underline{q}, i\epsilon_m + i\omega_\ell) G^A(\underline{k}, i\epsilon_m) \right]^2 \end{aligned} \quad (\text{E.7})$$

For $q\ell, \omega_\ell \tau \ll 1$ we can expand the Green's functions in \underline{q} and ω_ℓ to get the leading term,

$$\Pi(q, i\omega_\ell) = \Pi_0(q, i\omega_\ell) + \frac{2}{2\pi n_0 \tau^2 [\omega_\ell + Dq^2]} \frac{I_{pq}^2}{\beta} \frac{\omega_\ell}{2\pi} \quad (\text{E.8})$$

The integrals I_{pq} are defined and calculated in Appendix D.

The factor $\omega_\ell/2\pi$ comes from the frequency sum. We get, using eq. (D.6a)

$$\begin{aligned}\Pi(q, i\omega_\ell) &= \frac{2(z\pi n_0 \tau)^2}{2\pi n_0 \tau^2 [\omega_\ell + Dq^2]} \frac{\omega_\ell}{2\pi} + \Pi_0(q, i\omega_\ell) \\ &= \frac{2n_0 \omega_\ell}{\omega_\ell + Dq^2} + \Pi_0(q, i\omega_\ell) .\end{aligned}\quad (\text{E.9})$$

For the bare polarization $\Pi_0(q, i\omega_\ell)$ we get, after performing the frequency sums,

$$\begin{aligned}\Pi_0(q, i\omega_\ell) &= 2 \int \frac{d^d k}{(2\pi)^d} \int \frac{d\xi}{2\pi i} \left\{ (-f(\xi)) [G^R(k, \xi) - G^A(k, \xi)] G(k+q, \xi+i\omega_\ell) \right. \\ &\quad \left. - f(\xi-i\omega_\ell) [G^R(k+q, \xi) - G^A(k+q, \xi)] G(k, \xi-i\omega_\ell) \right\}\end{aligned}\quad (\text{E.10})$$

Using $f(\xi-i\omega_\ell) = f(\xi)$ and expanding again in q, ω_ℓ ,

$$\begin{aligned}\Pi_0(q, i\omega_\ell) &= \frac{1}{\pi} \int \frac{d^d k}{(2\pi)^d} \int d\xi f(\xi) \frac{1}{i} [G^A(k, \xi) - G^R(k, \xi)] \\ &\quad \times [G^R(k, \xi) + G^A(k, \xi)] \\ &= \frac{1}{\pi} \int \frac{d^d k}{(2\pi)^d} \int d\xi f(\xi) \rho(k, \xi) 2 \text{Re} G(k, \xi)\end{aligned}\quad (\text{E.11})$$

The spectral function and the real part of $G(k, \xi)$ are

$$\rho(k, \xi) = \frac{1/\tau}{(\xi - \omega_k)^2 + (1/2\tau)^2} \quad (\text{E.12a})$$

$$\text{Re} G(k, \xi) = \frac{(\xi - \omega_k)}{(\xi - \omega_k)^2 + (1/2\tau)^2} \quad (\text{E.12b})$$

It follows

$$\rho(k, \xi) 2 \text{Re} G(k, \xi) = -\frac{\partial}{\partial \xi} \rho(k, \xi) \quad (\text{E.13})$$

and

$$\begin{aligned}
 \Pi_0(q, i\omega_\ell) &= \frac{1}{\pi} \int \frac{d^d k}{(2\pi)^d} \int_{-\infty}^{+\infty} d\xi f(\xi) \left(-\frac{\partial}{\partial \xi} \rho(k, \xi) \right) \\
 &= -\frac{1}{\pi} \int \frac{d^d k}{(2\pi)^d} \int_{-\infty}^{+\infty} d\xi \left(-\frac{\partial \rho}{\partial \xi} \right) \rho(k, \xi) \\
 &= -\frac{1}{\pi} \int \frac{d^d k}{(2\pi)^d} \rho(k, 0)
 \end{aligned} \tag{E.14}$$

Hence the low q , ω_ℓ limit $\Pi^0(q, i\omega_\ell)$ is

$$\Pi_0(q, i\omega_\ell) = -2n_0 \tag{E.15}$$

Inserting this result in eq. (E.9) and using $\Pi(q, i\omega_\ell) = \Pi(q, -i\omega_\ell)$ we obtain,

$$\Pi(q, i\omega_\ell) = \frac{-2n_0 D q^2}{|\omega_\ell| + D q^2} \tag{E.16}$$

Using this result in eq. (E.1) we get for the averaged screened Coulomb interaction, to leading order in q and ω_ℓ ,

$$V_c(q, i\omega_\ell) = \frac{4\pi e^2}{q^2} \frac{|\omega_\ell| + D q^2}{|\omega_\ell| + D k^2} \quad ; \text{ in } 3D \tag{E.17a}$$

$$= \frac{2\pi e^2}{q} \frac{|\omega_\ell| + D q^2}{|\omega_\ell| + D k q} \quad ; \text{ in } 2D \tag{E.17b}$$

where k the inverse screening radius is

$$k^2 = 8\pi n_0 e^2 = \frac{4m e^2}{\pi} k_F \quad ; \text{ in } 3D \tag{E.18a}$$

$$k = 4\pi n_0 e^2 = 2m e^2 \quad ; \text{ in } 2D \tag{E.18b}$$

The spectral density $\sigma_c(q, \eta) \equiv 2 \text{Im} V_c^A(q, \eta)$ is, then, for $q\ell, \eta\tau \ll 1$,

$$\sigma_c(q, \eta) = \frac{8\pi e^2}{q^2} \frac{\eta \epsilon}{\eta^2 + \epsilon^2} \quad ; \text{ in } 3D \quad (E.19a)$$

$$= 4\pi e^2 \frac{\eta D\kappa}{\eta^2 + \epsilon Dq^2} \quad ; \text{ in } 2D \quad (E.19b)$$

where $\epsilon = D\kappa^2$. In our units me^2 is the inverse of the Bohr radius. Hence, in 3D $\epsilon = 4(\kappa_F \ell) a_0^{-1} \kappa_F / 3m\pi$ and in 2D $\epsilon = 4(\kappa_F \ell) a_0^{-2} / 2m$. In both cases $\epsilon \gg \epsilon_F$.

B. $q\ell \gg 1$.

It is shown in Appendix C that the integral $I(q; i\epsilon_m + i\omega_\ell, i\epsilon_m)$ is of order $1/q\ell$ at most, for $q\ell \gg 1$ (eq. C.10). Then, the particle-hole propagator D_0 is again given by eq. (E.5) and we see that each term in the frequency sum of the second term of eq. (E.3) is again smaller than the corresponding term in $\Pi_0(q, i\omega_\ell)$ by a factor $I(q; i\epsilon_m + i\omega_\ell, i\epsilon_m) \sim 1/q\ell$. Thus for $q\ell \gg 1$ we can neglect the second term in eq. (E.3) altogether and write,

$$\Pi(q, i\omega_\ell) \approx \Pi_0(q, i\omega_\ell) \quad (E.20)$$

We shall only be interested in the imaginary part of the advanced function $\Pi^A(q, \omega)$ for $\omega \ll \epsilon_F$. From eq. (E.10),

$$\begin{aligned} \Pi_2(q, \omega) &= 2 \int d\xi [f(\xi) - f(\xi + \omega)] \int \frac{d^d k}{(2\pi)^d} \rho(k, \xi) \rho(k+q, \xi + \omega) \\ &= 2 \int d\xi [f(\xi) - f(\xi + \omega)] \\ &\quad \times \int d^d \Omega \int d\omega_k n(\omega_k) \frac{1/\tau}{(\xi - \omega_k)^2 + (1/2\tau)^2} \frac{1/\tau}{(\xi + \omega - \omega_k + q)^2 + (1/2\tau)^2} \end{aligned}$$

where $d^d \Omega$ denotes the element of solid angle in d dimensions normalized to unity (eqs. C3).

The ω_k integral can be evaluated using the same contour

as in Appendix C (Fig. C.1). The contribution of the part of the contour between $-\mu - i\omega$, $-\mu$ can be estimated, using the same procedure as in Appendix C, to be of order $n_0/\tau^2 \epsilon_F^3$. The contribution from the poles of the spectral functions is smallest for large q ($\sim k_F$) and is of order $n_0/\tau \epsilon_F^2$. So we neglect the former contribution and write,

$$\begin{aligned} \Pi_2(q, \omega) &= 2 \int d\xi [f(\xi) - f(\xi + \omega)] n(\xi) \\ &\times \int d^d \Omega \frac{z/\tau}{[v_\xi q \cos\theta + (q^2/2m) - \omega]^2 + (1/\tau)^2} \\ &\approx 2 \int d\xi [f(\xi) - f(\xi + \omega)] \frac{\pi(\xi)}{v_\xi q} \\ &\times \int d^d \Omega \frac{z(q\ell)^{-1}}{\left(t - \frac{\omega}{v_\xi q} + \frac{q}{2k_\xi}\right)^2 + (q\ell)^{-2}}. \end{aligned} \quad (E.20)$$

In this expression $k_\xi \equiv \sqrt{2m(\mu + \xi)}$, $v_\xi \equiv k_\xi/m$ and $\tau \equiv \cos\theta$. The thermal occupation factors restrict $|\xi| < \text{Max}\{\omega, k_B T\}$ and so $v_\xi q \tau \sim v_F q \tau \sim q\ell$. In pure metals we get a similar expression with the last Lorentzian replaced by a delta-function $\delta\left(t - (\omega/v_\xi q) + q^2/2k_\xi\right)$. The variable t ranges between ± 1 and thus, if we have

$$\left| \frac{\omega}{v_\xi q} - \frac{q}{2k_\xi} \right| \ll 1 - \frac{1}{q\ell} \quad (E.21)$$

we can make the replacement

$$\frac{z(q\ell)^{-1}}{\left(t - \frac{\omega}{v_\xi q} + \frac{q}{2k_\xi}\right)^2 + (q\ell)^{-2}} \longrightarrow 2\pi \delta\left(t - \frac{\omega}{v_\xi q} + \frac{q}{2k_\xi}\right)$$

We are considering only $\omega \ll \epsilon_F$ and so the condition of eq. (E.21) may be replaced by

$$v_F q \gg \omega \Rightarrow \frac{q}{2k_F} \gg \frac{\omega}{4\epsilon_F} \quad (\text{E.22a})$$

$$1 - \frac{q}{2k_F} \gg \text{Max} \left\{ \frac{\omega}{4\epsilon_F}, \frac{1}{k_F \ell} \right\} \quad (\text{E.22b})$$

Including the initial restriction $q\ell \gg 1$ we can summarize these equations as

$$\delta \ll \frac{q}{2k_F} \ll 1 - \delta \quad (\text{E.23a})$$

$$\delta \sim \text{Max} \left\{ \frac{\omega}{\epsilon_F}, \frac{1}{k_F \ell} \right\} \ll 1 \quad (\text{E.23b})$$

Subject to these restrictions, one obtains, by replacing the Lorentzian in eq. (E.20) by the corresponding delta-function,

$$\pi_z(q, \omega) = \frac{\pi n_0 \omega}{v_f q} \quad ; \text{ in } 3D \quad (\text{E.24a})$$

$$= \frac{2n_0 \omega}{v_f q \sqrt{1 - (q/2k_F)^2}} \quad ; \text{ in } 2D \quad (\text{E.24b})$$

The Coulomb spectral function is

$$\sigma_c(q, \eta) = \frac{2 v_B^2(q) \pi_z(q, \eta)}{[1 - v_B(q) \pi_1(q, \eta)]^2 + [v_B(q) \pi_2(q, \eta)]^2} \quad (\text{E.25})$$

where $\pi_1(q, \eta) = \text{Re} \pi^R(q, \eta)$. We see from eq. (E.24) that $\pi_2(q, \eta)$ is linear in frequency for $\eta \ll \epsilon_F$ for almost all values of q . Thus, to leading order in η ,

$$\begin{aligned}
 \sigma_c(q, \eta) &= \frac{2V_B^2(q)}{[1 - V_B(q)\pi_1(q, 0)]^2} \pi_2(q, \eta) \\
 &= 2V_{SS}^2(q) \pi_2(q, \eta)
 \end{aligned}
 \tag{E.26}$$

where $V_{SS}(q)$, the static screened Coulomb interaction, is

$$V_{SS}(q) = \frac{V_B(q)}{1 - V_B(q)\pi_1(q, 0)}
 \tag{E.27}$$

REFERENCES

- Abrahams E, Anderson PW, Lee PA, Ramakrishnan TV, 1981
Phys. Rev. B24, 6783
- Abrahams E, Anderson PW, Licciardello DC, Ramakrishnan TV,
1979 Phys. Rev. Lett. 42, 673
- Abrahams E, Ramakrishnan TV, 1980 J. Non-Crystalline Solids
35, 15
- Abrikosov AA, Gor'kov LP, Dzyaloshinskii IE 1965 "Quantum
Field Theoretical Methods in Statistical Physics" (Oxford:
Pergamon)
- Al'tschuler BL, 1978 Sov. Phys. JEPT 48, 670
- Al'tschuler BL, Aronov AG 1979 Sov. Phys. JEPT 50, 968 and
JEPT Lett. 30, 482
- Al'tschuler BL, Aronov AG, Lee PA, 1980 Phys. Rev. Lett. 44,
1288
- Anderson PW, 1958 Phys. Rev. 102, 1008
- Anderson PW, Abrahams E, Ramakrishnan TV, 1979 Phys. Rev. Lett.
43, 718
- Ando T, Fowler AB, Stern F, 1982 Rev. Mod. Physics 54, 437
- Baym G, 1962 Phys. Rev. 127, 1391
- Baym G, Kadanoff LP, 1961 Phys. Rev. 124, 287
- Baym G, Pethick C, 1978 in "The Physics of Liquid and Solid
Helium" part 2 ed. K.H. Benneman and J.B. Ketterson
(New York, Wiley and Sons)
- Bergmann G, 1971 Phys. Rev. B3, 3797
- Bergmann G, 1982 Z. Physik B48, 5
- Bishop DJ, Dynes RC, Tsui DC, 1982 Phys. Rev. B26, 773
- Davies RA, Pepper M, 1983 J. Phys. C16, L353
- Doniach S, Sondheimer EH, 1974 "Green's Functions for Solid
State Physicists" (New York: W.A. Benjamin)
- Edwards SF, 1958 Phil. Mag. 3, 1020

- Fetter AL, Walecka JD, 1971 "Quantum Theory of Many Particle Systems" (New York: McGraw-Hill)
- Forster D, 1975 "Hydrodynamic Fluctuations, Broken Symmetry and Correlation Functions" (Reading Massachussets: W.A. Benjamin)
- Fukuyama H, 1980 J. Phys. Soc. Jpn. 48, 2169
- Fukuyama H, 1983 Technical Report of ISSP; in "Electron-Electron Interactions in Disordered Systems" ed. by M. Pollack and A.L. Efros (North Holland)
- Fukuyama H, Abrahams E, 1983 Phys. Rev. B27, 5976
- Guiliani GF, Quinn JG, 1982 Phys. Rev. B26, 4421
- Gor'kov LP, Larkin AI, Khmel'nitzkii DE, 1979 JEPT Lett. 30, 248
- Holstein T, 1964 Ann. Phys. NY 29, 410
- Kadanoff LP, Baym G, 1963 "Quantum Statistical Mechanics" (New York: W.A. Benjamin)
- Kawaguchi T, Kawaji S, 1980 J. Phys. Soc. Jpn 48, 699
- Keck B, Schmid A, 1976 J. Low Temp. Phys. 24, 611
- Langer JS, 1961 Phys. Rev. 124, 997
- MacDonald AH, 1980 Phys. Rev. Lett. 44, 486
- MacDonald AH, Taylor R, Geldart DW, 1981 Phys. Rev. B23, 6
- Migdal AB, 1958 Zh. Eksp. Teor. Fiz 34, 1438 (1958 Sov. Phys. JEPT 7, 996)
- Nozières P, 1964 "Interacting Fermi Systems" (New York: W.A. Benjamin)
- Pepper M, 1981 in "Disordered Systems and Localization" ed. by C. Castellani, C. di Castro, L. Peliti (Berlin: Springer Verlag)
- Poole DA, Pepper M, Hughes A, 1982 J. Phys. C15, L1137
- Prange RE, Kadanoff LP, 1964 Phys. Rev. 134, A566
- Prange RE, Sachs A, 1967 Phys. Rev. 158, 672
- Rice TM, 1968 Phys. Rev. 175, 858

- Rickayzen G, 1980 "Green's Functions and Condensed Matter"
(London: Academic Press)
- Schmid A, 1973 Z. Physik 259, 421
- Schmid A, 1974 Z. Physik 271, 251
- Schrieffer JR, 1964 "Theory of Superconductivity" (New York:
W.A. Benjamin)
- Takayama H, 1973 Z. Physik 263, 329
- Thouless DJ, Phys. Rev. Lett. 39, 1167
- Tsuneto T, 1960 Phys. Rev. 121, 402
- Uren MJ, Davies RA, Kaveh M, Pepper M, 1981 J. Phys. C14, L395
- Wheeler RG, 1981 Phys. Rev. B24, 4645
- Ziman J, 1962 "Electrons and Phonons" (Oxford: Oxford University
Press)